NUMERICAL SIMULATIONS OF FOUR-QUARK AND HYBRID MESONS IN LATTICE QUANTUM CHROMODYNAMICS

Thesis
submitted by

ALAN WILLIAM POLLOCK THOMSON

for the degree of

DOCTOR OF PHILOSOPHY

Department of Physics
University of Edinburgh
September 1985

To my mother and father
and to Ann-Marie

ACKNOWLEDGEMENTS

I would like to thank my supervisors, Ken Bowler, David Wallace, and also Ted Barnes, for pushing and prodding me whenever it might have been appropriate and for leaving me with a greater understanding of, and pleasure in, one of the finer aspects of life, namely, Natural Philosophy.

However, this would not have been possible but for the continuous help of the Edinburgh Regional Computing Centre over the last three years and, of course, the receipt of an SERC award.

I have appreciated, and still continue to do so, the friendship that is to be found in the Department of Physics. If I single out David Chalmers and Steven Goodyear in particular, it is only because we shared a, too often, cramped office.

It is also only just that I acknowledge the support of friends that I have known for somewhat longer. Although they may find much of what follows unintelligable, perhaps that is to their credit. They deserve equal praise for helping me find an appreciation of some of the less esoteric, but equally fine, qualities of life.

DECLARATION

Some of the work presented in chapters four and five was done in collaboration with Ted Barnes (Rutherford-Appleton Laboratory, presently at the University of Toronto, Canada). All other work is my own except where indicated.

ABSTRACT

We discuss the implementation of an $SU(3)_c$ gauge theory as a model of the hadronic interaction and illustrate the role played by non-perturbative fluctuations in the physical regime of strong coupling. The lattice formulation, an explicitly non-perturbative regularisation, is then introduced and numerical evidence for the veracity of $SU(3)_c$ is described in some detail. The quark model of Gell-Mann, Ne´eman and others is reconsidered in the light of the additional "colour" degree of freedom from the interacting field theory and multi-quark (e.g., $q^2\bar{q}^2$) quark-gluon ($q\bar{q}g$, "hybrid") bound states are anticipated. In the hitherto absence from experiment of 4-quark and $q\bar{q}g$ mesons, recent progress in calculating the masses of these states in the QCD spectrum by (semi-) analytic methods is reviewed.

Numerical results from lattice QCD for the masses of 4-quark and hybrid mesons are presented. Both the exotic and non-exotic scalar and vector channels are examined. The appearance of two pions in the 0^{++} channel on the 8^3x16 lattice implies, as a corollary, the incorporation of non-zero lattice 3-momentum in all effective particle masses. It is then argued that the lattice IR cut-off will prove crucial in determining the possibility of the production of true 4-quark resonances opposed to pairs of $q\bar{q}$ mesons. In the hybrid sector, gluon fields are defined in terms of products of the gauge link variables. The importance of the statistical averaging over (sizable) numbers of gauge configurations is emphasised. Approximate masses for the 0^{-+}, 0^{+-} and 1^{-+} hybrids are given. For both 4-quark and $q\bar{q}g$ states, comparisons with the (semi-) analytic results are made.

Protarchus: What question?

Socrates: Whether all this which they call the universe is left to the guidance of unreason and chance medley, or, on the contrary, as our fathers have declared, ordered and governed by a marvellous intelligence and wisdom.

Protarchus: Wide assunder are the two assertions, illustrious Socrates, for that which you were just now saying to me appears to be blasphemy, but the other assertion, that mind orders all things, is worthy of the aspect of the world, and of the sun, and of the moon, and of the stars and of the whole circle of the heavens; and never will I say or think otherwise.

Plato, "Philebus"

Philosophy [nature] is written in that great book which ever lies before our eyes- I mean the universe- but we cannot understand it if we do not first learn the language and grasp the symbols in which it is written. The book is written in the mathematical language, and the symbols are triangles, circles and other geometrical figures, without whose help it is impossible to comprehend a single word of it; without which one wanders in vain through a dark labyrinth.

Galileo Galilei, "The Assayer", 1610

CONTENTS

1.Gauge Symmetry and Quantum Field Theory

1.1 Introduction 1

1.2 The Quark Model of the Hadronic Spectrum: An Overview 2

1.3 Abelian and Non-Abelian Gauge Theories: Construction 6

1.4 The Perturbative Approach to a Quantum Field Theory 10

1.5 The Phase Structure of Non-Abelian Gauge Theories 18

2. The Lattice Formulation of QCD

2.1 Introduction 24

2.2 Definition of a Lattice Regularised Gauge Theory 25

2.3 Monte-Carlo Methods in Lattice Gauge Theories 32

2.4 Phase Structures of Abelian and Non-Abelian Gauge Theories 35

2.5 Non-Perturbative Features of the Gauge System 37

(a) String Tension 38

(b) Mass Gap 40

(c) The Deconfinement Temperature 42

2.6 Fermions in Lattice Gauge Theory 44

2.7 Calculational Methods for the Quark Propagator 50

2.8 The Hadron Spectrum: Combining the Quark Propagators 53

3. Multi-Quark and Hybrid Mesons in QCD

3.1 Introduction 61

3.2 Mass-Inequalities in Lattice Regularised Gauge Theories 65

3.3 QCD Sum Rules 69

3.4 The MIT Bag Model 76

3.5 Bag Model $Q^2\bar{Q}^2$ 82

4. Lattice Analysis of 4-Quark Mesons

4.1 Introduction: $Q^2\bar{Q}^2$ in Lattice and Continuum QCD 86

4.2 Definition of $Q^2\bar{Q}^2$ Operators 90

4.3 Numerical Results 94

4.4 Masses of Other Low-Spin States 104

(a) $O^{++}(\delta\delta)$ 106

(b) Other Exotic and Crypto-Exotic Mesons 107

5. Hybrid Mesons in Lattice QCD

5.1 Introduction 110

5.2 The Hypercubic Lattice Group 112

5.3 Lattice Studies of Hybrid Mesons: The Heavy $Q\bar{Q}$ Potential 116

5.4 Hybrid Mesons on the DAP 8^4 Lattice 118

6. Summary and Conclusions 128

Appendix 134

References 140

CHAPTER 1

Gauge Symmetry and Quantum Field Theory

1.1 Introduction

One can trace throughout the history of Man the importance of the concept of symmetry in shaping intellectual thought. Indeed the investigation by, for instance, the ancient Greeks, of the symmetries of simple objects was of considerable relevance to the development of Geometry, as we understand it today [Bronowski 1972]. The level of abstraction reached in physical theories today continues to reflect this preoccupation. We see the interplay between simple, almost naive, "pictorial" representations of phenomena and a complex and powerful calculational machinery derived from these centuries of effort. This accumulation of investigation and theorising has provided us with the ability to describe and predict multifarious aspects of the physical world, to such a degree, in fact, that many now feel that the basic principles underpinning the physical universe, or at least our "interaction" with it, are now becoming clearer.

In this opening chapter we wish to explore these principles with a view to illustrating that the mathematical descriptions of the four forces of nature share common roots. We refer to this by the title of the "gauge principle": the implementation of a local symmetry invariance in Quantum Field Theory (first demonstrated in the context of the SU(2) group by Yang and Mills [1954]. Moreover, one often finds that global symmetry invariance provides additional constraints on any field theory. The relevence of this to our major concern, the hadronic interaction, is demonstrated through introducing the "naive" quark model.

Having then discussed the explicit construction of a gauge invariant field theory, by example of Quantum Electrodynamics (QED) and Quantum Chromodynamics (QCD), we examine the range of applicability of the traditional method of calculation: a perturbation expansion (in powers of the coupling) around the non-interacting state. For the hadronic interaction (i.e., QCD) we find that many aspects of the theory are not exposed by this perturbation theory. We close the chapter by discussing the role of these non-perturbative phenomena; leading us naturally to the introduction, in chapter 2, of a non-perturbative scheme, the lattice regularised field theory.

1.2 The Quark Model of the Hadronic Spectrum: an overview

During the 1950's and 1960's, the number of sub-nuclear particles blossomed, somewhat to the consternation of Physicists believing that the universe should consist of a small number of "fundamental" particles. This view had been (and of course still is) widespread since the time of Mendeleev and the Periodic Table of the Elements. More importantly though, the results of scattering experiments revealed the probability of nucleon substructure with observations similar to those witnessed by Rutherford on particle scattering from atomic nuclei.

Gell-Mann [1964a,b] and Zweig [1964a,b] (for more general reviews on the Quark Model see also, for example, Close [1980], Kokkedee [1969]) introduced a symmetry scheme based on three "flavours" or types of "quarks" to explain some aspects of these dilemmas (today we believe that there are at least six flavours). Mesons were identified as quark-anti-quark configurations ($q\bar{q}$, the bar representing the conjugate representation of the symmetry

group) and baryons as three quark states (qqq). From the requirement that the quarks were complex variables, it was natural that the symmetry scheme be that of SU(3). The group theory of SU(3) tells us that if this scheme is correct then the following representations should be found [Hammermesh 1963]

$$q \otimes \bar{q} = \underset{\sim}{3} \otimes \underset{\sim}{\bar{3}} = \underset{\sim}{1} \oplus \underset{\sim}{8}$$
$$q \otimes q \otimes q = \underset{\sim}{3} \otimes \underset{\sim}{3} \otimes \underset{\sim}{3} = \underset{\sim}{1} \oplus \underset{\sim}{8} \oplus \underset{\sim}{8} \oplus \underset{\sim}{10} \qquad (1.1)$$

In chapters 3, 4 and 5, we will consider hadronic states which are composed of both multi-quark and mixed quark-gluon constituents, possibilities not understood within this phenomenological quark model, but arising specifically from the full interacting theory.

In table 1 we identify the low mass mesons and baryons by their flavour assignments. Table 2 shows the construction of wave-functions for these operators and lists their permutation properties. However, this on its own cannot be the complete story. If one expected, for example, that the quarks were scalar particles then a more natural heirarchy of masses would be that (in terms of the orbital angular momentum) $m(S) \leqslant m(P) \leqslant m(D)$. This is not what is found. The meson spectrum reveals that often the vector states are less massive that scalars and that pseudoscalars lie lowest of all [Close 1980]. The solution treats the quarks as spin 1/2 fermions and increases the overall group structure to include intrinsic and orbital angular momentum. Thus we write $SU(6)_{FS} \times O(3)$ for the combination of flavour and spin groups and O(3) for the orbital angular momentum (in some potential, e.g. harmonic oscillator). This extra group structure demonstrates explicitly the complicated spectroscopy of spin-spin and spin-orbit splittings of hadronic masses. For instance, a

Flavour	Charge	Strangeness	Meson
$u\bar{d}$	+1	0	π^+ ρ^+
$d\bar{u}$	-1	0	π^- ρ^-
$u\bar{u}$	0	0	π^0 ρ^0
$d\bar{d}$	0	0	η^0 ω^0
$s\bar{s}$	0	0	η'^0 ϕ^0
$u\bar{s}$	+1	+1	K^+ K^{*+}
$d\bar{s}$	0	+1	K^0 K^{*0}
$\bar{u}s$	-1	-1	K^- K^{*-}
$\bar{d}s$	0	-1	$\bar{K}^0$ $\bar{K}^{*0}$

Table 1.1 Identification of low-mass ($q\bar{q}$) mesons in terms of the SU(3) quark triplet (u,d,s). From Close [1980].

symmetry/ G-parity	Wavefunction	Meson
$\phi_S \chi_A (\phi_A \chi_S)$ ALL ‡	$\frac{1}{\sqrt{2}}(u\bar{d} \pm \bar{d}u)$	$\pi^+ \ (\rho^+)$
/ $-1 \ (+1)$	$-\frac{1}{\sqrt{2}}(d\bar{u} \pm \bar{u}d)$	$\pi^- \ (\rho^-)$
	$\frac{1}{2}[(d\bar{d} - u\bar{u}) \pm (d\bar{d} - u\bar{u})]$	$\pi^0 \ (\rho^0)$
	$\frac{1}{2\sqrt{3}}[(u\bar{u} + d\bar{d} - 2s\bar{s}) \pm (u\bar{u} + d\bar{d} - 2s\bar{s})]$	$\eta^0_8 \ (\omega^0_8)$
	$\frac{1}{\sqrt{6}}[(u\bar{u} + d\bar{d} - 2s\bar{s}) \pm (u\bar{u} + d\bar{d} - 2s\bar{s})]$	$\eta^0_1 \ (\omega^0_1)$
	$\frac{1}{\sqrt{2}}(u\bar{s} \pm \bar{s}u)$	$K^+ \ (K^{*+})$
	$\frac{1}{\sqrt{2}}(d\bar{s} \pm \bar{s}d)$	$K^0 \ (K^{*0})$
	$-\frac{1}{\sqrt{2}}(s\bar{d} \pm \bar{d}s)$	$\bar{K}^0 \ (\bar{K}^{*0})$
	$-\frac{1}{\sqrt{2}}(s\bar{u} \pm \bar{u}s)$	$K^- \ (K^{*-})$

‡ depending on ± sign

Table 1.2 Meson wave-functions with the explicit identification of the transformation properties under the $SU(3) \times SU(2)_{spin}$ subgroup of SU(6). Here, the subscripts "s" and "a" label interchange symmetry/antisymmetry under the respective $SU(3)_F$ ($SU(2)_S$) groups. φ (χ) is an SU(3) (SU(2)) wave-function. The non-zero charge states may be labelled by a G-parity: $G = Ci\tau_2$, with C= charge-conjugation. In particular, $G = C(-1)^I$, where I= total isospin. See Close [1980].

baryon composed of quarks with L=1 and S=1/2 or 3/2 yields

$$(^2\underset{\sim}{1}\,,\ ^4\underset{\sim}{8}\,,\ ^2\underset{\sim}{8}\,,\ ^2\underset{\sim}{10}) \qquad (1\cdot2)$$

$$\Rightarrow J^P = \left(\tfrac{1}{2}^-,\ \tfrac{3}{2}^-;\ \tfrac{1}{2}^-,\ \tfrac{3}{2}^-,\ \tfrac{5}{2}^-;\ \tfrac{1}{2}^-,\ \tfrac{3}{2}^-;\ \tfrac{1}{2}^-,\ \tfrac{3}{2}^-\right)$$

and we note that all of these have been observed [Close 1980]. Of course, for mesons and baryons, the L=0 states lie lowest in mass (see table 1 again).

Actually describing in detail all the aspects of the Quark Model would lead us somewhat beyond the direction of this chapter, but we may at least name the successes of the scheme before turning to its more obvious failings. Besides the qualitative explanation of the hadronic spectroscopy, the Quark Model is notable for its understanding and predictions on, e.g., electromagnetic interactions; quark excitations and radiative transitions; and calculations of magnetic moments [Bechi and Morpurgo 1965a,b, Morpurgo 1965, Copley et al 1969a,b, and also Okubo 1962, 1963]. Mostly one calculates in a non-relativistic approximation by "sandwiching" appropriate operators between hadronic wave-functions.

There are a number of theoretical and experimental results which were conclusive in finding the Quark Model, though a useful guide, to be inadequate. We can summarise (some) of the evidence as follows.

(a)According to the Pauli Exclusion Principle, three quarks in S-wave, e.g., the Δ^{++} (L=0,S=3/2), cannot occur. That is, the wave-function must be overall anti-symmetric but such a configuration is manifestly symmetric. Only if there is an additional degree of freedom in the wave-function can this result be avoided. The interaction theory which provides this additional degree of freedom will, as we

shall see, be that of $SU(3)_C$, the "colour" theory.

(b)The Adler-Bell-Jackiw theorem [Adler 1969, Bell and Jackiw 1969] tells us that the calculation of the process $\pi^0 \rightarrow 2\gamma$ proceeds by coupling two vector (γ) and one axial vector (π^0) current to a quark loop. By summing over all the quarks appearing in the loop, the i-th quark coupling with strength e_i^2 to the two vector fields and f_i^2 to the axial vector, then the resulting amplitude is proportional to [Close 1980]

$$\sum_{\substack{u,d \\ \text{quarks}}} f_3^2 e^2 = \frac{n_c}{2}\left(\frac{4}{9} - \frac{1}{9}\right) = \frac{n_c}{6} \qquad (1.3)$$

where the factor of $n_c=3$ meets the experimental requirements. This triangle graph appears in discussions on chiral symmetry breaking in the theory of the strong interactions. The anomaly, as it is called, arises from the inability to preserve a γ_5 symmetry in regularised and renormalised QFT (see later) unless there are sufficient quarks (and leptons) with appropriate charges, in the triangle, to sum to zero.

(c) e^+e^- annihilation shows that [Close 1980]

$$\frac{e^+e^- \rightarrow \text{hadrons}}{e^+e^- \rightarrow \mu^+\mu^-} = \sum_i e_i^2 = \frac{2n_c}{3} \qquad (1.4)$$

and again experiment requires that $n_c=3$.

(d) Other evidence involves e.g., semi-leptonic decays of charmed mesons [Brandelik et al 1977], or the Drell-Yan process ($p\bar{p} \rightarrow \mu^+\mu^-$) [Drell and Yan 1971, Drell et al 1970], which together with the result of deep inelastic scattering (scaling of the cross section in the regime of high energy and momentum transfer, i.e., $p^2 \rightarrow \infty$) [Bjorken 1967, 1969] all imply the inclusion of another degree of

freedom for the quark, q^a, a=1,2,3, the source of the "colour interaction".

We will investigate below the construction of the interaction theory based on a quark flavour-independant gauge theory whose aim is to generalise this Quark Model to a fully relativistic QFT. Let us first consider, as a simpler model based on the group U(1) ("phase" symmetry), the case of QED.

1.3 Abelian and Non-Abelian Gauge Theories: Construction

In this section our starting point will be the equations of motion for a complex (i.e., two real components) scalar field φ. These are [Ramond 1981, Itzykson and Zuber 1980, Cheng and Li 1984]

$$(\partial_\mu \partial^\mu - m^2)\,\phi(x) = 0 \qquad (1.5)$$

Using the Lagrangian formalism of dynamics this is derivable from a Lagrange density

$$\mathcal{L} = -(\partial_\mu \phi)^\dagger(\partial^\mu \phi) - \tfrac{1}{2} m^2 \phi^\dagger \phi \qquad (1.6)$$

$$\phi^\dagger = (\phi^*)^T$$

Suppose now that we are interested in building a theory to describe (electromagnetically) charged scalars. Firstly, it is reasonable to include a kinetic term for the photon (otherwise it is not a dynamical quantity) and this is

$$\mathcal{L} = -\tfrac{1}{4} F_{\mu\nu} F^{\mu\nu} \qquad (1.7)$$
$$F_{\mu\nu} = \partial_\mu A_\nu - \partial_\nu A_\mu$$

Regarding the total Lagrangian as composed of (1.6) and (1.7) it is evident that it will only be invariant under the following local transformations

$$A_\mu(x) \rightarrow A'_\mu(x') = A_\mu(x) - \partial_\mu \chi(x)$$
$$\phi(x) \rightarrow \phi'(x') = e^{i\chi(x)} \phi(x) \qquad (1.8)$$

if, and only if, we redefine the derivative

$$(\partial_\mu \phi)(x) \longrightarrow (\mathcal{D}_\mu \phi)(x) \qquad (1.9)$$
$$\mathcal{D}_\mu \equiv \partial_\mu - ig A_\mu$$

with g the gauge coupling constant. From the behaviour under the U(1) transformation of the scalar φ, we see the origin of the "phase" symmetry. The generalised derivative operator $\mathcal{D}(x)$ is called the covariant derivative (c.f. that in General Relativity). Thus the introduction of local symmetry transformations for the scalar field imply the appearance of "compensating" gauge fields A_μ.

The extension of this U(1) model to a more general non-abelian problem is complicated by the algebra of the group generators. For a general non-abelian symmetry group the generators obey commutation relations [Cheng and Li 1984]

$$[t_a, t_b] = f_{ab}{}^c t_c \qquad (1.10)$$

with $f_{ab}{}^c$ the (anti-symmetric) structure constants of that group. One associates with each of the generators a gauge field. So that, under local group transformations, parameterised by $\omega^a(x)$

$$A_\mu(x) \longrightarrow A_\mu'(x) = U A_\mu U^{-1} - i U \partial_\mu U^{-1} \qquad (1.11)$$
$$U(x) = \exp\{ i \omega^a(x) t^a \}$$

such that for matter (e.g., fermion) fields

$$(\mathcal{D}_\mu \psi)^a(x) = (U^a{}_b(x))(\mathcal{D}^b{}_c \psi^c)(x) \qquad (1.12)$$

$$\mathcal{D}_\mu = \partial_\mu - i A_\mu{}^a t^a$$

In particular, we note that

$$\delta A_\mu(x) = -(\mathcal{D}_\mu{}^a \omega^a)(x) \qquad (1.13)$$

with ω^a in the adjoint representation of the group (like the gauge fields themselves).

The analogue of the Electromagnetic field strength tensor (the connection 2-form [Cheng and Li 1984]) is the curvature

$$F_{\mu\nu} = -\frac{i}{g}[\mathcal{D}_\mu, \mathcal{D}_\nu] = \partial_\mu A_\nu - \partial_\nu A_\mu + ig[A_\mu, A_\nu]$$

$$\delta F_{\mu\nu}{}^a = f^a{}_{bc} F_{\mu\nu}{}^b \omega^c \qquad (1.14)$$

This obeys the Bianchi identities [Ramond 1981]

$$\mathcal{D}_\mu \tilde{F}_{\mu\nu} = 0 \quad ; \quad \tilde{F}_{\mu\nu} = \frac{1}{2} \varepsilon_{\mu\nu\lambda\sigma} F^{\lambda\sigma} \qquad (1.15)$$

with $\tilde{F}_{\mu\nu}$ the dual tensor.

The Yang-Mills [1954] equations of motion in the presence of a covariant source J_μ are [Ramond 1981]

$$\mathcal{D}_\mu F_{\mu\nu} = J_\nu \qquad (1.16)$$

and the action functional reads [Ramond 1981, Cheng and Li 1984, Itzykson and Zuber 1980]

$$S_{YM} = -\frac{1}{2g^2} \int d^4x \, F_{\mu\nu}{}^a F^{\mu\nu a} \qquad (1.17)$$

Quantum Chromodynamics (QCD) has this structure, with the specified gauge group $SU(3)_C$. The quark fields carry the fundamental representation and the gauge fields, the gluons, are in the adjoint representation (as we have already seen). For completeness, the quarks therefore are written as

$$q^a = \{ u^a, d^a, s^a, c^a, \ldots \} \qquad a = 1, 2, 3 \qquad (1.18)$$

and the commutator in SU(3) is

$$\left[\frac{\lambda_i}{2}, \frac{\lambda_j}{2} \right] = i f_{ij}{}^k \left(\frac{\lambda_k}{2} \right) \qquad (1.19)$$

One can "unpack" the condensed information in (1.17) to find three and four "leg" self-interactions. Note that it is the non-zero "colour charge" of the gluons that makes Yang-Mills (YM) theory a more complex problem than QED, where only one fermion-photon vertex occurs.

For the given set of f quarks, mass m_f, colour label a, the Lagrangian reads

$$\mathcal{L}_{QCD} = i \bar{q}^{af} \gamma_\mu D_\mu^{ab} q^{bf} - m_f \bar{q}^{af} q^{af} - \frac{1}{4} F_{\mu\nu}{}^a F^{\mu\nu a} \qquad (1.20)$$

The presentation here is completely general; any other non-abelian theory has precisely the same form. For example, by introducing additional scalar fields (see later on the role of scalar, Higgs, fields in discussions of gauge symmetry breaking) carrying some representation of the group we can easily write down the Lagrangian for the prototype unified theory, viz, the Electroweak theory devised through the combined efforts of Glashow [1961], Salam [1968], and Weinberg [1967] (for an introductory review on this topic see, for example, Aitchison and Hey, [1983], Aitchison [1983]). In contrast to QCD, the

Electroweak theory incorporates the spontaneous breakdown of an SU(2)xU(1) gauge group to the electromagnetic $U(1)_{EM}$ subgroup. The vacuum state does not share the symmetry of the Electroweak Lagrangian; the Higgs fields (introduced by Higgs [1964a,b, 1966], see also Englert and Brout [1964]) adopting a non-vanishing expectation value in the vacuum state.

1.4 The Perturbative Approach to a Quantum Field Theory

Our aim in this section is to outline the path-integral method of QFT and to emphasise the similarity (see also chapter 2) with the methods of statistical mechanics. What is relevant here is the connection between the green functions of the QFT and the correlation functions of the SM system. We will not consider the application of the resulting perturbation expansion in any depth, but only to such an extent that it illustrates those features that are vital in determining its validity as an approximation to the original path integral.

From elementary quantum mechanics, in terms of independant position and momentum operators Q, P respectively, the Heisenberg and Schrodinger "pictures" of quantum mechanics are related by [Amit 1984, Cheng and Li 1984, Ramond 1981, also see Dirac 1933, Feynman 1948, Schwinger 1951]

$$Q_H(t)\,|q\rangle = q\,|q\rangle \;;\; Q_S\,|q,t\rangle = q\,|q,t\rangle \qquad (1\cdot 21)$$
$$Q_H(t) = e^{iHt}\,Q_S\,e^{-iHt}$$

The Hamiltonian, H, is the operator for translations in time. Thus the Schwinger function, which determines the time development of a state can be written [Amit 1984]

$$F(q',t';q,t) = \langle q' | \exp\{iH(t'-t)\} | q \rangle \qquad (1.22)$$

To evaluate this expression, we divide the finite time interval into infinitesimal elements, ε, where $n\varepsilon = t'-t$, such that [Cheng and Li 1984, Ramond 1981]

$$F = \int dq_1 \cdots dq_n \{ \langle q', t' | q_n, t_n \rangle \langle q_n, t_n | q_{n-1}, t_{n-1} \rangle \cdots \langle q_1, t_1 | q, t \rangle \} \qquad (1.23)$$

Then it can be shown by expanding (1.22) [Amit 1984]

$$F = \int \frac{\mathcal{D}p\,\mathcal{D}q}{2\pi} \exp\left\{ i \int_t^{t'} (p\dot{q} - H(p,q))\, dt \right\} \qquad (1.24)$$

$$p = \frac{\partial \mathcal{L}}{\partial(\partial q/\partial t)} \; ; \quad \int \mathcal{D}p = \int \prod_{i=1}^{n} dp_i \; ; \quad \int \mathcal{D}q = \int \prod_{i=1}^{n} dq_i$$

where the sum is over all p,q such that $q(t)=q'$, $q(t)=q$.

For H quadratic in the momenta, we find, using the Fresnel integral that [Amit 1984]

$$F = \lim_{n\to\infty} \int \prod_i \frac{dq_i}{\mathcal{N}} \exp\left\{ i\varepsilon \sum_{j=1}^{n+1} \left[\frac{1}{2}\dot{q}_j^2 - V\left(\frac{q_j + q_{j+1}}{2}\right) \right] \right\} \qquad (1.25)$$

$$= \int \frac{\mathcal{D}q}{\mathcal{N}} \exp\left\{ i \int_t^{t'} \mathcal{L}\left(q, \frac{\partial q}{\partial t}\right) dt \right\}$$

where V is some specified potential function and $\mathcal{N}$ a constant. The fundamental quantities of interest, the green functions, are defined by [Amit 1984, Ramond 1981]

$$\langle q', t' | T\{q(t_1) \cdots q(t_n)\} | q, t \rangle = \int \frac{\mathcal{D}p\,\mathcal{D}q}{2\pi} q(t_1) \cdots q(t_n) \exp\left\{ i \int_t^{t'} \mathcal{L}\, dt \right\} \qquad (1.26)$$

i.e., as time ordered products of fields. They can be generated from the path integral by the inclusion of a source term in the Lagrangian. One replaces the boundary conditions $q(t')=q'$, $q(t)=q$, by $J(t)=0$ for $t>T$ or $t<-T$.

In terms of the Schwinger function, the generating functional is defined [Amit 1984]

$$Z\{J\} \propto {}_S\langle 0, +\infty \mid 0, -\infty \rangle_S \tag{1.27}$$

for Schrodinger basis states. This follows from

$$Z\{J\} \propto \lim_{t' \to \infty} \lim_{t \to -\infty} {}_S\langle q', t' \mid q, t \rangle_S \tag{1.28}$$

and the application of the appropriate boundary condition. One notes that in these asymptotic limits, the assumption is that the system tends to free particle states, i.e., plane wave solutions with some well defined ground state energy E_0.

The field theoretic expression for the generating functional, in terms of the field $\varphi(x,t)$ is

$$Z\{J\} = \frac{1}{N} \int \mathcal{D}\phi(x,t) \exp\left\{ i \int_t^{t'} \left[\mathcal{L}(\phi) + J\phi(x,t) \right] dt \right\} \tag{1.29}$$

with N a normalisation constant in the absence of the source. The green functions are then the moments of fields defined by

$$\left. \frac{\delta^n Z\{J\}}{\delta J(t_1) \ldots \delta J(t_n)} \right|_{J=0} \propto i^n \langle 0, +\infty \mid T\{\phi(t_1) \ldots \phi(t_n)\} \mid 0, -\infty \rangle \tag{1.30}$$

Perturbation theory involves recasting the Lagrangian as [Amit 1984]

$$\mathcal{L} = \mathcal{L}^0(\phi) + \mathcal{L}^{INT}(\phi) \tag{1.31}$$

where $\mathcal{L}^0$ is typically quadratic in the fields (i.e., a Gaussian integral). So, for a given theory, e.g., a $\phi^4(x)$ self-interaction, one can write

$$Z\{J\} = \exp\left[i \int d^4x \, \mathcal{L}^{INT}\left(-i \frac{\delta}{\delta J(x)} \right) \right] Z^0\{J\} \tag{1.32}$$

where

$$Z^{\circ}\{J\} = \int \mathcal{D}\phi \exp\left\{ i \int d^4x \left[\mathcal{L}^{\circ}(\phi) + J\phi + \tfrac{1}{2} i\epsilon\phi^2 \right] \right\} \tag{1.33}$$

The last term being inserted to provide convergence (damping possible oscillations in Minkowski space) for large times. In terms of the Feynman propagator $\Delta_F(x-y)$ (the matrix inverse of the Klein-Gordon operator)

$$\mathcal{L}^{\circ} = \tfrac{1}{2}\left(\partial_\mu \phi \, \partial^\mu \phi - m^2 \phi^2 \right) \tag{1.34}$$

$$Z^{\circ}\{J\} \propto \exp\left\{ \tfrac{i}{2} \int d^4x \int d^4y \, J(x) \Delta_F(x-y) J(y) \right\}$$

In extending these ideas to gauge theories, one encounters a critical problem. To quantise a gauge theory one introduces a complete set of initial value variables which obey the commutation relations (and for all time) [Lee 1975]. Because one can always make a gauge transformation vanishing at time zero, it is not possible to find that complete set unless we remove the gauge invariance by a constraint. We can illustrate how this is accomplished, in a heuristic fashion, as follows. The "gauge-fixing" finds a place in the path integral by the addition of a term (see later) [Cheng and Li 1984, Ramond 1981]

$$\exp\left\{ -\tfrac{i}{2} \int d^4x \, C^2(x) \right\} \tag{1.35}$$

with C some gauge non-invariant function of A_μ. It then becomes necessary to redefine the measure into gauge non-equivalent $\bar{A}_\mu$, such that the integration over gauge equivalent classes is factored out as a (harmless) multiplicative constant. Thus we seek

$$Z = \int \mathcal{D}A_\mu(x) \exp\left\{ i \int \mathcal{L} \, d^4x \right\} \tag{1.36}$$

$$\longrightarrow \int d\Lambda \int d\bar{A}_\mu(x) \exp\left\{ i \int \left(\mathcal{L} - \tfrac{C^2}{2} \right) d^4x \right\}$$

To be correct as it stands, this expression must be made independant of the choice of C(x), i.e., under gauge transformations. Under the change of variables, the measure contains the usual determinant factor, which, for the purpose of maintaining a local action, is recast as an integral over fermionic scalar fields [Faddeev and Popov 1967, Faddev and Slavnov 1980]. This Faddeev-Popov "ghost" factor [Faddeev and Popov 1967, Faddeev and Slavnov 1980], is interpreted, in a perturbation expansion, as an additional interaction for matter fields (one adds source terms for these "ghosts", but none appear as external particles).

The limitations of the perturbation theory are suggested by the fact that it is an expansion in powers of the coupling constant g. For QED at low energies, this is no problem as $\alpha=e^2/4\pi\approx1/137$. For the strong interactions, where $g^2 \geqslant 1$ at the hadronic scale, no finite set of terms in the expansion is likely to be useful. Only by exploiting the complete theory as represented by Z{J} can meaningful results be expected. As an asymptotic series, one really requires that the perturbation expansion be re-summable (by e.g., Borel summation techniques) and possess a small coupling constant. In QCD neither criterion is satisfied (we discuss this further in section 1.5).

There is however one aspect of the complete theory that is revealed, at least in part, by the perturbation series, that known as the renormalisation group (RG) equations. The RG equations represent a set of transformations between different renormalisations of the bare theory [Amit 1984]. A brief word of explanation of these terms is relevant here.

In actually evaluating Feynman diagrams, large momentum, UV divergences are endemic in the integrations. To define the finite, physical, parts of the parameters one must first regularise the integrals by, e.g., an explicit integral cut-off, Λ, or perhaps continuing analytically in the number of dimensions until convergence is assured [t'Hooft and Veltman 1972] One then sets some renormalisation conditions [Amit 1984, Cheng and Li 1984] such as requiring that the two point vertex function (the matrix inverse of the two point connected green function, see below) equals the renormalised mass at zero momentum

$$\Gamma^{(2)}(p) = p^2 + m^2 \equiv m_R^2 \quad \text{for } p^2 \equiv 0 \tag{1.37}$$

Typically there are a number of conditions that must be set simultaneously for all the parameters appearing in the Lagrangian. Then one subtracts off the divergent pieces, order by order in the expansion, so that the divergences remain only to the next order in the expansion. To show that this is possible to all orders is a complicated problem and one should refer, for example, to t'Hooft and Veltman [1972] (also see t'Hooft [1971a, b], Itzykson and Zuber [1980], Lee and Zinn-Justin [1972, 1973]) for more on this.

The requirements for any theory to be renormalisable are succinctly summarised by: (i) there exists a finite number of primitively divergent pieces, i.e., divergent graphs which do not contain divergent sub-graphs; (ii) a finite number of counter-terms are found, of the same form as bare terms appearing in the Lagrangian. A further necessary condition is that only dimensionless (or positive mass dimension) coupling constants are allowed.

Assuming that this process can be carried out, one will then have a definite relationship between the bare and

renormalised parameters. We can express this for the vertex functions (that sufficient subset of all green functions from which one can reconstruct all possible Feynman graphs) as [Amit 1984]

$$\Gamma_R^{(n)}(p_i ; g_i(\lambda), \lambda) = Z_\phi^{n/2} \Gamma_{bare}^{(n)}(p_i ; g, \Lambda) \qquad (1.38)$$

here, λ is the momentum scale at which the renormalisation takes place and Λ is the cut-off in the integration ($\Lambda \to \infty$). The RG equations convey the fact that the bare theory is independant of [Amit 1984] λ, i.e.,

$$\left(\lambda \frac{\partial}{\partial \lambda}\right)\Big|_{g,\Lambda} \left\{ Z_\phi^{-n/2} \Gamma_R^{(n)}(p_i ; g_i(\lambda), \lambda) \right\} = 0 \qquad (1.39)$$

This "β function" tells us how the coupling $g(\lambda)$ varies with the momentum scale, i.e., differing renormalisations of the bare theory. In particular, one can develop flow diagrams in the coupling constant space (i.e., if there is more than one) to determine the domains of attraction. A fixed point of the theory is a g^* such that $\beta(g^*)=0$. The fundamental result of such an analysis is that only non-abelian gauge theories are asymptotically free, i.e., $g^*=0$ is the stable fixed point in the limit that $\Lambda \to \infty$ [Gross and Wilcek 1973a,b, Politzer 1973, Zee 1973, Coleman and Gross 1973]. One sees that in this region, perturbation theory is valid. One hopes to obtain information on the full theory, to a certain extent, by following the flows of the coupling constant. Of course, a RG equation constructed from the perturbation series only has validity to the order in the expansion that one works to, but we should bear in mind that, at least, it serves as an approximation to the full RG equation [Amit 1984]. To give some substance to these points, let us investigate the RG equation for SU(N) gauge theory. To the order of two loops in the expansion, the β

function is calculated to be (including n_f quark fields in the fundamental representation) [Gross 1975]

$$\beta(g) = -\left(\frac{N}{16\pi^2}\right)\left[\frac{11}{3} - \frac{2n_f}{3}\right]g^3 - \left(\frac{N}{16\pi^2}\right)^2\left[\frac{34}{3} - \frac{(23N^2-3)n_f}{3N^3}\right]g^5 \quad (1.40)$$

A universal property of the theory is displayed by the fact that higher order terms in this expression are renormalisation-scheme dependant [Gross 1975]. By integrating (1.40), one deduces the feature of asymptotic freedom, where perturbation theory is valid, and the growing coupling in the infra-red regime, where it is not.

It is, however, precisely in the IR region of the theory that the properties of the hadronic spectrum are revealed, particularly the necessary confinement of colour charges and the resulting colour singlet bound state spectrum. Of further relevance, both within any Quark Model classification scheme and the full interacting theory, are the dynamical implications of global chiral symmetry breaking. This is the symmetry $SU(2)_V \times SU(2)_A$ of vector and axial vector quark currents appearing in the quark Lagrangian with the pion as the (approximate) Goldstone boson (see below and also chapter 2).

The physical applicability of any NAGT within perturbation theory will be in doubt in the IR regime due to soft (i.e., low energy, low momentum exchange) gluon production. Gluons are coloured and so can, in principle, construct infinite tree diagrams. There will be, inevitably, propagator singularities as $p^2 \to 0$ [Gross 1975, see also Bjorken and Drell 1964, 1965 for the resolution of this in QED].

To be able to handle these problems, e.g., by showing that non-perturbative effects remove these doubts, is imperative in establishing unbroken non-abelian gauge symmetries as relevant in the physical world. One can see that the growth of the coupling constant in the IR region of the theory may provide the escape that we need. Confinement itself should be sufficient to avoid these problems. What is required is a formalism, with appropriate calculational techniques, that lead us beyond weak coupling perturbation theory. To emphasise this point, in the next section we discuss some physical phenomena that specifically result from the different phase structures of physical theories and are not at all revealed by the perturbation theory.

1.5 The Phase Structure of Non-Abelian Gauge Theories

The definition of what constitutes the vacuum state of a QFT, or lowest energy state of a many-body system to use the SM analogy, is far from being a trivial point. From perturbation theory one might expect it to be the state with vanishing field excitation. It is worth emphasising, however, that there are instances where the possibility of <u>different</u> phases present in physical theories are describable within a perturbation theory. A simple example would be the ground state of a ferromagnetic system. This ordered state spontaneously breaks the rotational invariance of the Hamiltonian. Spontaneous symmetry breaking of such global symmetries was first investigated by Goldstone [1961] and Goldstone et al [1962] where it was demonstrated that the symmetry breaking is accompanied by the production of a massless spin zero boson.

When one considers the implications of spontaneous symmetry breaking in local field theories, the most relevant example is the Electroweak theory (which we touched on earlier). Note that for both global and local symmetries, the fact that the ground state of the system does not share the symmetry of the Lagrangian has to be supplied, as it were, by "hand", in that perturbation theory constructed around the "wrong" phase (i.e., the unstable symmetric state below the symmetry breaking scale) produces incorrect conclusions.

In pure NAGT, in general, there are more subtle effects connected with global aspects of the theory which imply that the naive vacuum is not the true vacuum. There is a rich structure of field configurations with non-vanishing (anti-) self dual solutions, the instantons, as the lowest energy (lowest action) states [Ramond 1981]. These instantons can be considered as "interpolating" or "tunneling" between the lowest action solutions [Belavin et al 1975, Coleman 1977, t'Hooft 1976, Jackiw and Rebbi 1976a, b]. We say that they are non-perturbative field configurations, in fact, they represent the effect of the inclusion of topological constraints on the local field theory. The key point is that results from a perturbative expansion are not reliable and do not capture all the "physics" that is there.

As a simple quantum mechanical analogy, we might consider a periodic, e.g., cosine, potential of some operator x. Within perturbation theory the expectation value $\langle x \rangle \neq 0$. Classically the ground state of the "system" must involve x in only one of the minima. Since we know that (quantum mechanically) the field can tunnel between wells, $\langle x \rangle$ is not so easily defined. In fact $\langle x \rangle = 0$ for the double well

potential (if the well is symmetric). In general we describe tunneling between n minima in the periodic potential via Bloch waves $e^{i\theta n}$. For an SU(N) gauge theory, where the tunneling between minima of the action is associated with instantons, we define a "winding number", n, analogously (the basic consideration is one of homotopy; see, for example, Cheng and Li [1984]). It takes the form [Belavin et al 1975]

$$n = \frac{1}{16\pi^2} \int d^4x \, Tr \left\{ \tilde{F}_{\mu\nu} F^{\mu\nu} \right\} \tag{1.41}$$

One can show that [Cheng and Li 1984]

$$n \propto \int_S d\sigma_\mu K^\mu \tag{1.42}$$

$$K_\mu = 4 \varepsilon_{\mu\nu\lambda\sigma} Tr \left[A_\nu \partial_\lambda A_\sigma + \tfrac{2}{3} A_\nu A_\lambda A_\sigma \right]$$

where S is the surface at infinity. If A_μ is pure gauge, i.e.,

$$A_\mu = U^{-1}(x) \partial_\mu U(x) \quad ; x \to \infty \tag{1.43}$$

then, for a gauge transformation $U = e^{i\tau\hat{\omega}\hat{\omega}}$

$$K_\mu = \frac{4}{3} \varepsilon_{\mu\nu\lambda\rho} Tr \left[(U^+ \partial_\nu U)(U^+ \partial_\lambda U)(U^+ \partial_\rho U) \right] \tag{1.44}$$

The Euclidean Yang-Mills action (1.17) is minimised for (anti-) self dual $F_{\mu\nu}$ and it can be shown that $S(A) = 8\pi^2 n/g^2$ [Coleman 1977, Cheng and Li 1984, Ramond 1981], with n the winding number. These finite action solutions are the instantons. It is important to remember that each minimum in the action represents inequivalent sectors of the perturbation theory, the perturbation expansion around any one will therefore not "see" that around any other [Cheng and Li 1984]. Also one finds explicitly that because these solutions contribute substantially to the path integral, the perturbation expansion cannot contain all the important aspects of the YM theory. Turning now to the

interpretation as tunneling amplitudes between different vacuua, we can understand this in terms of vacuua n,m from [Cheng and Li 1984]

$$\langle n|e^{-Ht}|m\rangle \propto \int \mathcal{D}A_\mu(x)\, e^{-S(A)} \qquad (1.45)$$

As such it is clear that the "true" θ vacuum state (the analogue of the statement in the quantum mechanical example that $\langle\varphi\rangle=0$) will be some linear superposition of all these n vaccuua, i.e.,

$$|\theta\rangle = \sum_m e^{-im\theta}|m\rangle \qquad (1.46)$$

In general NAGT the θ-term has the significance of labelling different Hilbert spaces of these field configurations, whilst in the specific case of QCD, the θ vacuum was necessary to explain the mass of the η meson [Glashow 1967, Kogut and Susskind 1975, Sutherland 1966]. Essentially, for a theory of two massless quarks, the (global) flavour symmetry possessed by the Lagrangian is $SU(2)_L xSU(2)_R xU(1)_V xU(1)_A$, and is spontaneously broken by the inclusion of non-zero quark masses to $SU(2)xU(1)_V$. The realisation, in the Goldstone mode, of the chiral SU(2) breakdown is the pion isotriplet (see Gell-Mann and Levy [1962], Dashen [1969]). The expectation would be that an isosinglet meson, approximately degenerate in mass with the pion, representing the $U(1)_A$ symmetry breakdown should be produced. The only possible meson suitable for identification with this Goldstone boson is the η. However, it is simply too massive, $m_\eta \approx 4m_\pi$ [Particle Data Group 1982]. We can illustrate how the θ-vacuum resolves this problem as follows. For N_f massless quarks, the divergence of the axial current is [Schierholz 1984 and references therein]

$$\partial_\mu j^\mu{}_5 = \frac{N_f}{32\pi^2} \mathrm{Tr}\, \tilde{F}_{\mu\nu a} F^{\mu\nu a} \equiv N_f q_t \qquad (1.47)$$

which leads to [Schierholz 1984]

$$m_s^2 = \lim_{n_c \to \infty} m_{ns}^2 + \frac{4N_f}{f_{ns}^2} \chi_t \qquad (1.48)$$

(m_s (m_{ns}) are the flavour singlet (non-singlet) pseudoscalar mesons; f_{ns} is the decay constant) where

$$\chi_t = \frac{1}{V} \langle Q^2 \rangle \quad ; \quad Q = \int_V d^4x\, q_t(x) \qquad (1.49)$$

Since q_t is a total divergence,

$$q_t = \frac{1}{16\pi^2} \partial_\mu \varepsilon_{\mu\nu\rho\sigma} \mathrm{Tr}\left[A_\nu \left(F_{\rho\sigma} - \tfrac{2}{3} A_\rho A_\sigma\right)\right] \qquad (1.50)$$

then $Q=0$, $m_s = m_{ns} = 0$ unless there are topologically non-trivial gauge field configurations. This is, of course, true for SU(N), i.e., eqn (1.43) and thus one has $m_\eta > m_\pi$. Finally, the value of χ_t is estimated by current algebra relations [Scheirholz 1984]

$$\chi_t = \frac{f_\pi^2}{4N_f} \left(m_l^2 + m_{l'}^2 - 2m_k^2\right) \underset{N_c=3}{=} (180\ \mathrm{MeV})^4 \qquad (1.51)$$

In general, instantons have been central in understanding quark and gluon condensates [Shifman et al 1979, Shuryak 1982a, b]. One might have hoped that QCD perturbation theory had some relevance at scales well short of the confinement length $(150)^{-1}$ MeV, but investigations have shown that the typical instanton "size" is more of the order of $(600)^{-1}$ MeV, and is instrumental, for example, in understanding how QCD Sum-Rule (chapter 3) calculations of hadronic properties are effective [Shifman et al 1979]. Notably though, the presence of light quarks tend to

suppress the instanton fluctuations of the pure gauge system, so the picture is not yet entirely clear [Shuryak 1982a, b].

The appearance of complex phenomena in the QCD vacuum whether at large or small g^2 means that we really do require a true non-perturbative calculus. In chapter 2 we take up this point and present a lattice discretisation of the QCD vacuum, developing a Monte-Carlo calculation designed to simulate quark and gluon dynamics. With this formalism one can demonstrate that the non-perturbative properties of QCD are in the direction we expect and are thus vitally important in any discussions on the QCD mass spectrum that we present in chapters 4 and 5.

CHAPTER 2

The Lattice Formulation of QCD

2.1 Introduction

In chapter 1, we developed the formalism of $SU(3)_c$ gauge theory in order to calculate processes in the theory of quark interactions, QCD. Investigating some aspects of the structure of QCD, amongst those of other non-abelian gauge theories, NAGT, we were led to question the applicability of "traditional", i.e., perturbative methods to what is essentially a strong coupling problem. In addition, one would like to understand such properties of the hadronic world as dynamical mass generation, confinement, chiral symmetry breaking in the quark Lagrangian, and the role and extent of topology in influencing these.

What we require is a method which supercedes as many of the problems associated with perturbation theory, as is possible, and, in view of the expected importance of non-perturbative phenomena in QCD [Shuryak 1982; Callen, Dashen and Gross 1979; Shifman, Vainshtein and Zahkarov 1979a,b; Berg and Luscher 1981; Luscher 1982], "samples" effectively all the important field configurations. As such a method, the lattice formulation of gauge theories, which we will consider now in some depth, provides an increasingly important method of analysis.

We will introduce the hypercubic regularisation of a (general) gauge theory, with the identification of the continuum limit (lattice spacing, $a \to 0$) of the pure gauge system. Some of those main features of QCD, the mass gap, string tension, confinement and de-confinement transition will be discussed with a view to confirming, or otherwise, their place in SU(3) gauge theory as revealed by the lattice calculation. The analogy with the statistical

mechanical system will be emphasised when we describe the main method of investigation, that of a Monte-Carlo simulation in a computer memory. Once having reviewed the status of the pure gauge models, we will be in a better position to introduce lattice formulations of the Dirac action, and to describe some of the problems that one is unable to avoid in any such transcription.

For the most part in this chapter, our emphasis will be on establishing the practicality and efficacy of the lattice Monte-Carlo method and the provision of computational tools that will be required for the investigation of "exotic" mesons in QCD (in chapters 4 and 5).

2.2 Definition of a Lattice Regularised Gauge Theory

As we recall from chapter 1, any quantum field theory requires a regularisation procedure (before renormalisation) in order that one may eventually extract the physically relevant components of the theory. The lattice formulation is no more than such a regularisation [Wilson 1974; Kogut 1979, 1983; Kadanoff 1977]. It has become increasingly common to employ a hypercubic lattice, although some investigation of the properties of gauge theories on other, e.g., random and simplicial lattices has been attempted [Christ, Friedberg and Lee 1982]. The advantage of the hypercube is in its conceptual simplicity; one may readily investigate (as we shall have occasion to do in chapter 5) its symmetry properties [Mandula, Zweig and Govaerts 1983; Baake, Gemundes and Oedingen 1982, 1983; Verstegen 1984], and the mounting of models in computer code, is probably more straightforward. One should be aware that in principle any lattice formulation, just as with different versions of the continuum gauge action, should lead to the same universal properties of QCD.

We have some expectation then that there is no lack of generality in specialising to the hypercube.

The gauge field connection resides on the links of our hypercubic lattice, emanating from the site n, in the direction μ (Figure 1). We require

$$U_\mu(n) = \exp\left[i B_\mu(n) \right] \; ; \; B_\mu(n) = \frac{a}{2} t^a A_\mu^a(n) \; ; \; U_{-\mu}(n+\mu) = U_\mu^{-1}(n) \tag{2.1}$$

as our definition of the gauge link variable $U_\mu(n)$, τ_a are the SU(3) group generators and $A_\mu^a(n)$ the gauge fields. The last statement of (2.1) follows on the grounds of consistency (Figure 1). At each of the lattice points we associate "matter" field variables such as scalars and fermions, with a colour frame of reference, i.e., co-ordinate axes in an internal symmetry space (Figure 1) [Kogut 1983]. Local gauge invariance, which is maintained unviolated on the lattice (in distinction to full Lorentz invariance, which is only a property of the continuum limit of the theory) asserts that the relative orientation of these colour frames of reference is irrelevant. The arbitrary gauge transformation matrices that impose this are given by

$$G(\chi(n)) = \exp\left[-\frac{ia}{2} \tau^a \chi^a(n) \right] \tag{2.2}$$

in terms of the parameter ("angle") χ(n). Thus relevant gauge actions will be gauge invariant if and only if under

$$U_\mu(n) \xrightarrow{G} G(n) U_\mu(n) G^{-1}(n+\mu) \tag{2.3}$$

they remain unchanged.

Let us pause for a moment to see how the lattice represents an acceptable regularisation of a QFT. Firstly, the non-zero lattice spacing is the analogue of an

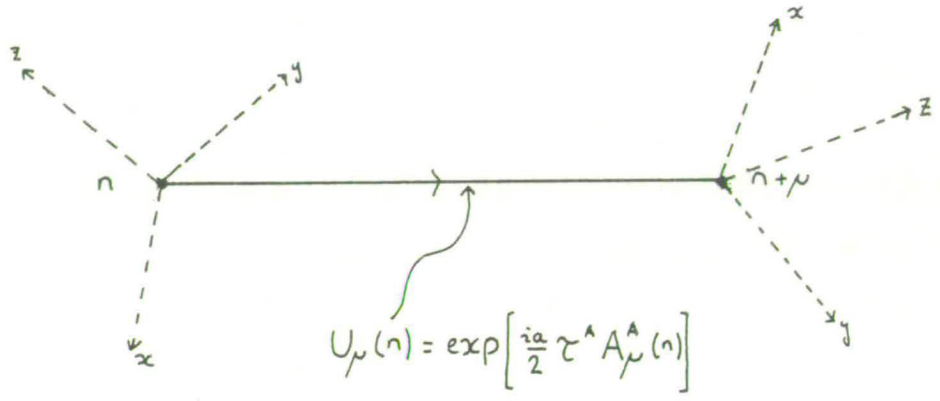

Figure 2.1 The definition of the gauge link variable $U_\mu(n)$. The "co-ordinate axes" demonstrate, in a schematic fashion, the role of $U_\mu(n)$ in "rotating" the colour frame of reference between lattice sites, i.e., imposing the local gauge invariance.

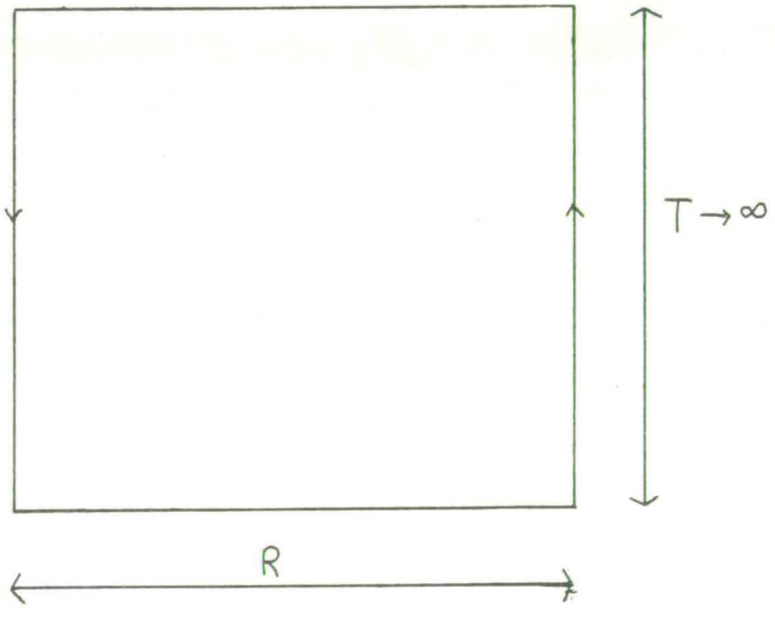

Figure 2.2 The world line of a (heavy) $q\bar{q}$ pair, seperated adiabatically at T=0 to a distance R, held there for a time $T \to \infty$, and then allowed to annihilate.

ultra-violet regulator (in any loop momentum integral) in the continuum theory. One must specify some procedure for letting $a \to 0$ that holds fixed any physical quantities, (as we shall show) [Wilson 1974]. In such a limit, we expect to recover all the symmetries of the continuum theory we are modelling [Lang and Rebbi 1982]. The second point is that no gauge fixing term is required in the gauge action. In any finite number of link variables stored in the computer memory, one cannot find that infinite multiplicative factor arising from the redundant integration over all gauge orbits, thus there is no explicit need to introduce a gauge choice [Wilson 1974].

One can develop the strong interplay between the lattice gauge theory, LGT, and the statistical mechanics, SM, of, for example, a ferromagnetic system. When one works in Euclidean space, i.e., performing a "Wick rotation" $t \to -i\tau$ in the definition of the functional integral, the analogy is much stronger.

Considered as a SM ensemble, one would map out the phases of the system, e.g., the presence of quark confining or Coulombic phases. In order to be able to do this we have to be able to express some function of the link variables that represent the gauge action embodied in the lattice.

For a theory which maintains strict gauge invariance, it is clear from (2.3) that this must involve products of links around closed paths. The simplest such choice, using the smallest squares, or "plaquettes", is due to Wilson [1974], and is

$$S_W = -\frac{1}{2g^2} \sum_{n,\mu,\nu} Tr \left\{ U_\mu(n) U_\nu(n+\mu) U_{-\mu}(n+\mu+\nu) U_{-\nu}(n+\nu) + h.c. \right\} \qquad (2.4)$$

This must of course reduce in the continuum limit to the conventional Yang Mills action

To show this one expands the fields $B_\mu(n)$ in a long wavelength (slowly varying as $a \to 0$) approximation [Kogut 1983, Creutz 1980]. Thus

$$U_\Box(n) = U_\mu(n)\,U_\nu(n+\mu)\,U_{-\mu}(n+\mu+\nu)\,U_{-\nu}(n+\nu) + h.c.$$
$$\simeq e^{iB_\mu}\, e^{i(B_\nu + a\partial_\mu B_\nu)}\, e^{-i(B_\mu + a\partial_\nu B_\mu)}\, e^{-iB_\nu} + h.c. \qquad (2.5)$$

By means of the Baker-Hausdorff inequality one can show

$$U_\Box \simeq \exp\{ia^2 g F_{\mu\nu}(n)\}\;;\; F_{\mu\nu}(n) = \partial_\mu A_\nu(n) - \partial_\nu A_\mu(n) + ig[A_\mu, A_\nu] \qquad (2.6)$$

Using the properties under the trace of SU(3) matrices it is then found

$$S \simeq -\frac{1}{2g^2}\int \frac{d^4x}{a^4}\,\frac{a^4 g^2}{2}\,(F_{\mu\nu}a^2)^2 + \mathcal{O}(a^2) \qquad (2.7)$$

[Yang and Mills 1954; Itzykson and Zuber 1980]. We shall see later how one might improve the agreement with the continuum limit of the theory to higher order in a.

Our first use of this action will be to establish the strong and weak coupling phases of the theory, hoping to give early indication that the model does reproduce some of the expected features of QCD.

To demonstrate strong coupling we imagine taking two colour sources q and $\bar{q}$, in principle infinitely massive, and seperating them adiabatically to a distance R and restraining them there for a time T ($T \to \infty$), then we let them come together and annihilate [Fischler 1977; Susskind 1976; Kogut 1983]. The world lines described by such a pair is shown in figure 2. The process is described by the

amplitude between initial and final states in the presence of the Euclidean Hamiltonian H. Thus, [Kogut 1983]

$$\langle i | e^{-H(R,T)T} | f \rangle = \frac{1}{Z} \int \mathcal{D}A_\mu \exp\left\{ -S + ig \int d^4x A_\mu J^\mu \right\}$$

$$J_\mu^a(x) = \frac{1}{2} \tau^a \text{ on contour } C \qquad (2.8)$$

One realises that with the identification of $|i\rangle$ and $|f\rangle$ and the independance of H from t,

$$e^{-V(R)} \langle i | f \rangle \Rightarrow V(R) = \lim_{T \to \infty} -\frac{1}{T} \ln \left\langle \mathrm{Tr} \left\{ P \left(\frac{ig}{2} \oint_C A_\mu^a \tau^a dx_\mu \right) \right\} \right\rangle \qquad (2.9)$$

for path-ordered products P. Note that this expectation value is also that of the Wilson loop variable [Wilson 1974; Creutz 1980; Pietarinen 1981; Bhanot and Rebbi 1981; Stack 1983], c.f., the plaquette operator, $U_\square$, introduced earlier.

$$\langle U_\square \rangle = \left\langle \prod_C U_\mu(n) \right\rangle = \left\langle P \left\{ \exp\left[\frac{ig}{2} \oint_C A^a \tau^a dx \right] \right\} \right\rangle \qquad (2.10)$$

It is possible to evaluate (2.10) when g^2 is large (strong coupling). One expands

$$e^{-S(U)} = \prod_C e^{-\beta \mathrm{Tr} U_\square} \quad ; \quad \beta = 1/g^2 \qquad (2.11)$$

and by virtue of the properties of integration over the group space [Kogut 1983], the leading order term is given by "tiling" the contour C with plaquette variables. Moreover, every power of U's is accompanied by a power of g^{-2}. Thus, to leading order,

$$\left\langle \prod_C U_\mu(n) \right\rangle \approx \left(\frac{1}{3g^2} \right)^{N_C} = \exp\left(-(\ln g^2) RT \right) \qquad (2.12)$$

where $N_C = RT$, gives us an "area" law behaviour. Evidentally, given that V(R) is as above (2.9), then

$$V(R) = \sigma R \qquad (2.13a)$$

$$\sigma = \ln g^2 + \ldots \qquad (2.136)$$

The area law is indicative of confinement, with a potential form that goes roughly linearly with the separation.

The exact form of V(R) depends on developing methods for handling the expansion of the action in inverse powers of g^2 (g large) and lies outside of the main line of our discussion [Kogut 1983, Munster 1981a, b].

One notes that in the strong coupling phase of the theory the Lorentz-rotational symmetry, i.e., O(4) is badly broken i.e., a is not in any sense, small. We claim that this symmetry is restored in the continuum limit, and we would like to be able to demonstrate that this "directional dependence" of, for example, physical masses, is not a surviving feature of the lattice theory. Lang and Rebbi [1982] have made some investigations of this problem and have shown that in the correct continuum limit of the model, one does indeed recover the full rotational symmetry. This will turn out to be an aspect of the weak coupling sector of the theory, which we now discuss.

From our knowledge of continuum renormalisation of QFT's, we recall that the definitions of the renormalised masses and couplings of the theory retain no dependence on the UV regulator, and that one is then free to let the regulator go to infinity. On the lattice, we make a similar claim and demonstrate it as follows. On dimensional grounds, a generic mass, m, must be such that

$$m = \frac{1}{a} f(g) \qquad (2.14)$$

where f(g) is some function of the bare coupling g^2. To define a renormalised mass means that, as $a \to 0$, $f(g) \to 0$

also, to hold m fixed. Therefore, as $a \to 0$, $g \to g^*$, where $f(g^*)=0$, i.e., a fixed point of the theory (chapter 1). What one notes is that such a <u>continuous</u> transition is a property of a second order phase transition with diverging correlation length ξ. That is, as $a \to 0$, the discrete nature of the lattice is lost and the space-time symmetries are restored, $\xi \to \infty$, or equivalently, the mass gap $M_G \sim \xi^{-1}$ of the theory vanishes. The fundamental result of QCD is that (asymptotic freedom, chapter 1) $g^*=0$ is the critical point [Gross and Wilcek 1973; Politzer 1973] and that in the region of $g \approx 0$, perturbation theory, perhaps renormalisation group improved, has some validity. We can use this fact, along with the unique requirement for renormalised quantities under a change in the length scale (cut-off) to determine the function f(g). We have

$$\left(a \frac{d}{da}\right) m = 0 \qquad (2.15)$$

and thus, using (2.14), find

$$f'(g) = -f(g)/\beta(g) \qquad (2.16)$$

with

$$\beta(g) = \left(a \frac{d}{da}\right) g(a) \qquad (2.17)$$

the usual β function of chapter 1 [Itzykson and Zuber 1980; Ramond 1981] There we noted that the β function was scheme-independant in its first two terms, i.e., [Gross 1975]

$$\beta(g) = -\beta_0 g^3 - \beta_1 g^5 \quad ; \quad \beta_0 = \frac{11}{3}\left[\frac{3}{16\pi^2}\right], \beta_1 = \frac{34}{3}\left[\frac{3}{16\pi^2}\right]^2 \qquad (2.18)$$

From (2.14) and (2.18) there follows

$$f(g) \propto (\beta_0 g^2)^{-\beta_1/2\beta_0^2} \exp\left[-\frac{\beta_0 g^2}{2}\right](1 + \mathcal{O}(g^2)) \qquad (2.19)$$

with the constant of proportionality, Λ_{latt}, defining the intrinsic scale of the theory such that, for example,

$$\sigma^{1/2} = c_\sigma \Lambda_{latt} \quad ; \quad M_a = c_a \Lambda_{latt} \qquad (2.20)$$

c_i = constants

Λ_{latt} has been related to other renormalisation schemes [Hasenfratz and Hasenfratz 1980; Dashen and Gross 1981] and

$$\Lambda_{mom}/\Lambda_{latt} = 83.5 \quad ; \quad \Lambda_{PV}/\Lambda_{latt} = 31.32 \qquad (2.21)$$

for SU(3). We will expect corrections to the right hand side of (2.19) if a is finite, estimated to be of order $a^2(\ln(a))^P$, P some power [Hasenfratz 1983].

Having seen the construction of a LGT and some of its more general properties, we now turn to the methods by which one can investigate numerically the space of possible configurations and the measurement of important observables. After discussing MC methods, we will describe what features are found in candidate (pure) gauge theories.

2.3 Monte Carlo Methods in Lattice Gauge Theories

Fundamentally, we are interested in the expectation values of observables O, defined in QFT (continued to Euclidean space) by [Creutz, Jacobs and Rebbi 1983]

$$\langle O \rangle = \frac{1}{Z} \int \mathcal{D}U \, O \, e^{-S(U)} \qquad (2.22)$$

Our aim is to "sample" this functional integral for those configurations which contribute most to the sum. In a finite, but reasonable (say 8^4) sample of links, trying to

evaluate (2.22) directly would be prohibitively expensive in computing time. One seeks to generate configurations of gauge fields U, such that the probability of encountering them in some stochastic sequence is proportional to their Boltzmann weight e^{-S} [Kogut 1983; Binder 1979]. Then we estimate the expectation value by averaging the observable over these N configurations, i.e.,

$$\langle O \rangle \simeq \frac{1}{N} \sum_i O(U_i) \qquad (2.23)$$

Evidently, one must specify some prescription which decides the transformation from one configuration to another. Let us write the probability of encountering a configuration U as $P_N(U)$ (i.e., after N steps of the sequence). Then, if $W(U \to U')$ is the transition probability for going from U to U', we see that [Kogut 1983; Binder 1979]

$$P_{N+1}(U) = \sum_{U'} W(U' \longrightarrow U) P_N(U') + \left(1 - \sum_{U'} W(U \to U')\right) P_N(U)$$

$$= P_N(U) + \sum_{U'} \left\{ P_N(U') W(U' \to U) - P_N(U) W(U \to U') \right\} \qquad (2.24)$$

If the system has reached equilibrium

$$\sum_{U'} P_N(U) W(U \to U') = \sum_{U'} P_N(U') W(U' \to U) \qquad (2.25)$$

i.e., $P_{N+1}(U) = P_N(U)$. One must have some measure by which it is meaningful to say that the system converges to equilibrium and that therefore, as required, $P_N(\text{stationary}) \alpha e^{-S}$. On this first point, we see that if

$$\frac{P_N(U_a)}{P_N(U_b)} > \frac{W(U_b \to U_a)}{W(U_a \to U_b)} \qquad (2.26)$$

then $P_{N+1}(U_a) < P_N(U_a)$ and $P_{N+1}(U_b) > P_N(U_b)$ and the system will tend to equilibrium [Kogut 1983].

There are two methods commonly employed to execute the second requirement, that of $P_n(\text{stationary}) \alpha e^{-S}$, the

Metropolis [Metropolis et al 1953] and the Heat Bath [Cabibbo and Marinari 1982; Creutz 1980] algorithms. Generally one will "step" (in some well defined way) through the lattice, vary one link at a time, and consider the change in the action resulting from this. On the basis of a choice in the way the link is chosen and then altered and what criteria the algorithm requires to be satisfied, the new link variable will either be accepted or rejected. In the Metropolis method [Metropolis et al 1953], one computes the change in the action for a new link variable selected in such a way that the group space can be reasonably well covered over the lattice sweep [Wilson 1979] (often one approximates continuous groups by their finite element sub-groups [Bhanot, Lang and Rebbi 1982]; this may be important if the group space is "large"). The new configuration is accepted if $\Delta S<0$, but is also accepted with conditional probability $\exp(-\Delta S)$ if $\Delta S>0$. This introduces quantum (thermal) fluctuations into the system on the basis of selecting a random number x, $0<x<1$ and accepting the new configuration if $\exp(-\Delta S)>x$.

The Heat Bath [Cabibbo and Marinari 1982] algorithm involves choosing the new link variable, U', with a probability

$$P(U') \propto e^{-S(U')}; \quad dP(U') = e^{-S(U')} dU' \qquad (2.27)$$

with all the other U's kept fixed. The difference between this and Metropolis amounts to repeating the latter an infinite number of times on each link [Kogut 1983]. Often one uses a "modified" Metropolis algorithm by repeating the procedure n times (most workers report some "optimal" value of n) on each link, in a sense interpolating between the two algorithms as we have described them.

Armed with a procedure to generate gauge configurations, (the work presented in chapters 4 and 5 will use the modified Metropolis method [Bowler et al 1983]) one can initiate a simulation with appropriate starting conditions. In principle, any starting conditions for the simulation would suffice, e.g., ordered U matrices ("cold" start), U matrices with random elements of the group space ("hot" start), or some combination of both [Creutz, Jacobs and Rebbi 1979a,b]. Unfortunately, the presence of metastable states in the space of configurations (see the discussion on phase structures below) can lead to inordinate time scales before equilibrium can be reached [Creutz et al 1979a,b]. Often some compromise is introduced, e.g., the "mixed" start, since the two other possibilities typically behave differently in the metastable region.

Inevitably, due to the finite size of the system and the choice of appropriate boundary conditions (normally periodic to try and avoid directly influencing the "interior" of the lattice volume), one will witness systematic discrepencies beyond the usual statistical errors. The latter, just by way of completeness behave as $\sim N^{-1/2}$ for N configurations. That is as a Poisson distribution for N different estimates, becoming Gaussian in the limit. These "finite size effects" will be relevant in later chapters.

2.4 Phase Structures of Abelian and Non-Abelian Gauge Theories

Abelian groups, e.g., U(1) or Z_n models, display confinement at strong coupling and a Coulombic (spin-wave) phase at weak coupling [Creutz et al 1979a; Lautrup and Nauenberg 1980; Creutz et al 1983; Guth 1980]. The detection of the phase transition separating these two regimes is obtained

by a simulation in which the coupling is varied over the configurations that are generated. One then observes hysteresis loops in the dependence of the Wilson loop expectation value on the coupling. This is characteristic of a system in which the diverging correlation length implies the impossibility of maintaining thermal equilibrium in any finite number of time steps over which one allows the system to propagate fluctuations. Of course, if there were a first order transition, then one would anticipate the appearance of metastability effects (i.e., two different stable states in the region of the transition [Creutz et al 1979a,b]) in such an investigation. In fact, the results are indicative of a continuous second order transition. It has also been shown that monopoles, defined in terms of closed colour loops [De Grand and Toussaint 1980, 1981; Tomboulis 1981; Halliday and Schwimmer 1981; Banks, Kogut and Susskind 1976], are not suppressed at small β (large g^2) and induce confinement of colour charges. Only when these loops are small (small g^2 and $a \to 0$) is their "macroscopic" size irrelevant to large scale order and disordering does not occur (one says that they "condense" at the phase transition). This shows indeed the relevance of topological effects in providing confinement [De Grand and Toussaint 1980, 1981; Kogut 1983; Mandelstam 1976; t'Hooft 1976].

In $SU(3)$, no phase transitions is expected in 4 dimensions and, indeed, none has yet been found in any simulation [Tomboulis 1982]. A particularly good way of illustrating this occurs in simulations based on finite-element subgroups [Bhanot and Rebbi 1981, Lisboa and Michael 1982; Rebbi 1980]. Then one does find a phase transition for some finite value of g^2. As the order of the subgroup increases, i.e., covering more and more of the continuous group space, the phase transition point is increasingly moved towards $g^2=0$. In the limit, one finds no

transition. One can compare this with the Z_n finite sub-groups of U(1). There, two critical regions are found, one of which moves off to infinity as $n \to \infty$, i.e., the full U(1) is used [Creutz et al 1983].

These results are typically obtained by using the Wilson form of the action [Wilson 1974]. Earlier in this chapter, we had occasion to comment on the desirability of obtaining universal features of continuum QCD. On the lattice, we might well expect that there will be artificial features, even spurious phase transitions, introduced by using different transcriptions of the Yang Mills action. A systematic analysis of the properties of as many actions as possible will help to reveal those properties of the lattice results that <u>are</u> universal. Much work has been directed at establishing the features of other lattice actions, such as that due to Manton, [1980] or the "Heat Kernel action" [Drouffe 1978; Menotti and Onofri 1981]. There are also (see later) more ambitious schemes designed to improve the lattice as an approximation to the continuum, e.g., the Symanzik "perturbatively improved action" approach [Symanzik 1982], and Monte-Carlo renormalisation group studies of the space of all possible couplings [Swendsen 1979, 1984]. As an example, we may note in passing that the groups SU(2) and SO(3) are locally isomorphic but differ in their global properties. Thus one might expect topological structures to play a role in the phase structures of the two models.

2.5 Non-perturbative Features of the Gauge system

We wish to investigate observables in the pure gauge models that directly arise from those aspects of QCD that are not quantifiable within the perturbation theory. In particular, we will look at the string tension, mass-gap,

and the deconfinement temperature. Having examined these in a quantitative fashion, we will extend the discussion to include those observables based on fermionic fields. This will then naturally lead us to a consideration of LGT calculations of the hadronic spectrum itself.

(A) The String Tension:

The potential of the heavy $q\bar{q}$ system was derived by measuring the expectation value of the Wilson loop and estimating the string tension, σ, from the fact that

$$V(I) = \sigma I = \lim_{J\to\infty} -\frac{1}{J} \ln \langle W(I,J) \rangle \qquad (2.28)$$

We should not be too surprised that there are corrections to this expression. Besides an "area law" dependence of the potential, the admission of quark self-energies and unphysical effects due to the plaquette corners, anticipates a more general parameterisation in terms of a "power series" in a. In considering this, Creutz [1980] constructed the operator

$$\chi(I,J) = -\ln\left(\frac{W(I,J)\,W(I-1,J-1)}{W(I,J-1)\,W(I-1,J)}\right) \qquad (2.29)$$

and with the form

$$V(I,J) = a\,IJ + b(I+J) + c \qquad (2.30)$$

we readily see that $\sigma=\chi(I,J)$. In fact, there are power-law corrections even to this [Hasenfratz 1983]. On dimensional grounds, $\sigma=C\Lambda_L^2$ (eqn (2.20)) and so, through the renormalisation group equation for SU(3), one finds $\sigma=f(g)^2/a^2$, a renormalisation group invariant. Monte Carlo experimental results were broadly supportive of the scaling curve (eqn (2.19)) behaviour for this [Creutz 1980] (though the $I\to\infty$ limit is not strictly possible: usually $I\geq 5$ or 6).

More recent, high statistics analysis [Barkai, Moriarty and Rebbi 1984, Otto and Stack 1984a, b] suggest, however, that this may be a premature conclusion for the range of β currently accessible. The early results however showed that as a function of g^2, one deduces a scaling "window", where (2.19) is obeyed, for SU(2) it is around $\beta=2/g^2\approx$ 2.3-2.5 [Bhanot and Rebbi 1981]. At strong coupling the measured result is as predicted earlier, whilst large β (small g^2) is compatible with the perturbation regime [Creutz et al 1983], where the loop sizes are smaller than the confinement scale (of the form $\sigma a^2\alpha$(constant)/β). From this, it has been deduced [Hasenfratz 1983; Bhanot and Rebbi 1981] that a=0.16 fermi (continuum $\sigma^{1/2}\approx$400 MeV), Λ_{latt}=(5.2±1.0) MeV. If 5-6 lattice spacings constitutes a rough assessment of the typical correlation length, then 0.6-0.8 fermi is consistent with observing the linear part in the potential (in scattering experiments) [Hasenfratz 1983].

One can also measure the rotational dependence of the heavy quark potential [Lang and Rebbi 1982] as suggested earlier and find that β=2.3-2.5 is here also the scaling region of SU(2). For completeness, the data for SU(3) itself finds [Creutz and Moriarty 1982; Hasenfratz 1983; see also Barkai, Moriarty and Rebbi 1984a, b]

$$\sigma = (2\cdot8 \pm 0\cdot4)\times10^{4}\Lambda^2 \;;\; \Lambda = 0\cdot0120\,\Lambda_{mom} \qquad (2\cdot31)$$
$$\beta = 5\cdot7 \rightarrow 6\cdot0$$

A final point here to note is that the relationship between σ, Λ_{latt}, and Λ_{mom} allows us to "fix the scale" of lattice gauge theory calculations, e.g., relate lattice and continuum masses. One may also, as we shall have occasion to do later, utilise physical particle masses, e.g., the ρ for this.

(B) The Mass-Gap

The mass-gap of the pure gauge theory (the scalar glueball; see chapters 3, 5) is a result of the lack of long-range forces within a confining theory [Kogut 1983; Creutz et al 1983]. Note that, in the absence of quarks, the lowest-lying excitation must be stable. To determine the numerical value of the mass-gap, we consider operators with the correct quantum numbers and measure their time-dependant correlations. Suppose O(t) is some suitable operator and

$$G(t) = \langle 0 | O(t)\, O^{\dagger}(0) | 0 \rangle - \langle 0 | O(0) | 0 \rangle^{2} \qquad (2.32)$$

the (connected) correlation function. To reveal the mass of this state, one inserts a complete set of energy eigenstates $|n\rangle$, so that

$$G(\underline{x}, t; \underline{x}', 0) = \sum_{n \neq 0} \langle 0 | O(\underline{x}) | n \rangle \langle n | O(\underline{x}') | 0 \rangle e^{\left[-E_n t - i\underline{p}\cdot(\underline{x}-\underline{x}')\right]} \qquad (2.33)$$

By summing over the spatial hyperplanes, i.e., projecting out the zero 3-momentum state, we define [Creutz et al 1983]

$$M_g(t) = -\ln \{ G(t)/G(t-1) \} \qquad (2.34)$$
$$G(t) = \sum_{\underline{x}} \sum_{n \neq 0} \langle n | 0 \rangle^{2} \exp\{-M_g t\}$$

with the explicit requirement that

$$M_g(\text{continuum}) = \lim_{t \to \infty} M_g(t) \qquad (2.35)$$

Evidently the scaling behaviour of m_g follows $m_g = C\Lambda_{latt}$ (with $a \sim \Lambda_{latt}^{-1}$).

In actually constructing appropriate operators, one employs the hypercubic symmetry group to select

combinations of Wilson loop operators in order to maximise the propagator signal. This will be discussed further in chapter 5, when some understanding of the hypercubic group will prove useful. However, it is generally found that correlations of operators over more than 3-4 time steps from the origin vanish into the statistical noise [Ishikawa, Schierholz and Teper 1982; Berg and Billoire 1982]. Moreover, at these short separations, power law corrections to (2.33) are important [Hasenfratz 1983], and so the exponential decay of the propagator may not be clear. In order to maximise the signal, one can apply a "variational method" to the set of eigenstates representing, for example, the 0^{++} operator [Berg and Billoire 1982]. That is, one seeks a upper bound on $M_g(t)$ through minimising the time-dependent log-ratios of the correlation function based on

$$O(t) = \sum_x \sum_i \alpha_i W^i(x,t) \qquad (2.36)$$

the $W_i(x,t)$ being different shapes of Wilson loops [Creutz et al 1983].

Results from this approach give reasonable (on statistical grounds) estimates even over 1-2 time steps [Berg and Billoire 1983; Ishikawa, Sato, Schierholz and Teper 1983; Michael and Teasdale 1983; de Forcand, Schierholz, Schneider and Teper 1985]. For SU(3),

$$M_g = M(0^{++}) = (280 \pm 50)\Lambda_{Latt} \qquad (2.37)$$

is a typical measurement [Berg and Billoire 1983]. Apart from the mass-gap itself, by combining operators in different representation of the hypercubic subgroup of O(4), one can construct glueball operators of different J^{PC}.

(C) The Deconfinement Temperature

Although a theory of confined quarks and gluons, QCD admits the possibility that, at sufficiently high temperature, the gluons (in the adjoint representation) can screen the colour charge of the quarks (fundamental representation) so that a quark-gluon plasma with essentially free quarks (asymptotic freedom) arises [Cabibbo and Parisi 1975; Shuryak 1980; Gross 1984; Polyakov 1978; Susskind 1979]. Recall that the free energy of a SM ensemble is given by

$$F = -T \ln Z_0 \qquad (k = 1) \tag{2.38}$$

with [Creutz et al 1983]

$$Z_0 = \int dx \langle x | e^{-\beta H} | x \rangle = \mathrm{Tr}\,(e^{-\beta H}) \tag{2.39}$$

One can write this as a path integral

$$Z_0 = \int_{\substack{\text{periodic} \\ \text{paths}}} \mathcal{D}\phi \; \exp\left\{ -\frac{1}{T} \int_0^{1/T} dt \int d^3x \, \mathcal{L}^0(\phi) \right\} ; \quad \phi(x, \tfrac{1}{T}) = \phi(x, 0) \tag{2.40}$$

In a lattice formulation, we make the identification that finite T effects (what we evidently require) are achieved by considering an infinite lattice in the 3-dimensional spatial directions but which is finite in the time (now temperature) direction [Gross 1984]. The temperature of the system (where Boltzmann's constant is set to unity), is given by [Gross 1984; Hasenfratz 1983] $t=(n_t a)^{-1}$, with n_t the number of lattice sites in the t-direction. It is clear from our earlier discussions on the heavy $q\bar{q}$ potential that the free energy change in the presence of a colour source is given by (2.38) with the operator

$$Tr\{P[\exp(ig\int_0^{1/T} A_0\,dt)]\} \qquad (2\cdot41)$$

inserted in the path integral [Creutz et al 1983].

We can now relate the deconfinement transition to a global symmetry violation in the QCD Lagrangian [Gross 1984; Hasenfratz 1983]. If one multiplies the U matrices, on any single hyperplane, which point in the t-direction only by an element of the centre of the group SU(3), $C_n=\exp(2\pi in/3)$, then, assuming that there are periodic boundary conditions in the t-direction, the action remains invariant. This is clearly true since any usual Wilson loops contain either zero or two oppositely aligned U matrices in the T-direction. However, the thermal Wilson loops, that is those operators that close upon themselves in the T-direction by virtue of the periodic boundary conditions are not invariant under the transformation. Thus W_t is an order parameter of the symmetry. If the symmetry is unbroken then

$$\langle W_t\rangle = z\langle W_t\rangle \Rightarrow \langle W_t\rangle = 0 \qquad (2\cdot42)$$

i.e., confinement. If

$$\langle W_t\rangle \neq 0 \qquad (2\cdot43)$$

then the charges must be screened. The deconfinement transition temperature has been estimated at [Kajantie et al 1981; Celik et al 1983; Hasenfratz 1983]

$$T_c = (76\pm1)\Lambda_{Latt} \qquad (2\cdot44)$$

In the presence of light quarks, the global symmetry is expected to be explicitly broken [Gross 1984]. The reason is connected with the "correct" boundary conditions on the quark fields. By analogy to rotating a charged fermion in

a magnetic field, in which the wave function changes sign, it has been suggested that anti-periodic boundary conditions are more natural for fermionic systems. This, of course, destroys any possibility of a global symmetry associated with the transition [Gross 1984]. It has been shown that the presence of a small m_q acts rather like a large external magnetic field in an Ising spin system, destroying the phase transition [Hasenfratz 1983; Gross 1984]. In the absence of a good order parameter, the existence of T_c in hadronic matter is still somewhat controversial [De Grand and De Tar 1983; Hasenfratz, Karsch and Stamatescu 1983].

2.6 Fermions in Lattice Gauge Theory

Now we must turn to the treatment of quarks and their interactions within LGT. In doing so, we will avoid discussing "ordinary" scalar matter for brevity. Some simple ways of handling the Dirac equation on the lattice will be presented and how some unavoidable problems (connected with chiral symmetry breaking) are encountered and treated. We will consider those points in some depth which refer most closely to the work of later chapters, especially those elements in the construction of mesonic lattice operators, and explicit calculations on the hadronic spectrum.

The fact that there are (at least) two ways of describing fermions on the lattice is most clearly illustrated by writing down a candidate action and considering the symmetries inherent in the prescription. We require a lattice (i.e., discrete) version of the Dirac action

$$S_F = \bar{\psi}(\not{\partial} + m)\psi \qquad (2.45)$$

where

$$\not{\partial}\psi = \gamma^\mu(\partial_\mu + igA_\mu)\psi \qquad (2.46)$$

in the usual way. The problem is the appearance of terms linear in the derivatives. To preserve the anti-hermiticity of the Dirac action, we choose the central difference transcription of the derivative operator [Kogut 1983]

$$\partial_\mu \psi(x) = \frac{1}{2a}\{\psi(x+\mu) - \psi(x-\mu)\} \qquad (2.47)$$

The unit cell on the lattice is now effectively 2a and for reasons we shall describe increases the number of fermion species from one (which we want) to 2^D, where D=dimensionality of the space.

Using this, let us consider the following representation of the fermion action [Kogut 1983; Karsten and Smit 1981]

$$S_F = a^4 \sum_n \Big\{ \sum_\mu \frac{1}{2a}\big(\bar{\psi}(n)\gamma_\mu U_\mu(n)\psi(n+\mu) - \bar{\psi}(n+\mu)\gamma_\mu U_\mu^\dagger(n)\psi(n)\big) + m\bar{\psi}(n)\psi(n)\Big\} \qquad (2.48)$$

In this expression, we have maintained gauge invariance by inserting U matrices in a covariant fashion. Note that the maximal global symmetry of this action is given , for n_f massless quarks as [Hasenfratz 1983; Kawamoto and Smit 1981]

$$SU(n_f)_V \times SU(n_f)_A \times U(1)_V \times U(1)_A \qquad (2.49)$$

This is where we encounter the doubling problem. Recall from chapter 1 that no quantum theory can preserve the axial symmetries [Adler 1969; Bell and Jackiw 1969; Karsten and Smit 1981]. For n_f=1, the divergence of the axial current contains a piece proportional to the "triangle"

graph, discussed in chapter 1 [Adler 1969]. In order to remove this anomaly, one must "add in" 2^D-1 other fermions in order that the total contribution to that graph is identically zero [Karsten and Smit 1981; Nielsen and Ninomiya 1981].

Conversely, by explicitly breaking the symmetries (chiral) of the axial currents, one <u>can</u> describe a single fermion species. There have been some attempts to circumvent this impasse by the use of non-local actions, but such approaches introduce problems of their own, e.g., relativistic non-covariance [Drell, Weinstein and Yankielowicz 1976a,b; Karsten and Smit 1978, 1979].

It is in this context that we see the appearance of different fermion lattice descriptions. Consider in 1+1 dimensions the energy momentum dispersion relations for the free Klein-Gordon and Dirac theories on the lattice. From the equations of motions it is readily found that

$$E_{ka}^2 = m^2 - \frac{2}{a^2}(\cos ka - 1) \; ; \; E_D = \pm \frac{\sin ka}{a} \qquad (2.50)$$

respectively [Kogut 1983]. The continuum limits of these yields, when $ka \ll 1$

$$E_{ka}^2 \simeq m^2 + k^2 + \mathcal{O}(k^4a^2) \; ; \; E_D \simeq \pm k + \mathcal{O}(k^3a^2) \qquad (2.51)$$

However, in the Dirac case, there is an additional fermion whose energy-momentum relation arises from $ka=\pi-k'a$, $k'a \ll 1$. In other words, there are two two-component spinors, degenerate in mass. One at the origin, and one at the edge of the Brillouin zone [Kogut 1983; Hasenfratz 1983].

The two methods commonly employed to break this degeneracy are Wilson's method [Wilson 1979], which relies on raising the energy at the zone boundary, and the Kogut-Susskind approach, K-S, [Kogut and Susskind 1975] which distributes the degrees of freedom of the 16 (in 4-d) fermions around the plaquette. In the latter, there remain only 4 degrees of freedom at each lattice site [Kawamoto and Smit 1981].

In Wilson's prescription, one has to give up completely the chiral symmetry, even for $m_q=0$. The K-S method retains, however, a remnant of the continuous chiral symmetry, as well as discrete γ_5 operations [Kogut 1983; Kluberg-Stern et al 1982]. We will be mainly interested in the Wilson formulation, as it forms the basis of our later calculations, but in describing the current state of lattice QCD it is relevant to comment on the K-S "staggered fermion" technique. The way that the Wilson form of the action elevates the masses at the edge of the Brillouin zone is by the introduction of a momentum dependent mass term, i,e.,

$$\frac{r}{2a}\sum_{n,\mu}\left\{\bar{\psi}(n)\psi(n+\mu)+\bar{\psi}(n+\mu)\psi(n)-2\bar{\psi}(n)\psi(n)\right\}a^4 \qquad (2\cdot52)$$

So that the full (free theory, for clarity) action then reads (on rescaling the fields) [Wilson 1977; Kogut 1983; Creutz et al 1983]

$$S_F=\sum_{n,\mu}\left\{\bar{\psi}(n)(r-\gamma_\mu)\psi(n+\mu)+\bar{\psi}(n+\mu)(r+\gamma_\mu)\psi(n)\right\}$$

$$+\sum_n (ma-8r)\bar{\psi}(n)\psi(n) \qquad (2\cdot53)$$

One solves for the propagator in momentum space (fourier representation of the inverse of the quadratic piece in the action) to find

$$G(p) = K\left[1 - K\sum_\mu \left\{(r+\gamma_\mu)e^{ip_\mu} + (r-\gamma_\mu)e^{-ip_\mu}\right\}\right]^{-1} \qquad (2.54)$$

$$K = (8r - ma)^{-1}$$

By investigating the parameter space of (m,r) we can see that m=r=0 implies

$$G(p) = \sum_\mu \gamma_\mu \sin p_\mu \Big/ \sum_\mu \sin^2 p_\mu \qquad (2.55)$$

i.e., 16 fermion flavours. For m=0, r≠0,

$$G(p) = \left[2\left(\sum_\mu \gamma_\mu \sin p_\mu\right) - 2r\left(\sum_\mu \cos p_\mu\right) + 8r\right]^{-1} \qquad (2.56)$$

with no remaining γ_5 symmetry (true for all r≠0). r=1 yields the continuum relativistic propagator (m=0) when K→ 1/8, i.e., $G(p) \sim p^{-1}$. K=1/8 is here the critical value of the hopping parameter, K_c, (from the fact that K enters in the term that propagates a quark from one site to the next).

In contrast to the Wilson formulation, the K-S approach does still observe some chiral symmetry for m=0. By way of completeness, but briefly, we note that there is a global phase rotation, independently at the even and odd sites of the lattice, $U(1)_e \times U(1)_o$ (there are additional discrete γ_5 operations) [Kluberg-Stern et al 1982; Kogut 1983]. This symmetry, when broken, will lead to the appearance of the Goldstone pion [Creutz et al 1983; Karsten and Smit 1981] since the usual current algebra expectation is that

$$\partial_\mu A_\mu^5 \propto m_\pi^2 \qquad (2.57)$$

The canonical transformation used in this approach reduces the effective number of flavours at each site to four by "spin-diagonalising" the fermion fields. We write [Kawamoto and Smit 1981; Karsten and Smit 1981]

$$\psi(n) = T(n)\chi(n) \; ; \quad \bar{\psi}(n) = \bar{\chi}(n)T^{\dagger}(n) \tag{2.58}$$

$$T(n) = (\gamma_1)^{n_1}(\gamma_2)^{n_2}(\gamma_3)^{n_3}(\gamma_4)^{n_4} \; ; \; n_\mu = (n_1, n_2, n_3, n_4)$$

By rescaling, the free Dirac action becomes

$$S_F^{KS} = \sum_{n,\mu} \left\{ \bar{\chi}(n)(-1)^{\phi}[\chi(n+\mu) - \chi(n-\mu)] \right\} + \sum_n \bar{\chi}(n)\chi(n) \tag{2.59}$$

where

$$(-1)^{\phi} = \begin{cases} (-1)^0 : & \mu = 1 \\ (-1)^{n_1} : & \mu = 2 \\ (-1)^{n_1+n_2} : & \mu = 3 \\ (-1)^{n_1+n_2+n_3} : & \mu = 4 \end{cases} \tag{2.60}$$

The interplay between the two methods in describing the hadron spectrum is an important test of the understanding of lattice fermions. Although we do not show it [see, for example, Bowler et al 1984], the K-S method allows simulations with much lower values of the quark mass (larger K), which is essentially a property of the techniques used to calculate the two different quark propagators. This is important, as it allows us to investigate more closely the region in which the full chiral symmetry and its spontaneous breakdown are observed. The mass spectra that are found with the two methods are not always consistent, but one has to be aware of the possibility of different renormalisations (following from the different transcriptions of the Dirac equation) of the bare quark mass. We noted that $K_c = 1/8$, for the free

Wilson case, but in the full interacting theory, K_c is necessarily renormalised. At strong coupling, $K_c \approx 1/4$, with intermediate couplings therefore somewhere between these limits [Hasenfratz 1983]. From its role in the action, an expansion of the quark propagator is essentially an expansion in powers of K. Finally, we recall that as $K \to K_c$, the mass of the lowest pseudoscalar excitation, the pion, goes to zero.

2.7 Calculational methods for the Quark Propagator

From our knowledge that QCD defines hadronic states to be colour singlet composite objects, we must find some method to calculate and combine quark propagators to obtain the mesonic and baryonic operators of interest. The expectation value of an operator is defined to be

$$\langle \theta \rangle = \frac{1}{Z} \int \prod_i \mathcal{D}\bar{\psi}_i \prod_j \mathcal{D}\psi_j \prod_{ij} \mathcal{D}U_{ij} \; \theta(U_{ij}; \bar{\psi}_i, \psi_j) e^{-S} \qquad (2.61)$$

with [Creutz et al 1983]

$$S = S_{gauge}(U) + \bar{\psi}(\not{\partial} + m)\psi \qquad (2.62)$$

in an obvious notation. The fermionic variables $\bar{\psi}, \psi$ obey a Grassmann algebra and so, except in 2-d where the positivity of the measure is guaranteed [Blanckenbeckler et al 1982], one cannot store the variables and phases in a computer memory. Fortunately, the fermionic action is quadratic, so we carry out the integration explicitly. Thus

$$\langle \theta \rangle = \frac{1}{Z} \int \prod \mathcal{D}U \; \langle \theta \rangle_U \det(\not{\partial} + m) e^{-S_g(U)} \qquad (2.63)$$

and now $\langle \theta \rangle_U$ is the expectation value of θ in the background gauge field. Evidently,

$$\langle \bar{\psi} \psi \rangle = \frac{1}{Z} \int \prod \mathcal{D}U \quad (\not{\phi}(U)+m)^{-1} \det(\not{\phi}(U)+m)\, e^{-S_G(U)} \qquad (2.64)$$

for the propagation of a quark in this gauge field. In this last expression, we can define

$$S_{eff} = S_G(U) - Tr\{ \ln(\not{\phi}(U)+m) \} \qquad (2.65)$$

where we understand the second term on the right hand side as the effect of including virtual quark loops on the (valence) quark propagator $(\not{\phi}+m)^{-1}$ [Creutz et al 1983; Hamber and Parisi 1981; Weingarten 1982]. In principle then, the evaluation of any expectation value is to be sought by using $S_{eff}(U)$, not $S_G(U)$ alone, and we must look for efficient ways to to determine $\Delta S_{eff}(U)$, induced by $U \rightarrow U'$. Although $\Delta S(U)$ is highly local, with only the nearest neighbour links affected by the change $U(n) \rightarrow U'(n)$, the expression $Tr(\ln(\not{\phi}+m))$ is highly non-local. For explanations of the various attempts to investigate this problem, one should refer to, for example, Fucito, Marinari, Parisi and Rebbi [1981]; Scalapino and Sugar [1981].

In all of the various approaches one must calculate the quark propagator G(n,0), derived from

$$[\not{\phi}(U)+m]\, G(n,0) = \delta_{n,0} \qquad (2.66)$$

The most widely used method for this involves some "relaxation" routine such as Jacobi, Gauss-Seidel [Weingarten 1982; Hamber and Parisi 1981; Marinari, Parisi and Rebbi 1981a], or Conjugate Gradient [Kogut et al 1982; Bowler et al 1984]. To outline the idea, we examine the simplest of these, that of the Jacobi method [Kogut 1983]. One considers the problem as one of matrix inversion, i.e., the solution to Mx=a. Then , in (real) computer time, we seek to solve

$$\frac{dx}{dt} = -[Mx(t)-b] = 0 \qquad (2.66)$$

by some iterative procedure. We can seperate the interaction part of M, by writing M=1-K, and then, if dt=ε is the computer "upgrading" time unit, then

$$x_{n+1} - x_n = -\varepsilon\left[(1-K)x_n - b\right] \qquad (2.67)$$

at the n-th time step. Thus [Kogut 1983]

$$x_{n+1} = \varepsilon b + (1 - \varepsilon + \varepsilon K)x_n \qquad (2.68)$$

One introduces a "source" or "seed" term x_0 at the space-time origin, and generates succesive approximations to the green function G(n,0). It is possible to increase the rapidity of convergence by adopting a Gauss-Seidel algorithm (obviously only if the largest eigenvalue of $1-\varepsilon-\varepsilon K$ is such that it is strictly less than 1). We label the matrix x_n, as $x_n(i)$, with i referring to a lattice site. Then we can evaluate $x_n(i+1)$ using $x_n(i=1,..,n)$, instead of $x_{n-1}(i=1,..,n)$ in (2.66) [Kogut 1983]. By "tuning" ε, one can optimise the whole process. The Conjugate Gradient method, a "steepest descent" approach, is faster still, particularly for K-S fermions [Bowler et al 1984], but as it is not employed in our later work, we will not consider it in any more detail.

With the unresolved problem of calculating the fermion determinant factor in the action, at the present time most groups have considered only the pure gauge action, i.e., ignoring internal fermion loops; the "quenched" or "valence" approximation [Weingarten 1982; Marinari, Parisi and Rebbi 1981b; Hamber and Parisi 1981]. That this may be a reasonable approximation follows from a number of considerations. We note that $(\det(\not{D}+m))$ appears with a power n_f, for the number of quark flavours present. In a perturbative expansion, each quark loop appears with a

counting factor n_f, and we see that $n_f \to 0$ suppresses such contributions. Additionally, each loop contains a 1/N (for SU(N)) factor, and large N expansions again suggest the suppression of these loops [Kawamoto and Smit 1981], relative to diagrams with internal gluons. One may also appeal to the phenomenological evidence which shows that the (naive) Quark model is relatively succesful (i.e., including only "valence" quarks) in, at least, the low-mass hadrons. Other arguments might include the effect of ignoring fermion flavours in the two-loop β function (~20% effect [Bowler et al 1984]) and the effectiveness of the OZI rule in suppressing quark annihilation diagrams [Close 1980].

2.8 The Hadron Spectrum: Combining the Quark Propagators

Bearing in mind that in the following chapters, we will concern ourselves with detailed calculations on some more "esoteric" states in the hadron spectrum, in this section we illustrate, in a general fashion, the methods of hadron mass measurement. Apart from defining the way in which the quark propagators are combined, we shall report on the findings in recent years of various groups on the spectrum of states itself.

Within the quenched approximation, one envisages the propagation of a meson (say) as in figure 3a. Obviously, we must exclude diagrams such as those of figure 3b which specify the propagation of flavour singlet mesons, but about which we are unable to say much. The problem essentially reflects the inability to calculate G(n,n) (c.f., fermion self-energy propagators, e.g., Amit [1984]), and the importance of fermion loops in the gluon propagator connecting the two quark propagators [Karsten and Smit 1981]. One has to accept, for the moment, the degeneracy

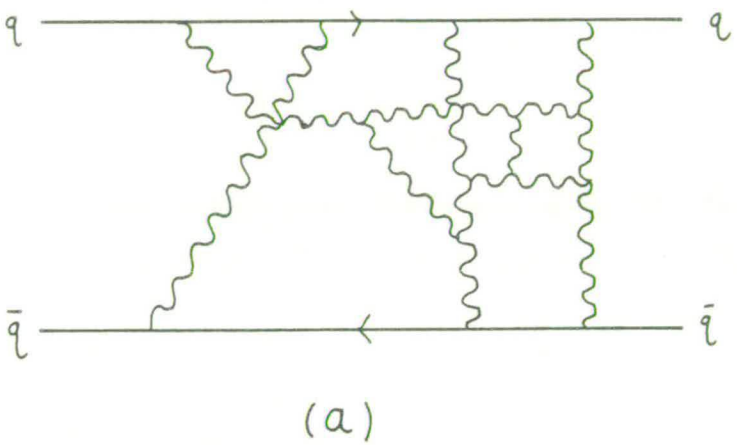

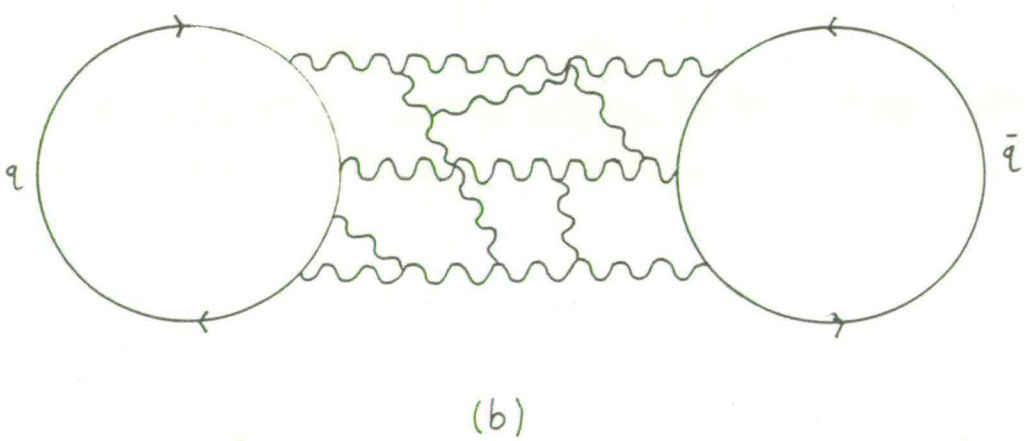

Figure 2.3 (a) A contribution, in the quenched approximation, to the propagation of a flavour non-singlet $q\bar{q}$ meson.

(b) A diagram contributing to a flavour singlet, e.g., η, meson. Ignoring (b) relative to (a) implies, for example, that the π and the η are degenerate in mass.

in mass resulting from this approximation. In addition to this, one typically works in the approximation of equal mass quarks.

The correlation function for a meson operator (consisting of two valence quarks) will be

$$\langle M(n) M^{\dagger}(0) \rangle = \frac{1}{Z} \int \mathcal{D}U \, \mathcal{D}\bar{\psi} \, \mathcal{D}\psi \; M(n) M^{\dagger}(0) \, e^{-S_G + \bar{\psi}(\not{D}+m)\psi} \tag{2.69}$$

The correct J^{PC} quantum numbers are specified by the inclusion of a suitable Dirac matrix Γ, so that

$$\langle M(n) M^{\dagger}(0) \rangle = \langle \bar{\psi}(n) \Gamma \psi(n) \; \bar{\psi}(0) \Gamma^{\dagger} \psi(0) \rangle \tag{2.70}$$

The expectation value then becomes

$$\frac{1}{Z} \int \mathcal{D}U \, \mathcal{D}\bar{\psi} \, \mathcal{D}\psi \; \bar{\psi}_{\alpha}(n) \, \Gamma_{\alpha\beta} \, \psi_{\beta}(n) \, \bar{\psi}_{\gamma}(0) \, \Gamma^{\dagger}_{\gamma\delta} \, \psi_{\delta}(0) \, e^{-S_G + \bar{\psi}(\not{D}+m)\psi} \tag{2.71}$$

This will simplify considerably in the quenched approximation (equal masses) to

$$\frac{1}{Z} \int \mathcal{D}U \, \mathrm{Tr} \left\{ \Gamma \, G(n,0) \, \Gamma^{\dagger} G(0,n) \right\} e^{-S_G} \tag{2.72}$$

Now it can be shown that

$$G^{ab}_{\alpha\beta}(0,n) = \gamma_5 \, G^{ba\,*}_{\beta\alpha}(n,0) \, \gamma_5 \tag{2.73}$$

and so

$$\langle M(n) M^{\dagger}(0) \rangle = \frac{1}{Z} \int \mathcal{D}U \, \mathrm{Tr} \left\{ \Gamma_A^{\dagger} G^{\dagger}(n,0) \Gamma_A \, G(n,0) \right\} e^{-S_G} \tag{2.74}$$

In terms of the colour and spinor labels, the trace reads explicitly

$$\mathrm{Tr} \left\{ \Gamma_A^{\dagger} G^{\dagger}(n,0) \Gamma_A \, G(n,0) \right\} = \sum_{\substack{a,b \\ \alpha,\beta}} \left(\Gamma_A \, G \right)^{ab}_{\alpha\beta} \left(\Gamma_A^{*} \, G^{*} \right)^{ba}_{\beta\alpha}$$

$$= \sum_{\substack{a,b \\ \alpha,\beta}} \sum_{\lambda,\nu} \Gamma^{A\dagger}_{\lambda\alpha} \Gamma^{A}_{\beta\nu} G^{ab}_{\lambda\beta}(n,0) G^{ab*}_{\alpha\nu}(n,0) \qquad (2.75)$$

In general, the quark green function contains both real and imaginary parts. The resulting correlation function is necessarily real and this follows from writing G=R+iF, and showing that if

$$\Gamma^{*A}_{\lambda\alpha} \Gamma^{A}_{\beta\nu} = \Gamma^{*A}_{\alpha\lambda} \Gamma^{A}_{\nu\beta} \qquad (2.76)$$

which must be true for all Γ^A, then the imaginary part vanishes identically.

As we saw earlier, the mass of the lowest interpolating state, in the channel specified by the Γ^A, is given by summing the propagator over the spatial hyperplanes, i.e.,

$$\sum_{n \neq n_4} \langle M(n) M^{\dagger}(0) \rangle \approx \sum_{\alpha} A_\alpha e^{-m_\alpha n_4} \qquad (2.77)$$

Then, as $t \to \infty$,

$$\sum_{n \neq n_4} \langle M(n) M^{\dagger}(0) \rangle \sim A_0 e^{-m_0 n_4} \qquad (2.78)$$

If the lattice is periodic in the t-direction, then the correct form of the large-t behaviour of the propagator is

$$A_0 \left(e^{-m_0 n_4} + e^{-m_0 (T-t)} \right) \qquad (2.79)$$

$nt = T$: where n = number of sites in t-direction

With the correct identification of the relevant operators, one now has a prescription for the measurement of hadron masses: (i) Generate pure gauge configurations according to some (e.g., Metropolis) algorithm; (ii) Calculate the quark green functions in this background gauge field by

some algorithm such as Gauss-Seidel; (iii) Evaluate the meson or baryon correlation functions on each of the configurations, in terms of matrix products of quark green functions; and (iv) average the propagator over all configurations and then sum over the spatial hyperplanes of the lattice.

By dividing up the set of generated configurations in some fashion ("binning" them), one can estimate the extent of the statistical errors in the averaged mass from measuring the masses within each block of configurations (quantifying the spread in the data). Of course, the preceding comments so far only refer to an analysis at one value of the quark mass (hopping parameter). The whole process may be repeated at various m_q and an extrapolation made to the critical quark mass region, where chiral symmetry is restored and spontaneously broken [Creutz et al 1983]. To estimate the position of m_c (K_c), one must extrapolate linearly in the pion mass squared (recall the current algebra prediction) [Karsten and Smit 1981]. One then increases $m_q=m-m_c$ (m=bare quark mass, that which appears in the Lagrangian) until agreement is reached on the splitting m_ϱ/m_π. In practice, however, one takes $m_\pi=0$ since m_π is so much smaller than the other hadronic masses that statistical noise masks the mass difference from zero. This allows one to fix the physical values of lattice masses by the input of the ϱ mass (or sometimes one uses the string tension [Hasenfratz 1983]; they must be related through their mutual dependance on the hadronic scale factor Λ_{latt}).

We describe in table 1, a distillation (by no means exhaustive) of results achieved in hadron mass calculations. One should particularly be aware of the results of Bowler et al [1984], on the grounds that the same gauge

	lattice spacing a (fm)	$m_\rho a$	$m_N a$	$m_\Delta a$	$m_\Delta a - m_N a$	m_N/m_ρ (expt ~1·20)	Comments
Fucito et al [1982]	0·139(11)	0·78(17)	1·14(18)	1·21(19)	0·07(37)	1·46(23)	$\beta = 6.0$; $5^3 \times 10$ Wilson; $r = 1$
Hamber and Parisi [1981]	0·176	0·71(9)	0·85(9)	1·16(9)	0·31(18)	1·20(20)	$\beta = 6.0$; $6^3 \times 10$ Wilson; $r = 1$
Weingarten [1983]	0·198(26)	0·61(15)	1·20(45)	1·49(38)	0·29(22)	1·97(88)	$\beta = 5.7$; $6^3 \times 14$ Wilson; $r = 1$
Bowler et al [1984]	0·136(8)	0·53(3)	1·11(10)	1·13(11)	0·02(1)	2·1(2)	$\beta = 5.7$; $8^3 \times 16$ Wilson; $r = 1$
Bowler et al [1984]	0·225(16)	0·88(6)	1·05(30)	-	-	1·19(33)	$\beta = 5.7$; $8^3 \times 16$ Susskind; $r = 0$
Lipps et al [1983]	0·094(6)	0·39(1)	0·60(2)	0·64(5)	0·04(11)	1·54(6)	$\beta = 6.0$; $10^3 \times 20$ Wilson; $r = 1$

Table 2.1 Collection of recent analyses of the hadron spectrum in QCD. Both Wilson and Kogut-Susskind actions and different lattice sizes are represented.

configurations and quark green functions are employed in our later work. Comparison with Bowler et al [1984] and others is therefore crucial in establishing confidence in the results of chapters 4 and 5. In this table, we have included, as indicated, work done on different sized lattices and occasionally different methods of calculating the green functions, etc.

In general, there are a number of considerations that may arise from these mass calculations. There are however essentially two points to be made here. One is understanding the limitations introduced through a finite lattice. Most workers are agreed that the pion is reasonably well exposed (at $\beta \approx 5.7-6.0$) on lattices (certainly) greater than 6^4. The glueball correlation length (string tension estimates in the scaling region) is typically 1-4 lattice spacings. The pion correlation length on 8^4 is $\sim$7-10 lattice units, even for unphysical, i.e., overly large, quark masses [Ishikawa, Teper and Schierholz 1982; Berg and Billoire 1982a,b; Bowler et al 1983]. The reduction in the quark mass matches an increasing lattice "path-length", in the sense of the hopping parameter expansion [Hasenfratz et al 1982], and one witnesses a slowing down in the convergence of algorithms for evaluating the quark propagator [Kogut 1983]. We have already commented on this effect in the comparison of Wilson's and the K-S methods of resolving the species doubling, but one should also be aware of the necessity of greater quark propagation distances for (at least some of the) heavier states, e.g., the ρ. There is a concommitant increase in (systematic) finite size effects from being unable to "probe" to these larger physical distances on fixed lattice volumes. At lower values of the hopping parameter the "graininess" of the lattice will also be more acute. One can think of this as sampling the meson wave function at

only a limited number of points in space-time. As the hopping parameter increases, the number of lattice sites, interior to the meson, also increases and gives one, in some sense, a better estimate of that wave function. Larger mesons, such as ϱ, δ, A, will require greater numbers of lattice sites to match the pion in terms of reliability. Evidently then, one would wish to investigate the spectrum on larger lattices. Computer memories capable of handling efficiently 16^4, and larger, are currently coming into use. It may be possible though, that better understanding of the properties of lattice actions themselves may allow more information to be extracted on the smaller lattices. This is the second point we make.

The Wilson form of the gauge action contains corrections of order a^2 to the Yang Mills continuum action [Kogut 1983]. For as long as a is non-zero, but still small, then perhaps the addition of more terms to the action that one simulates with may improve the agreement to higher order in a. This is the basis of the (Symanzik [1982]) perturbatively improved action programme. The other way to tailor the action is by the use of renormalisation group arguments. Suppose we added other terms to the Wilson gauge action carrying different representations of the gauge group [Bhanot and Creutz 1981] (recall the difference between SO(3) and SU(2) [Halliday and Schwimmer 1982]). In principle there is no limit to the numbers we add as long as in the continuum limit only the fundamental gauge action survives i.e., conventional Yang Mills theory. The fixed point in SU(3) gauge theory is $g^2=0$ ($\beta_f=\infty$). In the multiparameter coupling constant space of a lattice action, there will be a renormalised trajectory (dependent on the particular blocking scheme), starting at $\beta_f=\infty$, (the continuum theory) and flowing out into this space (the lattice regularised theory) [Swendsen 1979, 1984].

We may have hoped, though it is certainly not the case, that the usual Wilson action lay either on or close to this trajectory, and hence accurately reproduced continuum physics. An obvious improvement to the Wilson action would be made if we could find this trajectory, but unfortunately there is, as yet, no known calculation of this. Recently Swendsen [1984] has developed a method for using Monte Carlo techniques to improve our knowledge of this renormalised trajectory. The idea involves comparing "universal" quantities (e.g., ratios of hadron masses) on different size lattices. One attempts to adjust the definition of the lattice action on a smaller lattice and compare various expectation values with one that has resulted from a "blocking" of the dynamical variables on a larger lattice. By "blocking", we mean some combination (products) of the gauge fields on an n^D (e.g., 16^4) lattice that give rise to an action defined on an $(n/2)^D$ lattice. With some judicious choice of the blocking transformation, and a large enough coupling constant space, agreement between the two actions may perhaps be reached. Then more information can be extracted about the hadron spectrum on larger and larger lattices from simulations done on quite small lattices.

However, improvement is not necessarily guaranteed given that this trajectory is non-universal. In a multi-dimensional coupling constant space there will be many such paths, on the critical hypersurface, determined by the particular blocking scheme.

More pressing, in the light of recent evidence on the lack of scaling (i.e., (2.19)) observed for a number of measurables, e.g., the quark condensate [Barbour et al 1985], in the β region hitherto simulated in, is a re-assessment of the status of lattice QCD. In a sense, all these results demonstrate the improvements that have been made in lattice "technology". What remains is a clear need for a more systematic investigation of a range of

lattice sizes, actions and β values.

There is however some expectation that reliable quantitative analysis of the hadron spectrum through some optimisation of the Wilson r-parameter in conjunction with improvements in the lattice action may thus be possible, even without a full implementation of dynamical fermions, and with some remaining doubt over the "correct" value of β. This, however, represents a hope for the future. In the next few chapters, we shall systematically explore the spectrum of states that are not predicted within the quark model, but which arise solely from the nature of QCD itself, i.e., the propagation in free space of all colour singlet states. The simulations which have been performed do not include any of the sophisticated new techniques that are emerging, but we shall argue that the results that are obtained are reliable, particularly in comparison with other theoretical investigations.

CHAPTER 3

Multi-Quark and Hybrid Mesons in QCD

3.1 Introduction

In previous chapters the relationship between the quark model and QCD field theory (both manifested through the hadronic interaction) was not clearly spelt out. Ultimately one believes that the quark model is, in some sense, an approximation to the interacting field theory, but the fact that that connection may not be so transparent is readily demonstrated by the following consideration. In the quark model, one understands, for example, hard scattering processes (Drell-Yan, large p_T hadrons) more completely by introducing "intrinsic" p_T [Shuryak 1982] for constituent quarks ("partons" or "valons") typically of the order of 1 GeV, whereas, for example, the confinement scale is more of the order of 200 MeV. These constituent quarks are roughly additive in total scattering cross-section [Lipkin and Leck 1965; Levin and Frankfurt 1965; Nikolaev 1981], and are associated with some 350 MeV in energy. QCD, in contrast, deals with very light quarks (on that scale): $m_U \approx 5$ MeV, $m_D \approx 8$ MeV, $m_S \approx 150$ MeV, and which are treated as pointlike interacting objects. In other words, one has to be able to understand the way in which the features of the QCD field theory "conspire" to make the quark model a reasonable approximation in so many ways.

In this comparison, a particularly important area of investigation covers the role of "constituent glue" in the spectrum of states. We recall that the non-abelian gauge theory (NAGT) of QCD introduces gauge quanta, the gluons, in the adjoint representation of the group, to mediate the interaction processes. Like the quarks, they must be confined, but unlike the quark model, they can give rise to

a whole new range of hadronic states [Barnes, Close and de Viron 1983; Barnes, Close and Monaghan 1981,1982; Horn and Mandula 1978; Hasenfratz et al 1980; Balitsky, Dyakanov and Yung 1982; Jaffe 1977a,b; Jaffe and Johnson 1976; Donaghue and Johnson 1981; Barnes 1984; Chanowitz and Sharpe 1983]. The fundamental aspect of this spectrum is the appearance, at long distances (on the typical hadronic scale), of only colour singlet composite objects. With the colour degree of freedom at our disposal, there are many new combinations of quarks and glue, with no a priori mechanism for their suppression. Using the group theory of SU(3) let us construct some of these. Taking a quark, q^a, in the fundamental representation, $\underset{\sim}{3}$, of SU(3) (and $\bar{q}$ as a $\underset{\sim}{\bar{3}}$), we find

$$\begin{aligned} q \otimes q &= \underset{\sim}{3} \otimes \underset{\sim}{3} = \underset{\sim}{6} \oplus \underset{\sim}{\bar{3}} \\ q \otimes \bar{q} &= \underset{\sim}{3} \otimes \underset{\sim}{\bar{3}} = \underset{\sim}{1} \oplus \underset{\sim}{8} \\ \bar{q} \otimes \bar{q} &= \underset{\sim}{\bar{3}} \otimes \underset{\sim}{\bar{3}} = \underset{\sim}{\bar{6}} \oplus \underset{\sim}{3} \end{aligned} \qquad (3.1)$$

Now we realise that, for colour octet quark combinations and single gluons, $\underset{\sim}{8}\times\underset{\sim}{8}=\underset{\sim}{1}+\ldots$, so that states such as

$$\begin{aligned} q\bar{q}g &= (\underset{\sim}{1} \oplus \underset{\sim}{8}) \otimes \underset{\sim}{8} \; ; \; q^2\bar{q}^2 = (\underset{\sim}{6} \oplus \underset{\sim}{\bar{3}}) \otimes (\underset{\sim}{\bar{6}} \oplus \underset{\sim}{3}) \\ gg &= \underset{\sim}{8} \otimes \underset{\sim}{8} \; ; \; ggg = \underset{\sim}{8} \otimes \underset{\sim}{8} \otimes \underset{\sim}{8} \\ qqqg &= (\underset{\sim}{1} \oplus \underset{\sim}{8} \oplus \underset{\sim}{8} \oplus \underset{\sim}{10}) \otimes \underset{\sim}{8} \end{aligned} \qquad (3.2)$$

all have colour singlet contributions.

In this and the following two chapters, we shall explore extensively the spectrum of these states. Our considerations will involve a lattice QCD simulation of $q\bar{q}g$ and $q^2\bar{q}^2$ mesons to extract estimates for the masses of some low-spin states and a comparison with other calculations, more "analytic" in nature.

By way of nomenclature, $q\bar{q}g$ states are now commonly referred to as "hybrid" [Tarimoto 1982] mesons, although

the terms "hermaphrodite" [Barnes and Close 1982] and "meikton" [Chanowitz and Sharpe 1983] have also been applied. States composed solely of quarks (and anti-quarks) are generally called multi-quark, (where we will investigate only 4-quark, $q^2\bar{q}^2$, mesons), and those colour singlet objects containing pure glue are "glueballs" (see previous chapter on the mass-gap). We shall have little to say on the glueball sector. Much work has been directed at detailing the spectrum, and one is referred to, for example, Barnes [1984 and references therein] for a summary of their status in research and experiment. One must say at the outset that no conclusive proof of the existence of hybrid and multi-quark mesons has been given [Barnes 1984]. Partly, the problem is clouded by their mixing with "conventional" $q\bar{q}$ and q^3. It is, however, the possibility of the existence of (low-mass in particular) <u>exotic</u> states that make their identification unquestionable. Exotic, in this respect, means those mesons or baryons that have quantum numbers unobtainable within the naive quark model. We can demonstrate this for a $q\bar{q}$ system. Such a meson necessarily has a parity label $P=(-1)^{L+1}$ and a charge conjugation $C=(-1)^{L+S}$, where L=total orbital angular momentum and S=total intrinsic spin [Particle Data Group 1982]. Given this, one can easily see that 0^{+-}, 0^{--}, 1^{-+}, 2^{+-}, ... are not possible $q\bar{q}$ assignments. There are, as we have observed previously, such states in the spectrum of hybrid and 4-quark mesons. However, most of the possible states will be "crypto-exotic", that is non-$q\bar{q}$ mesons with "conventional" quantum numbers.

What will be demonstrated is that some of the exotic mesons, especially the 1^{-+}, can be expected to have masses which are not exceptionally high ($m(1^{-+}) \backsim 1-2$ GeV), and hence should be experimentally detectable [Barnes et al 1983; Chanowitz and Sharpe 1983; Jaffe 1977a]. Their existence

will not establish outright the veracity of QCD as the theory of the strong interaction but will give valuable information on the essential differences between the quark model approximation and any (correct) QFT approach.

By way of "setting the scale" for the spectrum, we can make a rough assessment on the basis of taking $\sim$350 MeV for constituent quarks and $\sim$500-700 MeV for constituent gluons [de Viron and Weyers 1981; Bernard 1982; Cornwall and Soni 1982; Parisi and Petronzio 1980]. The former is an estimate based on a "typical" $q\bar{q}$ meson mass of 700 MeV, and the latter follows from an analysis of the energy required to "break" a colour string. Evidently, we expect that $m(q\bar{q}g)\sim 1200-1400$ MeV and $m(q^2\bar{q}^2)\sim 1400$ MeV (all for u, d quarks: for s-quarks, add $\sim$ 150 MeV per s-quark).

In the absence of any firm experimental guidance on these states, we will review the major calculational schemes for resolving these additional spectra. This will give us scope to illustrate the extent to which predominantly analytic calculations can adequately cope with a strong coupling problem. Most of our discussion will focus on the MIT "Bag Model" and QCD "Sum Rules" methods. In both, one seeks a comprehensive parameterisation of the important non-perturbative features of QCD (see chapter 1). The two methods differ in the way that they approach this but share an attempt to perform a (first order) perturbative calculation in the strong coupling α_c to introduce spectroscopic "fine detail".

A more recent avenue of investigation involves deriving inequalities relating different operators that excite appropriate mesons out of the vacuum. In some respects (which we shall explain) this provides a useful ordering of the hadronic spectrum but it does not, however, produce

quantified mass estimates. It is however, particularly well suited to comparison with a lattice Monte-Carlo analysis, being based (usually) on a hypercubic lattice regularisation of QCD.

This computationally more simple method will be considered first, to provide some "benchmark" against which we can estimate the strengths of the other schemes. During the discussion on the QCD Sum-Rules and the MIT Bag Model, we will provide, where it might be instructive, some consideration of the general production and decay characteristics of the more interesting states. One should note that lattice studies of $q\bar{q}g$ and 4-quark mesons (any that is, already existing in the literature) has been deferred to later chapters, where, we feel, comparison with our work is more illuminating.

3.2 Mass Inequalities in Lattice-Regularised Gauge Theories

In discussing the formalism of operator inequalities, we will concentrate, for brevity, on those works which deal specifically with multi-quark and hybrid mesons [Goodyear 1984; Espriu, Gross and Wheater 1984]. In fact, no lack of generality in the method follows from this. Indeed, in these particular cases, more complicated operator inequalities are often needed (in comparison with "ordinary" hadrons [Weingarten 1983; Witten 1983; Nussinov 1984]) to extract relations between different meson propagators.

The main requirement of this approach is establishing the equivalence of operator and expectation value inequalities [Espriu et al 1984] through the positivity of the measure. Only gauge theories with no inherent CP violation are involved (no θ-term in the gauge action; fermion-anti-fermion-gauge couplings strictly real). Witten

[1983] deduced relations between (π^0, π^+) and also (A, ϱ) by employing different mass heavy quarks. However, he also had to consider the limiting case of letting the number of colours become large. It is technically simpler, and allows $N_c=3$, to consider only equal mass quarks since quark propagators then share the same form (see below). The hypercubic latticed regularised (Wilson) theory of QCD is (see also chapter 4) [Wilson 1974, 1977; Goodyear 1984; Espriu et al 1984]

$$S = \frac{1}{g_0^2} \sum_{\text{plaquettes } \square} \mathrm{Re}\{\mathrm{Tr}\, U_\square\} + \sum_{x,y} \bar{\psi}(x) M(x,y) \psi(y) = S_G + S_F \qquad (3.3)$$

where g_0, m_0 are the bare coupling and quark mass, and

$$M(x,y) = (4 + m_0 a)\delta_{x,y} - \frac{1}{2}\sum_\mu \{(1-\gamma_\mu)U(x,y)\delta_{y,x+\mu} + (1+\gamma_\mu)U(x,y)\delta_{y,x-\mu}\} \qquad (3.4)$$

μ is the unit vector in the μ-th direction. In this, as one can see, we have set r=1, that is, the usual solution to the fermion doubling problem [Kogut 1983, Creutz, Jacobs and Rebbi 1983]. As it stands, equation (3.3) represents the action for one quark species, but one considers this for i quarks, and so there is an implicit summation over i. Of course, given that the fermion integral is quadratic in the fields, we can carry out the integration explicitly (as in chapter 2) to establish that det(M) is real i.e., the eigenvalues of M^{-1} are either real or pairs of complex conjugates. If n_f, the number of quark flavours, is even then the "measure"

$$\frac{1}{Z}\int \mathcal{D}U\ (\det M)^{n_f} e^{-S_G(U)} \qquad (3.5)$$

is positive definite.

We now have a definite prescription for the evaluation of the expectation values. One writes down the appropriate mesonic current and constructs the two-point

connected correlation function. As an example, we consider the 0^{++} 4-quark meson in the approximation that no quark annihilation terms are involved. To include such contributions is certainly relevant in producing π-η splitting but is computationaly demanding in that it requires a knowledge of $M_{ab}^{-1}(x,x)$, i.e., non-propagating valence quarks (c.f., fermion self-energy propagators). Therefore, we write

$$O^{++}(n) \equiv \delta(n) = \sum_{a,b} \bar{\psi}^{i}_{a} \gamma_5 \psi^{j}_{b} \bar{\psi}^{k}_{b} \gamma_5 \psi^{\ell}_{a} \qquad (3.6)$$

a,b = colour indices ; i,j = flavour indices

with the proviso that $i,k \neq j,l$. For the u, d system, such an operator does give an isospin 2 meson (i.e., where there <u>are</u> no quark annihilation graphs) but it is necessarily degenerate in mass with all other isospin states in this approximation. Thus [Espriu et al 1984; Goodyear 1984]

$$\langle 0 | \delta(x)\, \delta^{\dagger}(0) | 0 \rangle = \qquad (3.7)$$

$$\left\langle \sum_{\substack{a,b \\ a',b'}} \mathrm{Tr}_{(\mathrm{spin})} \left[M^{-1}_{aa'}(x,y) \gamma_5 M^{-1}_{bb'}(y,x) \gamma_5 M^{-1}_{aa'}(x,y) \gamma_5 M^{-1}_{bb'}(y,x) \gamma_5 \right] \right\rangle$$

Consider now another operator with $\Gamma^{A} \neq \gamma_5$, say

$$\sigma(x) = \sum_{a,b} \bar{\psi}^{i}_{a}(x) \Gamma^{A} \psi^{j}_{b}(x) \bar{\psi}^{k}_{b}(x) \Gamma^{B} \psi^{\ell}_{a}(x) \qquad (3.8)$$

Entirely similarly then,

$$\langle 0 | \sigma(x)\, \sigma^{\dagger}(0) | 0 \rangle = \qquad (3.9)$$

$$\left\langle \sum_{\substack{a,b \\ a',b'}} \mathrm{Tr}_{(\mathrm{spin})} \left[\Gamma_A^{\dagger} M^{-1}_{aa'}(x,y) \Gamma_A M^{-1}_{bb'}(y,x) \right] \mathrm{Tr}_{(\mathrm{spin})} \left[\Gamma_B^{\dagger} M^{-1}_{aa'}(x,y) \Gamma_B M^{-1}_{bb'}(y,x) \right] \right\rangle$$

It is the structure of these expressions, containing multiple sums and square moduli, that suggest the use of, for example, the Cauchy-Schwarz and other inequalities in order to exploit their basic similarities. We quote some of these useful inequalities [Espriu et al 1984; Goodyear

1984]

$$\langle |A|^2 \rangle \geq \langle |A| \rangle^2 \; ; \; \left| \sum_n a_n \right| \leq \sum_n |a_n| \qquad (3.10)$$

$$\langle A^r \rangle^{1/r} \leq \langle A^{\alpha s} \rangle^{1/s} \langle A^{\beta t} \rangle^{1/t} \; : \; \alpha, \beta > 0 \; , \alpha + \beta = 1.$$
$$r, s, t > 0 \; , \; \frac{1}{r} = \frac{1}{s} + \frac{1}{t}$$

In using these one will lose the strict equality of course, of (3.9) for example, but will gain a definite bounding of the resulting inequalities by operators with the simplest Γ matrix structures. In particular, generalised meson operators with π $q\bar{q}$ operator constituents will bound all other mesons from **above** [Weingarten 1983; Espriu et al 1984]. We can see this from (3.7) and (3.9) as the former gives the strict equality

$$\langle 0 | \delta(x) \delta^\dagger(0) | 0 \rangle = \left\langle \sum_{\substack{a,b \\ a',b'}} \left| Tr_{(spin)} \left(M^{-1}_{aa'}(x,y) M^{-1\,*}_{bb'}(x,y) \right) \right|^2 \right\rangle \qquad (3.11)$$

and the latter, by means of the Cauchy-Schwarz relation, gives (with A a constant)

$$\left| \langle 0 | \sigma(x) \sigma^\dagger(0) | 0 \rangle \right| \leq A \left\langle \sum_{\substack{a,b \\ a',b'}} \left| Tr_{(spin)} \left(M^{-1}_{aa'}(x,y) M^{-1\,*}_{bb'}(x,y) \right) \right|^2 \right\rangle \qquad (3.12)$$

If the expectation values fall off at large times (chapter 2) as

$$\langle 0 | \delta(x) \delta^\dagger(0) | 0 \rangle \sim e^{-m_\delta t} \; ; \; \langle 0 | \sigma(x) \sigma^\dagger(0) | 0 \rangle \sim e^{-m_\sigma t} \qquad (3.13)$$

then evidently $m_\sigma \geq m_\delta$.

Rather than continue to derive various inequalities in a rigorous manner, we feel that it is sufficient to summarise the known relations (to date). Dealing solely with the $q\bar{q}g$ and 4-quark sectors, it has been found that

(i) $J^P = 0^{++}$ is the lightest 4-quark state [Espriu et al 1984; Goodyear 1984]

(ii) $(1-2^{-n})m_{\pi} \leq m_{\delta} \leq m_{\pi}$ [Espriu et al 1984] where $\delta = 0^{++}$ and n is the largest integer such that $2^{n} \leq n_{f}-2$

(iii) from (ii), letting i=k, j=l. i.e., including "crossing diagrams" leads to the same bounds in (i), (ii), [Goodyear 1984]

(iv) $m_{AA} \leq 2m_{A}$ where "A" signifies a $q\bar{q}$ operator [Goodyear 1984]

(v) $m_{AB} \geq (m_{AA}+m_{BB})/2$ same convention as (iv) [Goodyear 1984]

(vi) $m_{b} \geq 3m_{\delta}/4$, B=any baryon [Goodyear 1984]

(vii) $m_{h} \geq m_{\delta}/2$, h=lightest flavour non-singlet hybrid [Espriu et al 1984]

(viii) $|\langle 0|\bar{\psi}\sigma_{\mu\nu}\psi' G^{\mu\nu}|0\rangle| \leq 4\left|\langle 0|G_{\mu\nu}G^{\mu\nu}|0\rangle^{1/2}\langle 0|\bar{\psi}\gamma_{5}\psi'\bar{\psi}'\gamma_{5}\psi|0\rangle^{1/2}\right|$

n.b., an inequality between condensates, where G=gluon field, ψ' is a quark flavour degenerate in mass with ψ [Espriu et al 1984]

As we pointed out earlier on, such an analysis is particularly relevant for a comparison with a Monte-Carlo simulation on a hypercubic lattice regularised gauge theory. What is not quantifiable, as will be immediately obvious from the above list of results, is a precise determination of the actual mass scales involved. In addition, one may also add the point that the expected exponential fall-off in time is only reliable if the states in each channel are well seperated in energy (compared to any resonance width) [Espriu et al 1984]. Although computationally neat, and mathematically rigorous, there is only a limited scope for this approach and we feel that, for our interests, more headway is possible with the other methods that we will now consider.

3.3 QCD Sum Rules

. The seminal article of Shifman, Vainshtein and Zahkarov (SVZ from now on) [1979a,b] on the QCD Sum Rule analysis introduces one to an extensive literature, complex in its treatment of the "long-distance", non-perturbative features

of QCD and hence the hadron spectrum. In this review of the methods that are employed, we will restrict ourselves, for the sake of clarity, to those points which are central to grasping the effectiveness of the formalism. In any investigation of the topological properties of QCD, one might well expect a considerable influence to be exerted from instanton-like phenomena, and indeed, if the Sum Rule results are a guide, this appears to be the case [Shifman et al 1979a,b; Belavin, Polyakov, Schwartz and Tyupkin 1975; Callan, Dashen and Gross 1978; Baulieu, Ellis, Gaillard and Zakrzewski 1978]. However, a systematic investigation of all those interesting facets of QCD involving instanton calculus would lead us too far from our aim of illustrating the nature of "analytic" work on the QCD spectrum of states. The reader is directed to the article of SVZ [1979a,b], and also the papers of Callan et al [1978]; Andrei and Gross [1978]; Baulieu et al [1978]; Polyakov [1979] for further details on many of these points.

Essentially, the underlying idea in this scheme is to make some headway in evaluating the expectation values of hadronic operators by making use of Wilson's Operator Product Expansion [Wilson 1969; Symanzik 1971]. This states that

$$i\int e^{iqx} d^4x \langle 0 | T\{ J_\mu(x) J_\nu(0)\} |0\rangle \underset{q^2\to-\infty}{=} (q_\mu q_\nu - q_\mu q^2) \sum_n C_n O_n \qquad (3.14)$$

where the O(n) are local (gauge and Lorentz scalar) operators ordered, in the expansion, by their dimension. The C_n are the Wilson coefficients and fall off in inverse powers of q^2. The O(n) are a parameterisation of the non-perturbative fluctuations, for example the quark and gluon condensates

$$\langle 0 | \bar{\psi}\psi | 0\rangle \qquad \langle 0 | G_{\mu\nu} G^{\mu\nu} | 0\rangle \qquad (3.15)$$

which vanish in perturbation theory, but which are known to be non-zero [SVZ 1979a,b]. The Wilson co-efficients are evaluated in perturbation theory ($q^2 \to \infty$) where asymptotic

freedom ensures that such an expansion is meaningful [Gross and Wilcek 1973; Politzer 1973].

The justification of the OPE [Wilson 1969; Symanzik 1971] has been shown for QFT to be rigorous, but we may also appeal to the intuitive picture that a product of local operators at mass scales much higher than the characteristic scale of the problem (the hadronic scale), should appear as a single local operator [Gross 1975].

The advantage of the OPE, if it holds in the QCD vacuum, is in its explicit dependence on a number of condensates, and that it specifically relates the hadronic spectrum to the fundamental Lagrangian of QCD itself [SVZ 1979a,b] (see also the lattice formulation). The lowest dimension operators that are relevant (apart from the unit operator) are

$$O_M = m\bar{\psi}\psi \quad (\text{dimension } 4) \; ; \; O_G = G_{\mu\nu}^a G^{\mu\nu a} \quad (\text{dimension } 4)$$

$$O_\sigma = m\bar{\psi}\sigma_{\mu\nu}\tau^a\psi G^{\mu\nu a} \quad (\text{dim. } 6) \; ; \; O_\Gamma = \bar{\psi}\Gamma^A\psi\bar{\psi}\Gamma^A\psi \quad (\text{dim. } 6)$$

$$O_F = f^{abc} G_{\mu\nu}^a G^{\nu\rho b} G_{\rho\mu}^c \quad (\text{dim. } 6) \qquad (3.16)$$

Notice that, in the limit $q^2 \to \infty$, one would expect these lowest dimension operators to be the most significant. In some sense then, the series should be bounded [SVZ 1979a,b]. However, one must qualify this remark. In fact, it has been shown [Callan et al 1978; SVZ 1979a,b] that instanton effects break down the validity of the expansion beyond a mass dimension of about 11. The reason for this is connected with the non-negligible contribution of "small" instantons, i.e., even in the region where perturbation theory should be valid (see also chapter 1) [SVZ 1979a,b]. Quite what the OPE means beyond this point is unclear [SVZ 1979a,b], but results on "conventional" mesons and baryons based on the contributions of only a <u>few</u> terms give a good agreement with the experimental data (see [SVZ 1979a,b; Reinders, Yazaki and Rubenstein 1982, 1983a,b; Ioffe 1981; Shuryak 1983]).

Having given some background to the nature of this approach, let us turn to how one actually produces a "Sum Rule" from the OPE (3.14). It proves simpler to demonstrate this for the "conventional" $q\bar{q}$ mesons. In fact, no calculation is known to exist for 4-quark mesons, although there are a number of analyses of the hybrid sector. The reason for this, we believe, rests in the relatively large number of fermion contractions (i.e., quark propagators) implicit on the left hand side of (3.14) for any 4-quark operator. As we shall see, keeping track of the terms generated in the perturbation theory expansion of (3.14) is a tricky matter, and the 4-quark case is undoubtedly more complicated still.

A systematic method for developing the perturbation theory has developed in recent years and involves "expanding" the quark and gluon fields as "quantum fluctuations" around some classical fields, obeying the equations of motion, that give rise to the non-perturbative contributions [SVZ 1979a,b; Govaerts, de Viron, Gusbin and Weyers 1983, 1984; Shuryak and Vainshtein 1982; Shifman 1982]. So we shift

$$A_\mu^a \longrightarrow A_\mu^a + \phi_\mu^a \qquad (3.17)$$
$$\psi \longrightarrow \psi + \varepsilon$$

where $\varphi(x)$, $\varepsilon(x)$ are the fields in the functional integral. The variables φ, ε give rises to propagators in the "background" fields which one inverts to obtain the green functions. In doing so, it is found to be easier to fix the gauge freedom of the "background" fields in order that the physical gluon "background" field (giving rise to, e.g., the gluon condensate) becomes explicit in the expression (3.14). That is, we set [Schwinger 1979; Dubikov and Smilga 1981; Shifman 1980]

$$x^\mu A_\mu(x) = 0 \qquad (3.18)$$

so that

$$A_\mu{}^a(x) = \int_0^1 d\rho\, \rho x^\nu G_{\nu\mu}{}^a(x) \qquad (3.19)$$
$$= \sum_{n=0}^{\infty} \frac{1}{(n+2)n!} x^{\alpha_1} \cdots x^{\alpha_n} (D_{\alpha_1} \cdots D_{\alpha_n} G_{\nu\mu})^a(0)$$

The co-efficient of the unit operator on the right hand side of (3.14) is the trace in

$$i \int e^{iqx} d^4x \; \overline{\bar\epsilon(x) \gamma_\mu \epsilon(x) \bar\epsilon(0) \gamma^\nu \epsilon(0)} \qquad (3.20)$$

and that of the quark "mass" condensate (from (3.16) is

$$i \int e^{iqx} d^4x \, \bar\psi(x) \gamma_\mu \overline{\epsilon(x) \bar\epsilon(0)} \gamma^\nu \psi(0) \qquad (3.21)$$
$$+ i \int e^{iqx} d^4x \, \bar\epsilon(x) \gamma_\mu \psi(x) \bar\psi(0) \gamma^\nu \epsilon(0)$$

both taken at zeroth order in α_c, and in the "background" gluon field [Govaerts et al 1984; Shuryak and Vainshtein 1982].

One then extracts the leading singularities in these expressions by means of the result [Bogoliubov and Shirkov]

$$\int \frac{d^4x}{(2\pi)^4} \frac{e^{iqx}}{(x^2 - a^2 \pm i\epsilon)} = -\frac{1}{4\pi^2} \delta(q^2) + \frac{a^2}{8\pi} \theta(q^2) \left[\frac{J_1(a\sqrt{q^2})}{a\sqrt{q^2}} \mp \frac{N_1(a\sqrt{q^2})}{a\sqrt{q^2}} \right]$$
$$\mp \frac{ia^2}{4\pi^2} \theta(-q^2) \frac{K_1(a\sqrt{-q^2})}{a\sqrt{-q^2}} \qquad (3.22)$$

Keeping track of all the terms generated in the expansion, and also those important contributions at first order in α_c and the gluon field $G_{\mu\nu}$ is obviously a laborious proceedure. We will not pursue this, but merely quote the result for the ϱ-meson correlation function [SVZ 1979a,b]

$$\Pi(q^2) = \sum_n c_n O_n = -\frac{1}{4\pi^2} \left(1 + \frac{\alpha_s}{\pi}\right) \ln\left(\frac{q^2}{\mu^2}\right) + \frac{2m}{q^4} \langle \bar\psi \psi \rangle$$
$$+ \frac{\alpha_s}{12\pi q^4} \langle G_{\mu\nu}{}^a G^{\nu\mu a} \rangle - \frac{2\pi\alpha_s}{q^6} \langle \bar\psi \gamma_\sigma \gamma_5 \tau^a \psi \bar\psi \gamma^\sigma \gamma_5 \tau^a \psi \rangle$$
$$+ \cdots \qquad (3.23)$$

To obtain "Sum Rules" from the OPE, one uses dispersion relations to relate them to physical states [SVZ 1979a,b;

Shuryak 1982]. As motivation for this we note that the imaginary part of $\Pi(q^2)$ is related to physical processes [SVZ 1979a,b; Applequist and Georgi 1973; Zee 1973] i.e.,

$$\mathrm{Im}\ \Pi(q^2) = \frac{\sigma(e^+e^- \longrightarrow \text{hadrons};\ \text{isospin} = 1)}{\sigma(e^+e^- \longrightarrow \mu^+\mu^-)} \qquad (3.24)$$

In general, the (1-dimensional) fourier transform of the spectral function obeys [Shuryak 1982; SVZ 1979a,b]

$$\mathrm{Re}\ \Pi(s') = \frac{1}{\pi}\int ds\ \frac{\mathrm{Im}\ \Pi(s)}{s'-s} \qquad (3.25)$$

Normally one is interested in the Borel transformation of the spectral function. This "transforms" the power series (in q^2) into an exponential, with better convergence properties [SVZ 1979a,b]. To extract the lowest mass, it is standard to adopt the prescription that, in any given channel, there is only one resonance state and writes [SVZ 1979a,b; Govaerts et al 1984]

$$\mathrm{Im}\ \Pi(s) = \pi g_R^2 (m_e^2)^4 \delta(s - m_R^2) + \pi\,\theta(s-s_0)\left\{\text{power corrections in } s\right\} \qquad (3.26)$$

to saturate $\Pi(s)$. Here, g_R, m_R are the renormalised coupling and mass and s_0 is some continuum momentum threshold. The power corrections are specified by the paticular channel that one investigates [SVZ 1979a,b]. In (3.26), g_R^2, m_r^2 are treated as free parameters in a least-squares fit to s_0.

There are many aspects of the OPE in the QCD vacuum and the derived "Sum Rules" that are deserving of comment. However, the above example goes some way to relating the kind of considerations that are relevent in the analysis. The reader is referred to [SVZ 1979a,b; Govaerts et al 1984; Shuryak 1982] for further information.

The application of these methods to the spectrum of hybrid mesons has been almost exclusively due to Govaerts et al [1983, 1984]; Lattore, Narrison, Pascuard and Tarrach [1984]; Balitsky D'Yakanov and Yung [1982a,b]. A typical $q\bar{q}g$ operator would have the form

$$J_\mu(x) = \bar{\psi}(x)\,\Gamma_\nu\,\tau^a\,\psi(x)\,G_{\nu\mu}^a(x) \qquad (3.27)$$

where, for example, $\Gamma_\nu=\gamma_i$ yields the 1^{-+} exotic meson, and $\Gamma_\nu=\gamma_0$, the 0^{++}. Evidently, one can consider many possible $q\bar{q}g$ operators on the basis of this, and we shall have cause to examine them extensively in chapter 5. For the moment, we present in table 1, a "master" set of results, drawn from a sample of all recently (within the last few years) reported findings. References for this data are provided by the accompanying explanatory paragraph to the table. What we have shown is a comparison of the data on $q\bar{q}g$ and 4-quark mesons in various calculational schemes. Our aim here is to show the degree, or lack of it, not only between different methods applied to the $q\bar{q}g$ or 4-quark mesons, but also a "cross-comparison" of the different states themselves. This gives, at a glance, a better impression of the important energy scales involved. We consider only the lightest, i.e., u, d system states for direct comparison with the lattice results of chapters 4 and 5. As an aside, a recent analysis of Govaerts, Reinders and Weyers [1985], looked at heavy quark (i.e., $c\bar{c}g$, $b\bar{b}g$) hybrids. The simplicity that arises from this approximation is the relative unimportance in the OPE of the quark condensate relative to the gluon condensate [Govaerts et al 1985], a result which does not hold for light-quark systems. Note that the results of table 1 for the "Sum Rules" are quoted as statistically significant to the level of about 10%.

	masses in GeV	0^{++}	0^{+-}	0^{--}	0^{-+}	1^{-+}	1^{+-}	1^{--}	1^{++}
$q^2\bar{q}^2$	Jaffe [1977a,b] (Bag)	1·15 (5)	-	-	-	-	-	—	1·45 (5)
$q\bar{q}g$	de Viron and Weyers [1981] (Bag)	1·69 (14)	1·93 (19)	1·32 (13)	1·87 (19)	1·57 (16)	1·76 (18)	1·32 (13)	1·60 (16)
	Charowitz and Sharpe [1983] (Bag)	1·41	-	-	-	-	1·76	-	1·56
	Barnes et al [1983] (Bag)	-	-	-	1·30 (10)	1·50 (10)	-	1·60 (10)	-
	Govaerts et al [1984] (Sum Rules)	3·40 (34)	-	3·40 (34)	-	1·30 (13)	1·00 (10)	-	-
	Latorre et al [1983] (Sum Rules)	-	-	3·10 (20)	3·10 (20)	1·70 (10)	-	1·70 (10	-

Table 3.1 Summary of 4-quark and hybrid exotic and non-exotic meson masses. The $q^2\bar{q}^2$ are due soley to Jaffe [1977a,b] in the Bag-Model. No P=-1 mesons are calculated there, but the 0^{+-} and 1^{+-} will mix with 0^{++} and 1^{++} when charged. The masses here quoted have been selected from the various authors to correspond to operators that feature in the lattice simulation. For further data, see the references.

The major conclusion has to be the lightness of vector hybrid mesons, in the 1-2 GeV region. In particular the exotic 1^{-+} is not at some experimentally unobtainable mass, an idea that might have been invoked to explain its apparent absence from experiment. The scalar sector, on the other hand, does appear somewhat massive, to the extent that one might yet believe them to be difficult to detect (but this in itself cannot be a guarantee). What is important is the degree to which these general trends might be borne out by the lattice calculations (see chapter 5).

3.4 The MIT Bag Model

A framework within which we are able to discuss both $q\bar{q}g$ and 4-quark mesons is provided by the MIT Bag Model [Chodos, Jaffe, Johnson, Thorn and Weisskopf 1974; de Grand, Jaffe, Johnson and Kiskis 1975]. This is, at heart, a relatively simple idea in that one envisages quarks and gluons propagating (on-shell) only within a spherical cavity $4\pi R^2/3$. Confinement is built in, ab initio, by the inclusion, in the phenomenological Hamiltonian, of a "bag pressure" term. In contrast to the "Sum Rules" approach, this term results from a "once and for all" fit to the masses of the low-mass hadrons [de Grand et al 1975]. In principle then, we might anticipate that the "Sum Rules", with a greater number of terms parameterising the long-distance properties of the theory, would provide a better estimate of the masses of "unusual" states. Both methods overlap to some extent on the predictions of the masses of the low-lying vector $q\bar{q}g$ but differ substantially on the masses of the scalars. This will open the way for the lattice calculations of the following chapters.

The zeroth order approximation to a hadronic mass is the sum of quark (and gluon mode) kinetic energies and the "bag pressure term" [Chodos et al 1974; Barnes 1984]. That is, we solve

$$(\not{p} - m)\psi(x) = 0 \qquad (3.28)$$

inside the surface S (figure 1) Confinement is provided explicitly by the term

$$\frac{4}{3}\pi R^3 B_0 \quad : \quad B_0 \simeq (146\ \text{MeV})^4 \qquad (3.29)$$

which is estimated from a fit to well-established hadrons [de Grand et al 1975]. This we will discuss further below. One then minimises the energy

$$E(q\bar{q}) = \frac{2x}{R} + \frac{4}{3}\pi R^3 B_0 \qquad (3.30)$$

$$x = kR \quad ; \quad k = \text{quark eigenmode}$$

(a factor of n for n quarks in the kinetic energy part) in order that a stable bag radius be determined. Thus

$$\frac{\partial E}{\partial R}\Big|_{R=R_0} = 0 \quad \Rightarrow \quad R_0 = \left(\frac{x}{2\pi B_0}\right)^{1/4} \qquad (3.31)$$

With these parameters,

$$E_0 = \frac{2x}{R_0}\left(1 + \frac{1}{3}\right) = 1.05\ \text{GeV} \qquad (3.32)$$

$$R_0 = 1.02\ \text{fermi}$$

At this order, the bag contributes 1/4 of the mass of the hadron and that <u>all</u> the mesons, or all the baryons, are degenerate in mass. We have a certain "freedom" to alter the value of B_0 (and this can be important for discussions of the spectroscopy, see later), but the experimentally observed splittings can never arise [Barnes et al 1983; Barnes 1984]. It is, of course, higher order exchanges in, for example, transverse gluons that give rise to these

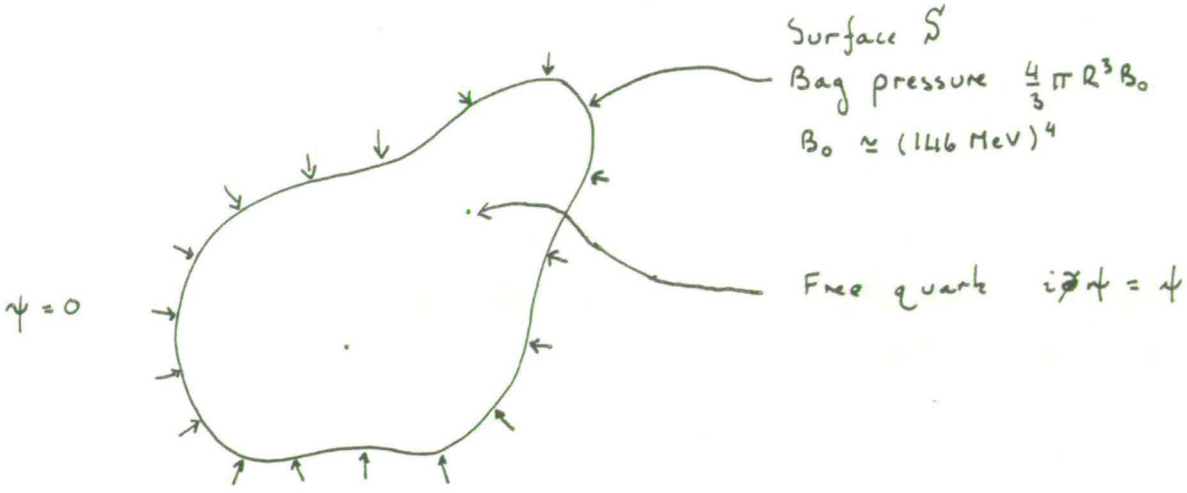

Figure 3.1 A schematic interpretation of the MIT Bag-Model. The QCD vacuum is internal to the surface S and is maintained (confinement) by the term $4\pi R^3 B_0/3$.

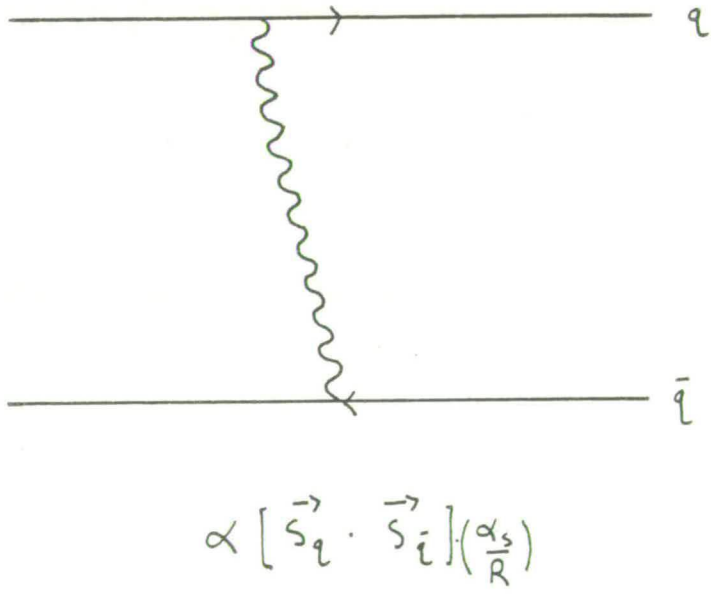

Figure 3.2 One transverse gluon exchange process yielding the first order estimate to the $q\bar{q}$ meson mass.

splittings. Bag model calculations are restricted to one gluon exchange processes such as figure 2. We note, from our familiarity with the predictions of the quark model, that such an approximation is not a priori unreasonable. The addition of just <u>one</u> gluon exchange improves impressively the spectrum of states and many of its properties [see, e.g., de Grand et al 1975; Barnes 1984; de Viron and Weyers 1981; Close and Horgan 1980].

In the interaction Hamiltonian we will encounter a term

$$H_{int} = \sum_{a=1}^{8} j_\mu^a A^{\mu a} \; ; \quad j_\mu^a = \bar{\psi} \Gamma_\mu \tau^a \psi \qquad (3.33)$$

for which it is evidently necessary to introduce gluon "propagators" in the same way as we did for the quark fields. In the spherical cavity the gluon modes are the solutions of

$$n^\nu G_{\mu\nu} = 0 \qquad (3.34)$$

$$G_{\mu\nu} = \partial_\mu A_\nu - \partial_\nu A_\mu - ig[A_\mu, A_\nu]$$

n_μ = outward normal to surface S

and, similarly to the result of electromagnetism, exist in transversely polarised states: transverse magnetic, TM, or transverse electric, TE, components. In table 2, we list the lowest energy eigenmodes [de Viron and Weyers 1981]. One gluon exchange in the π-ϱ case gives rise to a spin-spin contribution

$$\delta E = \left[\frac{128\pi}{3} \cdot \frac{b_1^2}{x_g} \cdot \frac{\alpha_s}{R} \right] \vec{s}_q \cdot \vec{s}_{\bar{q}} \qquad (3.35)$$

where b_1 is an integral over the bag wave functions and is known [Barnes et al 1983]. x_g is the lowest gluon eigenmode (the fact that there is a significant difference in the N=1 TE and TM modes has important consequences for spectroscopy [Barnes et al 1983]) and α_s is the strong

MODE		χ_g N = 1	N = 2 .....
TRANSVERSE ELECTRIC	1^+	2·744	6·117
	2^-	3·870	7·443 ...
	⋮		⋮
TRANSVERSE MAGNETIC	1^-	4·493	7·725
	2^+	5·763	9·905 ...
	⋮		⋮

Table 3.2 N gluon eigenmodes (TE or TM) in a spherical cavity, where $\chi_g = \varepsilon R$; ε_g = energy eigenvalue, R= bag radius. From Barnes [1984].

coupling. The correct value of $\delta E = E_\rho - E_\pi$ thus fixes the parameter α_s (R is known).

It is worthwhile to set in perspective this method by pointing out some of the approximations that are almost universally adopted. Firstly, self-energy corrections to the quarks and gluons are not calculated. In order that they may be included in the analysis, the phenomenological masses for the quarks are employed [de Grand et al 1975; Jaffe 1977a,b]. The trouble here is that the self energy of the "valence" gluon is difficult to quantify [de Viron and Weyers 1981] although one may appeal to estimates based on the string tension. Secondly, in the "zeroth order" Hamiltonian, it is more common to introduce a mass dependance on the i-th quark through

$$E_{KE} = \frac{1}{R} \sum_{i=1}^{n_f} \left(\chi^2(m_i R) + m_i^2 R^2 \right)^{1/2} \qquad (3.36)$$

and, from consideration of the quantum mechanical aspects of cavity perturbation theory, a term estimating the effect of confining quarks and gluons to a sphere of radius R, (the zero-point energy) is added [de Grand et al 1975; Jaffe and Johnson 1976; Jaffe 1977a,b]

$$E_0 = -\frac{z_0}{R} \quad : \quad z_0 = 1.84 \qquad (3.37)$$

Although some attempts have been made to analyse decay processes in the Bag Model, problems are encountered due to the non-spherical geometry involved [Chanowitz and Sharpe 1983b; Maciel and Paton 1982].

Combining all these additional components, in the u, d, system [Barnes 1984] E_0 is given by

$$E_0(R) = E^{(0)} + \frac{4}{3}\pi R^3 B_0 - \frac{z_0}{R} \qquad (3.38a)$$

$$E_{(0)} = \sum_i \frac{x_i}{R} \qquad \begin{cases} x_{u,d} = 2.043 \\ x_{q_{TE}} = 2.744 \\ x_{q_{TM}} = 4.493 \end{cases} \qquad (3.38b)$$

All the $O(\alpha_s)$ contributions to a $q\bar{q}g$ meson are summarised by the diagrams of figure 3, in units of α_s/R [Barnes and Close 1982]. Notably, in this case, the existence of "valence" gluons in the Bag, gives rise to scattering processes involving these eigenmodes [Barnes and Close 1982; Barnes et al 1983]. The total energy shift is negative and is, in the particularly interesting case of the 1^{-+}, [Barnes and Close 1982]

$$\Delta E(1^{-+}) = -0.30 \frac{\alpha_s}{R} \qquad (3.39)$$

Thus we see that the cost in energy of adding an $\underset{\sim}{8}$ gluon is reduced by the large colour attraction that arises from the two $\underset{\sim}{8}$ substates [Barnes et al 1983]. This will also be an important characteristic of 4-quark mesons (below) [Jaffe 1977a,b]. In particular, such "unusual" states are not pushed up to very high masses, thus making them conveniently unobservable. Another noteworthy comment is the absence of any large contribution from graph topologies that relate the $q\bar{q}g$ and 4-quark sectors (figure 3), i.e., $q\bar{q}$ annihilation into a transverse gluon [Barnes and Close 1982; Barnes et al 1983; Jaffe 1977a].

In table 1 again, we have collected together the Bag Model results on the spectrum of $q\bar{q}g$ states. The list, as before for the Sum Rule calculation, is not exhaustive, but gives a reasonable cross-section of available results. There is a certain amount of consistency within the Bag Model results themselves, but it is clear that a large discrepency exists between Bag and Sum Rules in the case of the scalar mesons. It becomes apparent that the

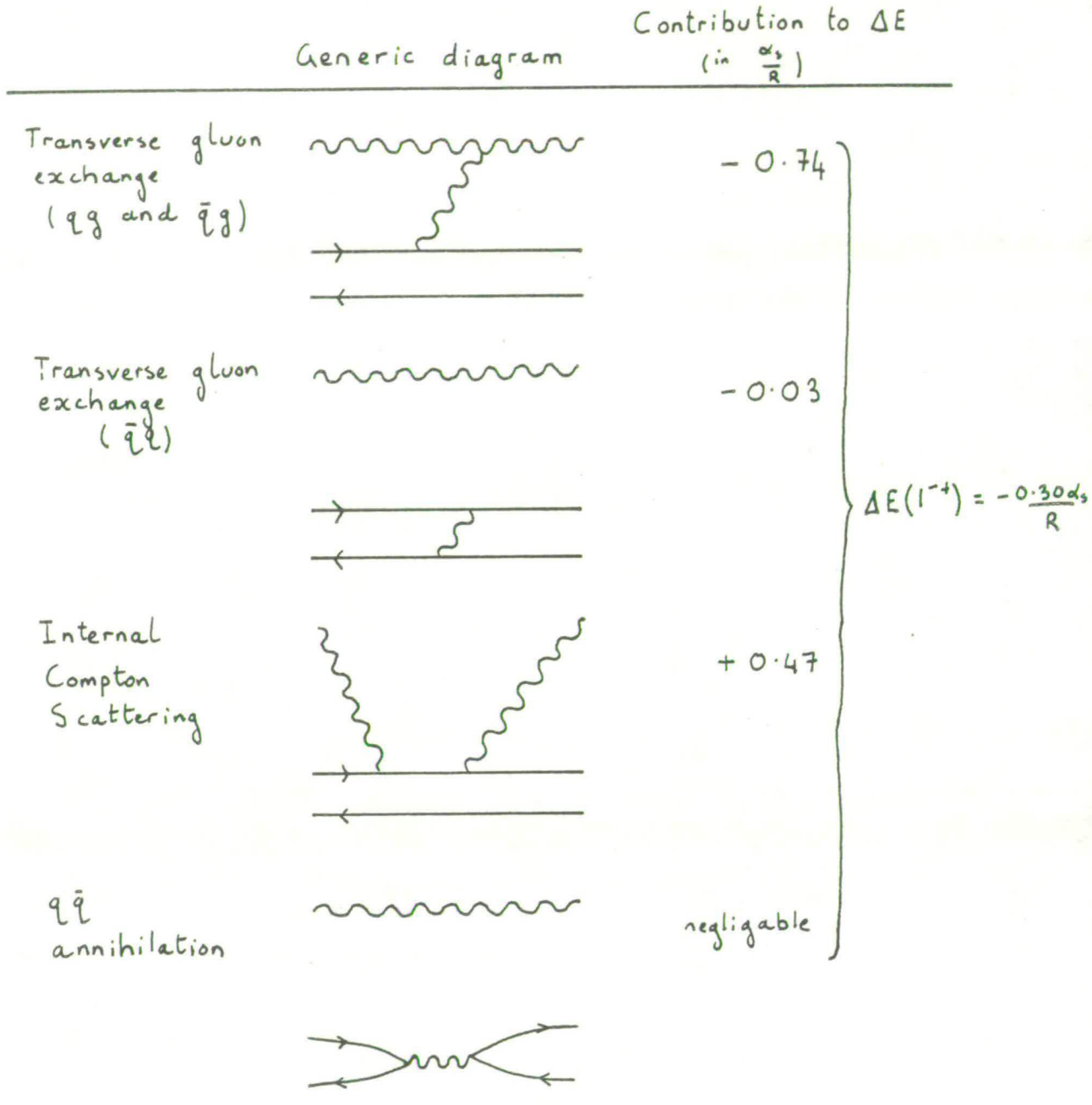

Figure 3.3 The $O(\alpha_s)$ energy shifts in the case of the 1^{-+} bag model calculation after Barnes and Close [1982].

inevitable approximations introduced into these two important methods must be investigated more extensively. We shall however take an alternative approach in the following chapter, calculating the spectrum via lattice Monte Carlo. The fact that, in the Bag Model, the overall scale of the spectrum depends crucially on the "pressure term", and will inevitably be affected by spin-independant effects (generally not well understood [Barnes et al 1983; Barnes 1984; Chanowitz and Sharpe 1983a]) gives rise to uncertainties in E_0, estimable as being some 30% at the very least [Barnes 1984]. Of course, the unambiguous signal of an exotic, e.g., the 1^{-+}, would tie down much more precisely the efficacy of the "Bag" in predicting masses of these kind of states. With such an uncertainty over E_0, there is a certain leeway in interpreting (if any doubt should exist) "conventional" $q\bar{q}$ mesons as possible crypto-exotic states. One should refer to, e.g., [Barnes 1984] for more on this. As an example consider the $\iota(1400)$. With a Bag Model prediction for the 0^{-+} $q\bar{q}g$ at around 1400 MeV, there are features of the decay channels (but recall the earlier remarks on bag fission) that have been claimed to be more explainable in terms of the $q\bar{q}g$, rather than the accepted view of the $\iota(1400)$ as a radially-excited η [Barnes 1984]. It is fair to say that this possibility is not highly regarded [Particle Data Group 1982]. Of course, the Bag Model result for this meson , like that of any other, is sensistive to the value of E_0. One may also note that if this term were some 200 MeV lower, then the πA decay channel would be closed to the 1^{-+} exotic. Then there would be only $\pi\pi\varrho$, 4π channels available but, overall, the situation is definitely not clear.

As a remark applicable to both $q\bar{q}g$ and 4-quark mesons, one should be aware of the importance of the role of intermediate gluon states in production experiments

[Barnes et al 1983; Barnes and Close 1982]. Channels with "hard" glue (large q^2) are expected to be productive. Thus

$$\psi \longrightarrow \Upsilon X \quad ; \quad \psi \longrightarrow \text{hadrons} \; ; \; p\bar{p} \longrightarrow \text{anything} \tag{3.40}$$

are interesting experimentally.

3.5 Bag Model $Q^2\bar{Q}^2$

The major work on Bag Model 4-quark mesons is that due to Jaffe [1977a,b]. It is fair to say that the status of 4-quark mesons seems to be where he left it and so we feel that it is appropriate here to outline, in a general fashion, his method. The basic addition to the zeroth order Hamiltonian of the Bag (3.38) is the interaction term [Jaffe 1977a,b]

$$H_{int} = \frac{-g^2}{2} \sum_{i \neq j} \sum_{a} \int d^3x \, \vec{B}_i^{\,a}(x) \, \vec{B}_j^{\,a}(x) \tag{3.41}$$

which can be shown [Gell-Mann 1964] to be

$$H_{int} = -\frac{\alpha_s}{R} \sum_{i>j} \sum_{a} \vec{\sigma}_i \cdot \vec{\sigma}_j \, \lambda_i^a \cdot \lambda_j^a \, M(m_i R ; m_j R) \tag{3.42}$$

in which $M(m_iR;m_jR)$ is the integral over cavity wave functions (for non-zero quark mass) that arose before. Having evaluated the integral numerically , and removed it from the summation, we are left solely with calculating the colour and spin sum.

The basic symmetries of the Lagrangian are classifiable as $SU(6)_{CS} \times SU(3)_F$, where the first term is the combination of the colour and spin groups and the latter is the flavour symmetry (for three quarks). In the original quark model, one would have dealt with an $SU(6)_{FS} \times O(3)_{AM}$ of flavour-spin and orbital angular momentum. The lowest mass states there would then have been singlets under the O(3) [Close

1980]. In the 4-quark case, the colour-spin group is the result of an interacting (QCD) theory, and gives rise to SU(6) multiplets mixed by the gluon interactions (acting in a flavour independent way). If we ascribe to a quark, q, the $\underset{\sim}{6}$ dimensional representation of SU(6) (and $\bar{q}$, the $\underset{\sim}{\bar{6}}$ conjugate representation), then

$$\left.\begin{aligned} \underset{\sim}{6}\otimes\underset{\sim}{6} &= \underset{\sim}{15}\oplus\underset{\sim}{21} \\ \underset{\sim}{\bar{6}}\otimes\underset{\sim}{\bar{6}} &= \underset{\sim}{\bar{15}}\oplus\underset{\sim}{\bar{21}} \end{aligned}\right\} \quad q^2\otimes\bar{q}^2 = \underset{\sim}{1}\oplus\underset{\sim}{35}\oplus\underset{\sim}{189}\oplus\underset{\sim}{280}\oplus\underset{\sim}{405} \qquad (3.43)$$

with the lower dimensionality representations being antisymmetric. Overall antisymmetric wave-functions, including the flavour group, are readily constructed

$$\begin{aligned} &([21]\,\bar{3})\otimes([\bar{21}]\,3) \\ &([15]\,6)\otimes([\bar{15}]\,\bar{6}) \\ &([15]\,6)\otimes([\bar{21}]\,3) \\ &([21]\,\bar{3})\otimes([\bar{15}]\,\bar{6}) \end{aligned} \qquad (3.44)$$

A major point in Jaffe's [1977a,b] analysis is the approximation of the integral over wave-functions in states with definite strange quark content, i.e., E_0 is diagonal in $s\bar{s}$ pairs. This is a generalisation of the "magic mixing" observed in the ω-ϕ, f-f′ sectors. There, the $SU(3)_F$ representations mix so that

$$\begin{aligned} \eta_s &= (1/3)^{1/2}\,\eta_{\underset{\sim}{1}} - (2/3)^{1/2}\,\eta_{\underset{\sim}{8}} \\ \eta_0 &= (2/3)^{1/2}\,\eta_{\underset{\sim}{1}} - (1/3)^{1/2}\,\eta_{\underset{\sim}{8}} \end{aligned} \qquad (3.45)$$

where the subscripts indicate the dimensionality and where the physical $\phi=\eta_s$ contains an $s\bar{s}$ pair (and η_0, the ω, does not). One has to extract from (3.44) mesons with definite transformation properties under the $SU(2)_S$ subgroup (prescribed J^P) and which are $SU(3)_C$ singlets. We evaluate (3.42) in terms of the Casimir operators of SU(6), SU(2), SU(3) as

$$-\sum_{a}\sum_{i>j}\sigma_i\cdot\sigma_j\,\lambda_i^a\cdot\lambda_j^a = 8N + \tfrac{1}{2}C_6(\text{tot}) + \tfrac{8}{3}S_{\text{tot}}(S_{\text{tot}}+1) + C_3(q) + \tfrac{8}{3}S_q(S_q+1) - C_6(q) + C_3(\bar{q}) + \tfrac{8}{3}S_{\bar{q}}(S_{\bar{q}}+1) - C_6(\bar{q}) \quad (3.46)$$

Since the C_6 operator will dominate, we can see that the magnetic gluon interaction is most attrative when (i) C_6(tot) is as small as possible, and (ii) $q,\bar{q}$ are (seperately) in the largest representations of $SU(6)_{CS}$. With the addition to the zeroth order estimate, the results are those of Table 1 (quoted to ±50 MeV).

From this data it is clear that evidence of multi-quark states should be found in experiment. Jaffe [1977a] takes the view that the relative lightness of the non-exotic 0^{++} flavour nonet suggests a re-interpretation of the existing $q\bar{q}$ L=1 nonet as, in fact, a crypto-exotic multiplet. He makes the following identifications of the members of that multiplet

$$\varepsilon(700) = u\bar{u}\,d\bar{d} \quad ; \quad S^*(993) = \tfrac{1}{\sqrt{2}}s\bar{s}(u\bar{u}+d\bar{d})$$
$$\delta(970) = u\bar{d}\,s\bar{s} \quad ; \quad \kappa(1300) = u\bar{s}\,d\bar{d} \quad (3.47)$$

This would immediately resolve why the S^* is degenerate with the δ(976) (S^* decays predominantly to $K\bar{K}$, but δ couples fairly evenly to $K\bar{K}$ and ηπ). The ε naturally falls apart to 2π (it is very broad in that channel, with no $K\bar{K}$ decay). In the quark model, $q\bar{q}$, L=1 nonet, one would have expected, from the S^*-δ degeneracy, that "magic mixing" is in evidence [Jaffe 1977a,b; Particle Data Group 1982]. However, then ε should couple to $K\bar{K}$ (i.e., the ε is understood there as predominantly $s\bar{s}$ in nature) and S^* to ππ (S^* has no $s\bar{s}$ component). In fact, [Particle Data Group 1982], the current status of these resonances is that the ε(700) has been removed from the reckoning altogether on

the basis of a lack of corroborating evidence, and has been replaced by the $\varepsilon(1300)$. The most recent version of the Particle Data Table summarising all experiments to date with bearing on the S^*-δ, claimed that there were grounds for expecting virtual 4-quark components in 0^{++} nonet wave-functions but that the quark model description was still adequate. There are, moreover, additional complications suggested from within Jaffe's calculation itself. Although the one gluon exchange calculation is expected by many to be a reasonable approximation, there is some uncertainty that corrections arising from the non spin-spin forces, in particular the colour Coulomb term may be relevant. In the calculation of Barnes et al [1983] on the $q\bar{q}g$ spectrum, this colour Coulomb term was a non-negligable contribution to the overall energy shift.

It is clear that the status of both $q\bar{q}g$ and 4-quark mesons in experiment is far from clear. However, as we have repeatedly stressed, it is most important to clarify the position of these states that arise from the nature of QCD itself, in order that one might more fully understand the properties of that theory. In the following chapter we examine 4-quark mesons in lattice QCD and find that there also does one expect low-mass exotics. If not realised in nature, then some method of suppressing them must be found. Arising even from this brief discription of the various models, one might well wish to question the meaning of "valence" gluons in the $q\bar{q}g$ spectrum. There is more difficulty though in similarly disposing of the 4-quark spectrum, (but recall the Particle Data Groups comments on "virtual" 4-quark components in $Q\bar{Q}$ meson nonets). This is backed-up by the lattice calculation. The lattice hybrid calculation, we shall find, is beset with a number of problems of its own, so only some guidance on these questions can be offered.

CHAPTER 4

Lattice Analysis of 4-quark Mesons

4.1 Introduction: $Q^2\bar{Q}^2$ in Lattice and Continuum QCD

We have seen that, as a non-perturbative technique, lattice gauge theory stands, perhaps, as the best method yet to exploit fully the $SU(3)_c$ group of quark interactions. Our aim in this chapter is to use the lattice formulation of QCD to clarify the behaviour of multi-quark mesons and predict masses for some low-spin states.

One would expect that such an approach would at least provide a comparison with, and should hopefully avoid the (computationally necessary) simplifications introduced in, other work which has been done in investigating these states.

In chapter 3, we reviewed the status of 4-quark mesons in the Bag Model and Operator Inequality formalisms, commenting on the lack of any investigation by means of the (possibly more consistent approach of) QCD Sum Rules. Before proceeding to a presentation of our results in a lattice Monte Carlo calculation, we take up a comment of chapter 3 and evaluate the work of Fucito, Patel and Gupta [1983], who performed a more restricted analysis than ourselves using Wilson fermions on the lattice. Their results and conclusions are to be questioned, and, in particular, at $\beta=6.0$, the proximity to the deconfinement transition on a $6^3 \times 10$ lattice is of major importance.

Fucito et al [1983] followed the proposal of Jaffe [1977a,b] (see also chapter 3) and defined the quark flavour content of 0^+, L=1 quark model nonet mesons as

$$\varepsilon(n) = [\bar{u}\Gamma_1 u \bar{d}\Gamma_2 d](n) \;;\; \delta(n) = [\bar{u}\Gamma_1 d \bar{s}\Gamma_2 s](n)$$
$$S^*(n) = 2^{-1/2}[\bar{u}\Gamma_1 u + \bar{d}\Gamma_2 d](n);\; \kappa(n) = [\bar{u}\Gamma_1 s \bar{d}\Gamma_2 s](n) \qquad (4.1)$$

The calculation involved a comparison of the results using $\Gamma_1 = \Gamma_2 = 1$, and $\Gamma_1 = \Gamma_2 = \gamma_5$. These designations correspond to choices made later in our simulations which are labelled $0^{++}(\delta\delta)$ and $0^{++}(\pi\pi)$.

In extracting mass estimates from the above lattice operators, two important points of theirs should be noted. One was the neglect (see also below) of $Q\bar{Q}$ annihilation terms (chapter 2), equivalent to working with four different quark flavours. The other was the inclusion of a different (bare) quark mass for the strange quark in (4.1). As to their findings, the major conclusion is the appearance of a bound state in the 0^+ channel, i.e., below the two pion mass threshold. But this only occurs at the largest value of the hopping parameter ($k = 1/m_q$) At lower k, no such feature is found, thus there is some <u>unexplained</u> "crossover" phenomenon. The masses of operators with $\Gamma = 1$ are always lower than those with $\Gamma = \gamma_5$ and the mass of the 0^+ $Q\bar{Q}$ meson appears higher than that of the 0^-. From this they claim that the 0^{++} meson (the $\Gamma = 1$ combination) is a genuine resonance and not some π-π "artifact" (i.e., the $\Gamma = \gamma_5$ choice), and expect it to mix with the 0^+ $Q\bar{Q}$ meson. The inverse lattice spacing, u- and s- quark hopping parameters, and the masses of the 4-quark states are found to be

$$a^{-1} = 1051 \text{ MeV}$$
$$k_u = 0.1596 \qquad (4.2a)$$
$$k_s = 0.1469$$

$$m_\varepsilon = (290 \pm 350)\,\text{MeV} \qquad (\text{experiment} \sim 1350\,\text{MeV})$$

$$m_\delta = m_{s^*} = (1060 \pm 250)\,\text{MeV} \qquad (\text{expt} \sim 980 - 975\,\text{MeV}) \qquad (4\cdot2b)$$

$$m_\kappa = (675 \pm 300)\,\text{MeV} \qquad (\text{expt} \sim 1350\,\text{MeV})$$

$$m_{\pi\pi} = (400 \pm 310)\,\text{MeV} \qquad (\text{expt} \sim 270\,\text{MeV})$$

To deduce these masses, n quark propagators with hopping parameter k_u (the u, d quarks say) and 4-n s-quark propagators with hopping parameters, k_s, were combined (ostensibly) in the same way as our calculation below (for equal mass quarks), and so we make no further comment here. The three hopping parameter values used were

$$k_u, k_s \in \{0\cdot145, 0\cdot150, 0\cdot153\} \qquad (4\cdot3)$$

Then the masses were extracted at each k from the linear combination

$$M = A\left(\frac{n}{k_u} + \frac{(4-n)}{k_s}\right) - B \qquad (4\cdot4)$$

with A, B fitting parameters. The quoted errors are given from dividing the configuration sample of 33 into 3 blocks of 11 configurations.

the gauge field configurations were calculated on a lattice whose parameters were chosen precisely to investigate the effects of the deconfinement transition on hadron masses [Fucito et al 1983 and references therein]. One should also be aware that Bowler et al [1984] report the existence of finite size effects in $Q\bar{Q}$ meson masses (e.g., π-ϱ degeneracy) at β=6.0. These 33 configurations, each separated by 300 sweeps, were constructed by a Metropolis algorithm (10 hits per link) using the Wilson action at β=6.0. The quark propagators were calculated in the quenched approximation with r=1. They noted in that work that $t \approx 10$ did not prove sufficient to reveal the "asymptotic" behaviour of the hadron masses. Apart, then, from explicitly demonstrating the effects of the metastable region on all masses, they attempted to control these effects by looking at the impact of those quark paths that "wind" around the lattice. We recall from chapter 2 that below the transition temperature, thermal Wilson loops are suppressed, but have a non-zero expectation value above T_c. This was shown to correspond to the breaking of the global Z(3) symmetry of the action. In the same way, above the transition, there is no suppression of quark paths, included in a hadron mass fit, that wrap around the lattice. Their main effort was to try and remove a significant fraction of these paths by averaging all the quark and hadron propagators over periodic and anti-periodic boundary conditions. This would account for those paths with an odd winding number. However, hadron masses calculated in this way were still a long way from the physical values. The π and the ϱ are almost degenerate, as are the nucleon, N, and the Δ. In addition they report $a^{-1} \approx 800$ MeV, in poor agreement with the string tension esimates.

To summarise our observations on the work of Fucito et al [1983], we may say that it provides interesting evidence on the effects of the deconfinement transition on hadron masses, but that no worth can really be attached to their mass-estimates (and unusual behaviour) of the 4-quark mesons. A comprehensive examination of the 4-quark sector is still found wanting. This is what we now turn to.

In section 4.2, we begin by defining 0^{++}, 1^{+-}, 2^{++} 4-quark operators from matrix products of $Q\bar{Q}$ operators with π,ϱ quantum numbers. Our aim here will be to establish the systematics of the simulation and the significance of the method. Section 4.3 contains the details of this numerical calculation and a discussion on the implications of the results. We close in section 4.4 by then extending the analysis to a more general set of 4-quark operators and reporting on the results obtained.

4.2 Definition of $Q^2\bar{Q}^2$ meson operators.

A general 4-quark operator will have the form

$$M(n) = \left(\bar{\psi}^{d}_{\delta} \Gamma^{2}_{\delta\gamma} \psi^{c}_{\gamma} \bar{\psi}^{b}_{\beta} \Gamma^{2}_{\beta\alpha} \psi^{a}_{\alpha} \right)(n) \qquad (4.5)$$

where we project out the propagating colour singlet by means of the tensors $\delta_{ab}\delta_{cd}$ or $\delta_{ad}\delta_{bc}$. Let all the primed labels and superscript "F" refer to the operator at the site n, and all unprimed labels and "I" refer to the space-time origin, 0. Then the 4-quark correlation function is

$$\langle M(n) M^{\dagger}(0) \rangle =$$

$$\left\langle \left[\bar{\psi}^{d'}_{\delta'} \Gamma^{F2}_{\delta'\gamma'} \psi^{c'}_{\gamma'} \bar{\psi}^{b'}_{\beta'} \Gamma^{F2}_{\beta'\alpha'} \psi^{a'}_{\alpha'} \right](n) \left[\bar{\psi}^{a}_{\alpha} \Gamma^{I2}_{\alpha\beta} \psi^{b}_{\beta} \bar{\psi}^{c}_{\gamma} \Gamma^{I2}_{\gamma\delta} \psi^{d}_{\delta} \right](0) \right\rangle \qquad (4.6)$$

The expectation value is with respect to the functional integral over gauge and fermionic fields. Now by using (2.73), redefining $\tilde{\Gamma}=\Gamma\gamma_5$, and then dropping the tilde for clarity,

$$\langle M(n)M^{+}(0)\rangle = \sum_{i=1}^{4} T_i =$$

$$\begin{aligned}
\sum_{Q} \mathrm{Tr}\Big\{ & \Big[\Gamma^{F1}_{\alpha'\rho'}\,\Gamma^{I1}_{\beta\alpha}\,G^{b'b}_{\rho'\rho}\,G^{a'a*}_{\alpha'\alpha}\Big]\Big[\Gamma^{F2}_{\gamma'\delta'}\,\Gamma^{I2}_{\delta\gamma}\,G^{d'd}_{\delta'\delta}\,G^{c'c*}_{\gamma'\gamma}\Big] \\
& - \Big[\Gamma^{F1}_{\alpha'\rho'}\,\Gamma^{F2}_{\gamma'\delta'}\,\Gamma^{I2}_{\beta\alpha}\,\Gamma^{I2}_{\delta\gamma}\,G^{d'b}_{\delta'\rho}\,G^{c'c*}_{\gamma'\gamma}\,G^{b'd}_{\rho'\delta}\,G^{a'a*}_{\alpha'\alpha}\Big] \\
& - \Big[\Gamma^{F1}_{\alpha'\rho'}\,\Gamma^{F2}_{\gamma'\delta'}\,\Gamma^{I2}_{\beta\alpha}\,\Gamma^{I2}_{\delta\gamma}\,G^{d'd}_{\delta'\delta}\,G^{c'a*}_{\gamma'\alpha}\,G^{b'b}_{\rho'\rho}\,G^{a'c*}_{\alpha'\gamma}\Big] \\
& + \Big[\Gamma^{F1}_{\alpha'\rho'}\,\Gamma^{I2}_{\delta\gamma}\,G^{b'd}_{\rho'\delta}\,G^{a'c*}_{\alpha'\gamma}\Big]\Big[\Gamma^{F2}_{\gamma'\delta'}\,\Gamma^{I1}_{\beta\alpha}\,G^{d'b}_{\delta'\rho}\,G^{c'a*}_{\gamma'\alpha}\Big]\Big\}_{Q}
\end{aligned} \qquad (4.7)$$

to an overall phase. In this, the trace is in colour space, defined by means of the above projection operators, and the subscript "Q" denotes the quenched average in the expectation value.

Under the constraint of being an overall colour singlet at each lattice point, there are four ways that the colour contractions for each 4-quark state can be performed. By referring to figure 1, we see that this corresponds to each "end" of the diagram being composed of either two colour singlets or two colour octets. The "two" here refers to a description in terms of $Q\bar{Q}$ "basis" states. The sense in which we mean "basis" will be defined below.

Fig.1(a)-(d) are the contributions to the 4-quark 2-point connected operator in the case where we have only two quark flavours (each quark line is traced in flavour space), e.g., up and down, I=2, (i.e., no quark annhilation graphs, so that there is no mixing with standard $Q\bar{Q}$ mesons). We also calculate all operators in the approximation Fig.1(a) alone, that is, four different quark flavours. The equality of the quark mass parameters for each of the flavours appearing in these operators also imply the degeneracy in mass of all isospin states. This will be demonstrated in the actual

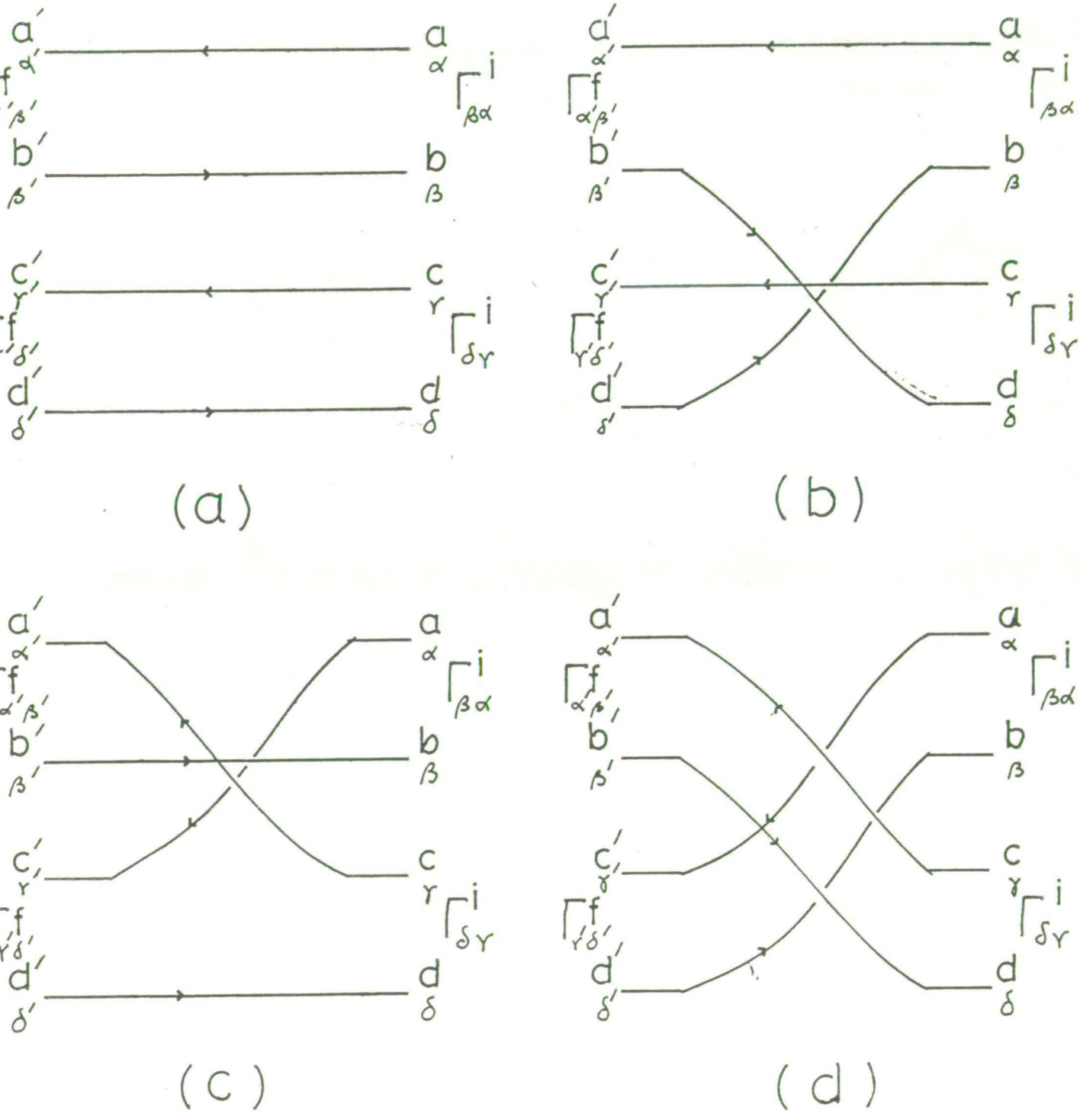

Figure 4.1 Diagrams contributing to the I=2, two quark flavour case.

simulation.

From the structure of terms $T_{2'}$ T_3 it is clear that if one were to Fierz transform the matrix indices on the Γ's there is an interpretation of these contributions also as products of terms like those in square brackets in (4.7a) The motivation for such a Fierz transformation is based on the particular index structure of the stored quark green functions [Bowler et al 1984]. By such a transformation we are then able to carry out, in one program, the full average (i.e., the four contributions $T_1 \to T_{4'}$ each of which consists of four colour combinations). This saves on CPU time.

A subtlety that arises from the Fierz re-shuffle of Dirac indices is in the corresponding alteration of colour labels. From fig. 1(b),(c), one sees that the "crossed" lines carry spinor and colour labels. On Γ matrices, the Fierz transformation follows from the completeness of the 16 matrices Γ^i, i=1,..,16. These obey

$$\sum_{i=1}^{16} \Gamma^i_{ab} \Gamma^i_{cd} = 4 \delta_{ad} \delta_{cb} \qquad (4.8)$$
$$Tr(\Gamma^i \Gamma^j) = 4 \delta^{ij}$$

Thus we find

$$4 \Gamma^i_{ae} \Gamma^j_{cf} = \sum_{i=1}^{16} \Gamma^i_{ab} \Gamma^j_{bf} \Gamma^i_{cd} \Gamma^j_{de} = \sum_{i=1}^{16} C_{(ij)} \Gamma^i_{af} \Gamma^i_{ce} \qquad (4.9)$$

where $C_{(ij)} = \frac{1}{16} Tr \Gamma^i \Gamma^j \Gamma^i \Gamma^j$

The completeness of the set of 3x3 colour matrices requires the inclusion of the unit matrix, i.e.,

$$\delta_{ad} \delta_{cb} = \frac{1}{3} \delta_{ab} \delta_{cd} + \frac{1}{2} \sum_{i=1}^{8} \lambda^i_{ab} \lambda^i_{cd} \qquad (4.10)$$
$$Tr(\lambda^i \lambda^j) = 2 \delta^{ij}$$

Thus, under the combined Fierz transformation of (4.8) and (4.10), colour octet contributions to the expectation value

carry an additional relative factor of 3/2.

Having expressed all the contributions $T_1 \to T_4$ as matrix products in the way of T_1 we may introduce the $Q\bar{Q}$ "basis" functions. For example, from (4.7a) each of the square bracket terms carries a J^{PC} given by the Γ matrix, which is identical at site n and 0. In the numerical simulation, we construct such objects, and and perform, using the colour singlet projection operators, the matrix multiplication with another such object.

As stated earlier, this preliminary (and section 3) investigation of multi-quark mesons will employ only π- and ϱ-meson operators as our $Q\bar{Q}$ basis operators. Loosely, we must be guided by the lattice behaviour of π and ϱ $Q\bar{Q}$ meson operators. These give the "best" mass estimates from a statistical point of view and are found to have the largest propagator signals (see Bowler et al [1983, 1984]). This will be of relevance when one recognises that even some $Q\bar{Q}$ mesons and QQQ baryons operators are found to have small signals. We want to maximise the possibility of achieving good mass estimates for all the 4-quark states considered but will have cause later to note that problems with some of the propagator signals do still arise.

So we choose to use initially as $Q^2\bar{Q}^2$ operators, the following:

$$
\begin{aligned}
0^{++}(\pi\pi) &= \bar{\chi}\Gamma_5\chi\,\bar{\chi}\Gamma_5\chi \\
0^{++}(\rho\rho) &= \bar{\chi}\Gamma_i\chi\,\bar{\chi}\Gamma_i\chi \\
1^{+-}(\pi\rho) &= \bar{\chi}\Gamma_5\chi\,\bar{\chi}\Gamma_i\chi \\
2^{++}(\rho\rho) &= \bar{\chi}\Gamma_i\chi\,\bar{\chi}\Gamma_j\chi - \tfrac{1}{3}\bar{\chi}\Gamma_i\chi\,\bar{\chi}\Gamma_i\chi
\end{aligned}
\qquad (4.11)
$$

One cannot construct a 1^{++} from 2 <u>similar</u> lattice operators

(carrying the same representation of the rotation group; symmetric under particle interchange), the only other possible combination using π and ϱ operators is the 2^{++}, which we have investigated. Parenthetically, we may note that, as discussed by Jaffe [1977a,b], the spin 2 4-quark meson will either fall apart into two rhos or into two pions in a relative D-wave. Although we construct the spin 2 via ϱ- operators, one might then expect to see two π's in the final analysis, if that combination with the inclusion of the D-wave kinetic energy is lighter than $2m_{\varrho}$.

4.3 Numerical Results

We use the standard Wilson action [Wilson 1974, 1977, Bhanot and Creutz 1981, Bhanot 1982] for gauge and fermionic sectors, generating the gauge configurations via the Metropolis algorithm [Bowler et al 1983, 1984], and the quark green functions (for Wilson fermions) by a relaxation routine.

One combines the quark green functions (propagating a quark from the origin to any site n) to form the $Q\bar{Q}$ "basis" functions, as described in section (4.2). The trace over colour and spin labels is then performed for the 4-quark operator suitably defined as a matrix product of these $Q\bar{Q}$ operators and the result is averaged over all configurations at each of the three quark mass parameter values. The mass of the lowest-lying state in the spectrum of each 4-quark operator is estimated from the smaller argument of a two-exponential fit to the the resultant propagator. Finally, the 4-quark meson mass is deduced from a linear extrapolation (in m_q) to where the pion $(\text{mass})^2$ vanishes (the critical value of the hopping parameter, k, where chiral symmetry is restored and

spontaneously broken). Physical masses (in MeV) are found by setting the scale with the ϱ mass.

The simulation was performed at 3 hopping parameter values ($k=1/2m_q$): k=0.1625; 0.1575; 0.1520 with 16 configurations per m_q. Runs were performed at $\beta=5.7$ (i.e., solely in the fundamental representation of the gauge action) on a 8^3x16 lattice, periodic in space, with fixed time boundaries. Statistical errors were calculated from the spread in mass estimates on 4 successive blocks of 4 configurations. As noted previously, for the $Q^2\bar{Q}^2$ mesons an additional improvement in statistics was available from averaging the 4 possible colour combinations. The calculations were performed on an I.C.L Distributed Array Processor (DAP) at Edinburgh.

Details on the configuration and quark green function calculations are reported in Bowler et al [1984], but we would like to note, for completeness, a few of the more important points. Firstly, in generating the gauge field configurations, 10^4 lattice sweeps were allowed for equilibration and each of the 16 resulting configurations were separated by 2400 lattice sweeps. All matrix multiplies on the gauge fields and in the quark propagators were done in 24 bit arithmetic, sufficiently accurate for the problem at hand. The 8^3x16 lattice itself was constructed from two identical copies of an 8^4 lattice, the extension being in the time direction (see appendix for a discussion on the DAP). In terms of the DAP software features, the 8^4 structure is mapped on to the 64^2 array of processors by means of four logical masks (appendix). The extension of the lattice to 16 time steps is suggested from the fact that the optimised Gauss-Seidel algorithm for the quark propagator connects even to odd sites (and vice versa). That is, the routine [Hamber and Parisi 1981,

Weingarten 1982] with covariant derivative $\not{D}$, and relaxation parameter ε

$$G'(n,0) = G(n,0) + \varepsilon[-(\not{\phi}+m)G(n,0) + \mathbb{1}] \qquad (4\cdot12)$$

$$= (1-\varepsilon m)G(n,0) - \varepsilon\not{\phi}G(n,0) + \varepsilon\mathbb{1}$$

reduces to, at the l, l+1 step,

$$G^{(l+1)}_{even} = (1-\varepsilon m)G^{(l)}_{even} - \varepsilon\not{\phi}G^{(l)}_{odd} + \varepsilon\mathbb{1} \qquad (4\cdot13)$$

$$G^{(l+1)}_{odd} = (1-\varepsilon m)G^{(l)}_{odd} - \varepsilon\not{\phi}G^{(l+1)}_{even}$$

where one evaluates (4.13a) first, and then (4.13b) (with the origin an even site). The boundary conditions used in our work were periodic in space, and fixed in time. An investigation by Bowler et al [1984] into varying these conditions led to only a 1-2% effect in the propagators.

A fairly heavy usage of host CPU time resulted from the program details, given that each time-slice green function has to be transferred from disc to DAP store, repeated for each choice of Γ. This led to some restraint on the number of 4-quark mesons that were investigated. It also precluded adding, in general, Fierz re-arranged terms for the vector and tensor states; this would have required order(16^2) additional calculations for each operator. For the particular case of the 0^{++}, we report below on a test of the expected degeneracy in mass between 2-qf and 4-qf simulation.

In order to check the program, we calculated $Q\bar{Q}$ meson masses at each of the three quark mass values, and compared with Bowler et al [1984]. At the lowest quark mass, the quark green functions were precisely those used in the simulation of Bowler et al. At the intermediate value, corresponding to a value used by Bowler et al, and at the highest value, which did not correspond to one of

their parameters, the masses obtained from recalculated quark propagators, agreed with that analysis. In all these calculations, we used the same criterion of convergence in the Gauss-Seidel algorithm.

We find for the critical value of the hopping parameter k, lattice and inverse lattice spacing, and m_ϱ in lattice units

$$\begin{aligned} k_c &= (0.1698 \pm 0.0008) \\ a &= (0.131 \pm {}^{0.005}_{0.013})\ \text{fermi} \\ a^{-1} &= (1510 \pm {}^{190}_{60})\ \text{MeV} \\ m_\rho a &= (0.510 \pm {}^{0.022}_{0.058}) \end{aligned} \qquad (4.14)$$

These results are in good agreement with those of Bowler et al [1984] who find

$$\begin{aligned} k_c &= (0.1695 \pm 0.0007) \\ a &= (0.136 \pm 0.008)\ \text{fermi} \\ a^{-1} &= (1450 \pm 90)\ \text{MeV} \\ m_\rho a &= (0.530 \pm 0.030) \end{aligned} \qquad (4.15)$$

by using five values of the hopping parameter, as opposed to the three values that we consider. We thus conclude that there is a roughly equivalent measure of significance in our results.

Let us now turn to the 4-quark states of (4.11). We demonstrate in figures 2 and 3 the behaviour of the log-ratios for two of these mesons. Figure 2 is the 0^{++} constructed from two rho $Q\bar{Q}$ operators (y-components) and is in the assumption of two quark flavours. Figure 3 represents the same calculation in the 4 quark flavour assumption. We shall deal with the comparison of these graphs immediately below. Figures 4 and 5 are included, at

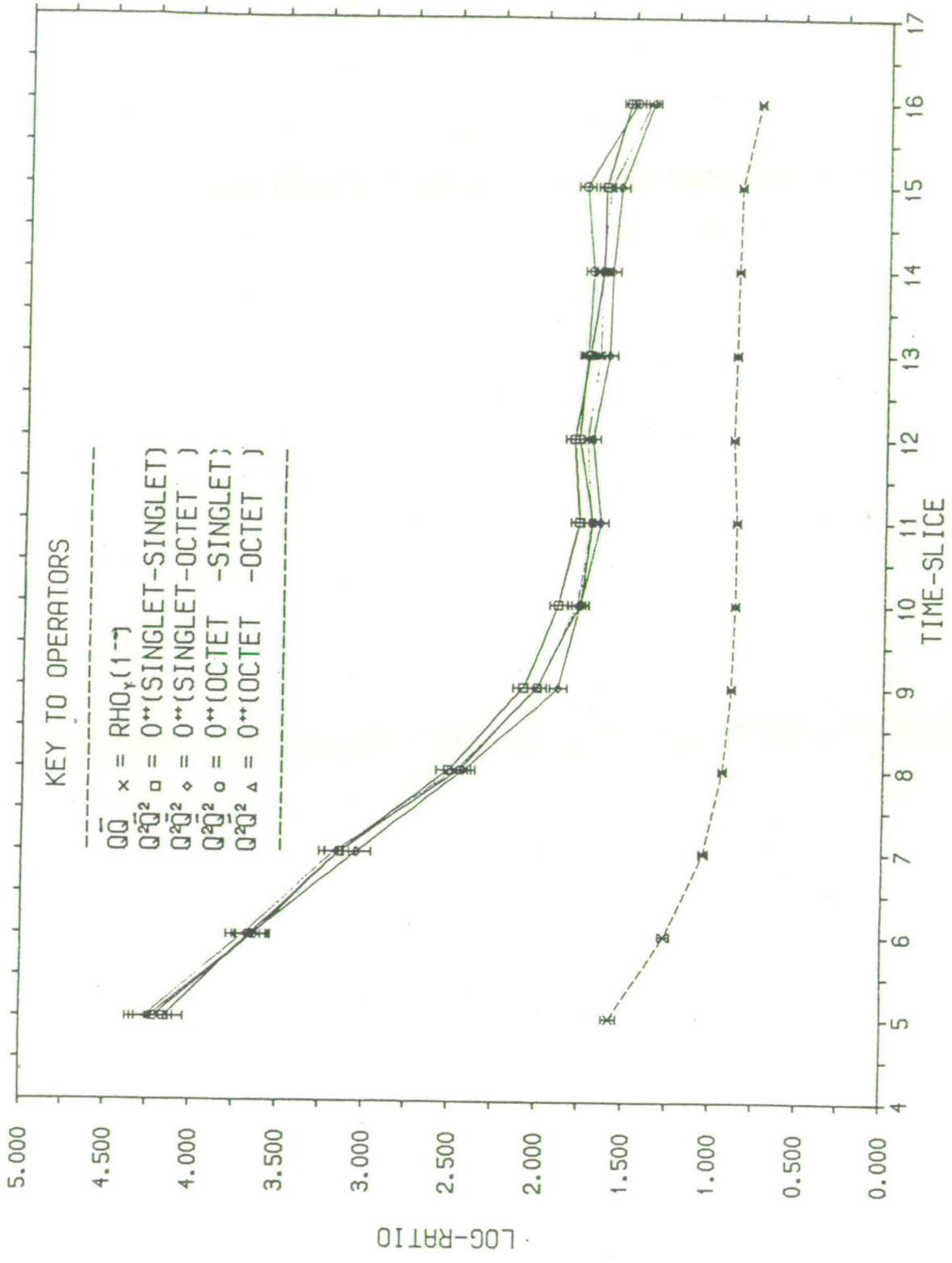

Figure 4.2 Log-ratio plots, i.e., m(t)= ln(G(t)/G(t-1)) versus time-slice t for the 0^{++} 4-quark meson in the two quark flavour analysis. Shown here is the y-component of the $\varrho\varrho$ scalar product at m_q =3.1746

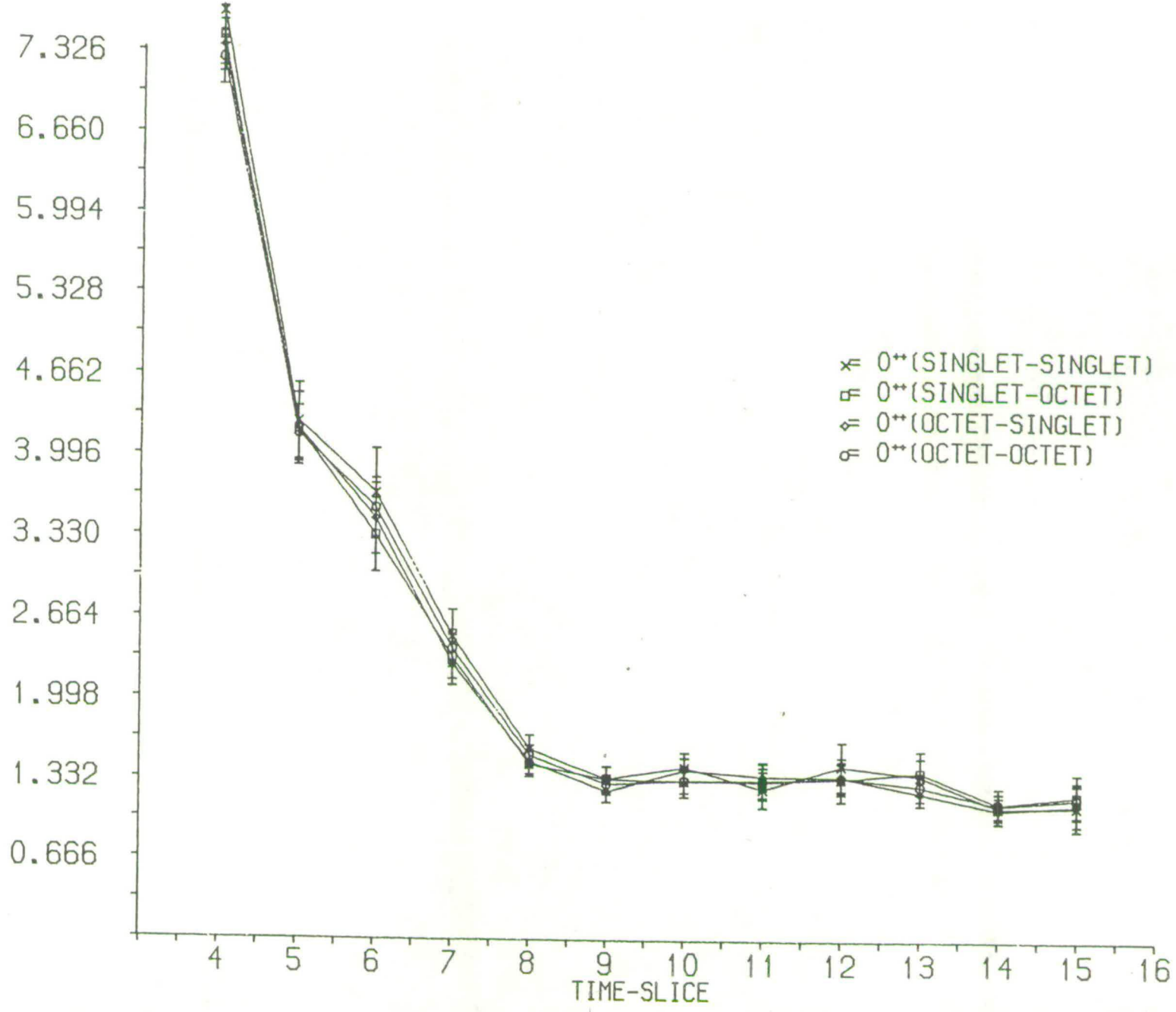

Figure 4.3 Same as Fig. 4.2 but in the approximation of four different quark flavours, $m_l = 3.0769$.

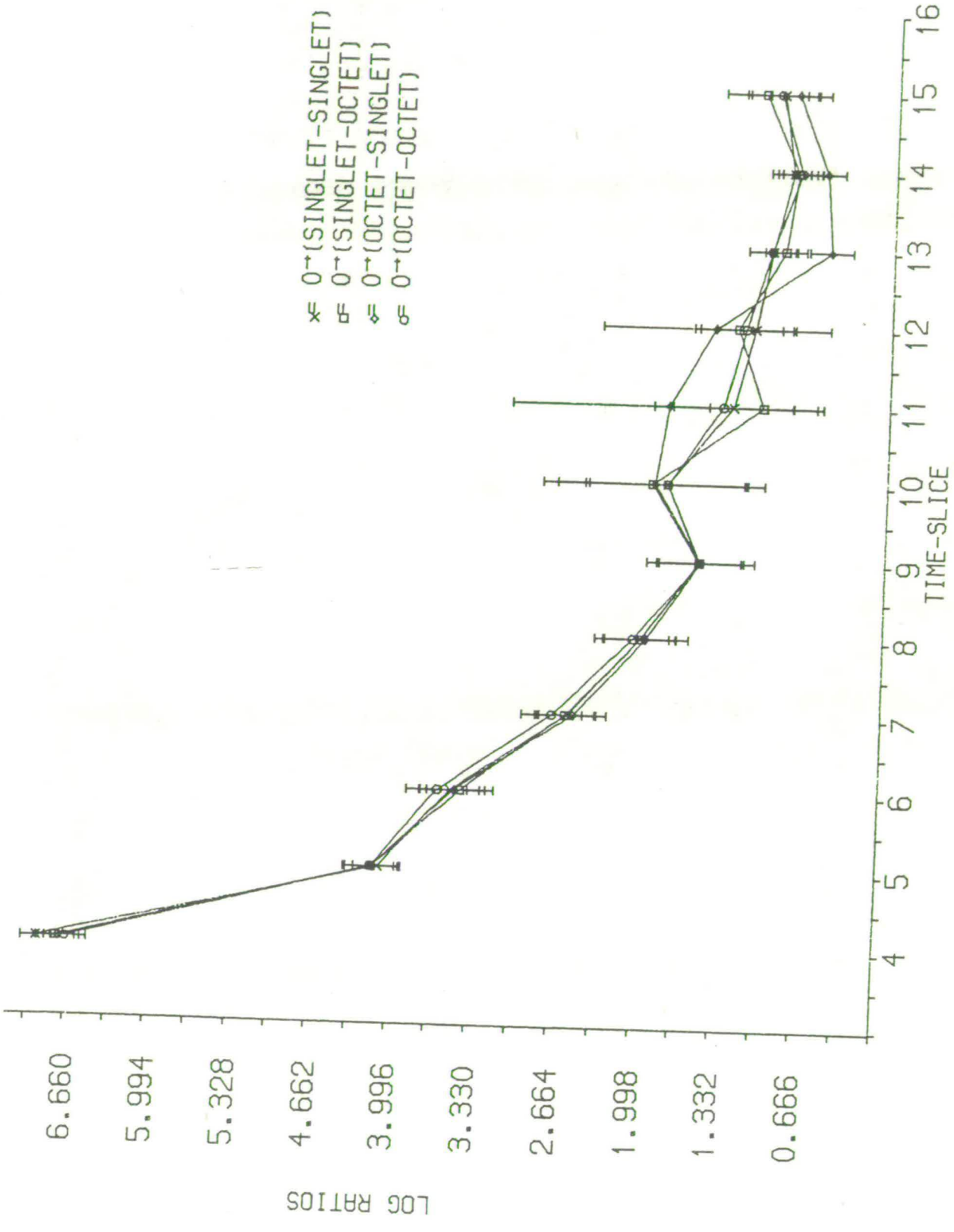

Figure 4.4 The same plot as Fig. 4.2 for the 0^{-+} non-exotic. Note that the noise is significant around time-slice 9-10.

$m_q = 3.0769$

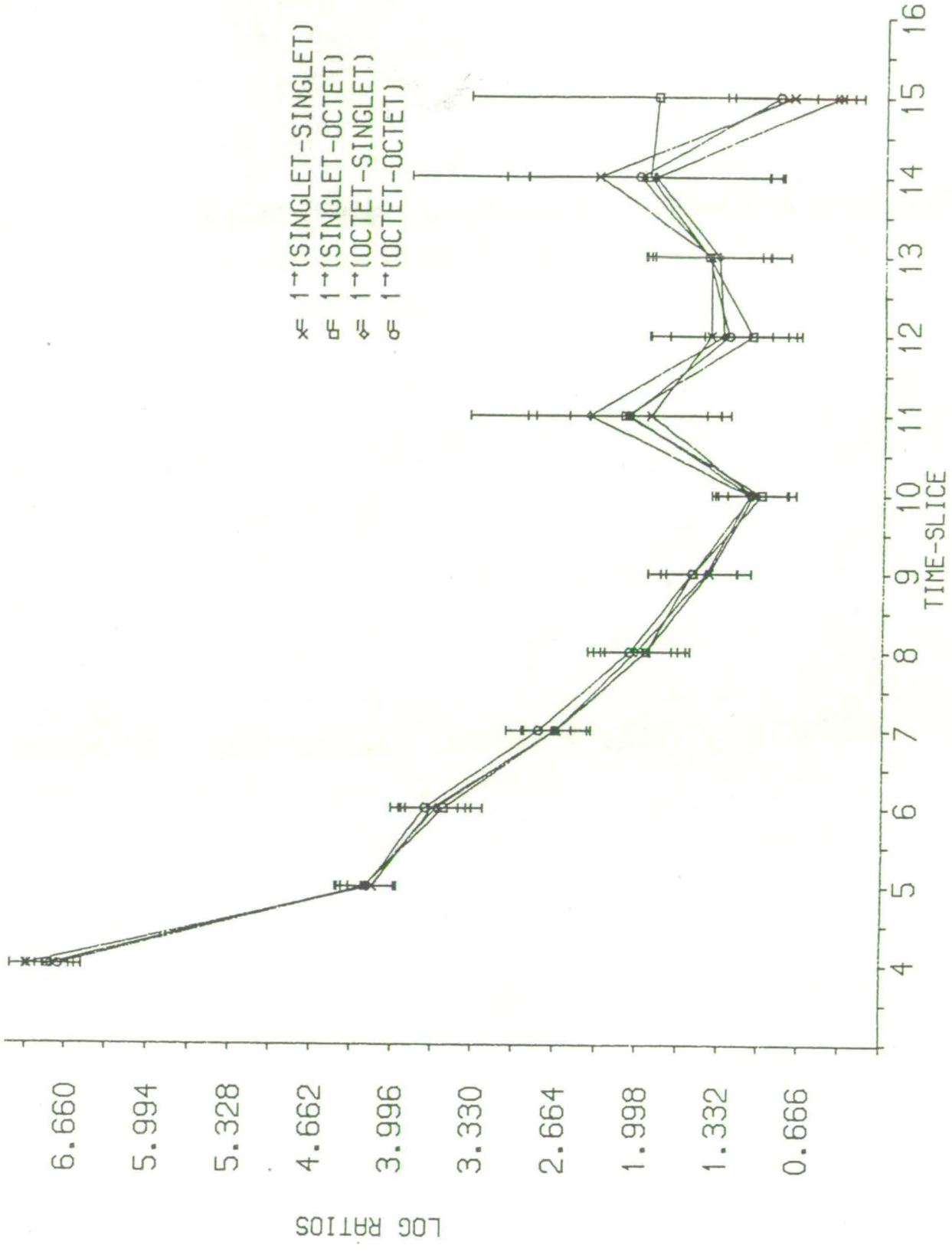

Figure 4.5 Same as Fig. 4.2 for the 1^{-+} exotic 4-quark meson. $m_q = 3.0769$

this stage, merely for comparison sake, and represent the same plot in the cases of the 0^{-+} and 1^{-+} mesons. The detail on these graphs is discussed in section 4.4. An overall impression that one gets from all these figures is the extent to which the propagators are generally "well-behaved" only up to time slices 9-10. The suggestion is that here the amplitudes on decaying exponentials are not large enough to allow the greater extrapolation in time, without higher statistics. This will be an important point when considering the success of this approach to 4-quark meson masses.

In table 1, we give the results of the calculation, for the operators of (4.11), at the 3 quark mass values quoted.

Comparing the 2 quark-flavours (2-qf), and the 4-quark flavours (4-qf) approximations, for the 0^{++} state, one sees immediately that the errors in the latter are significantly smaller than in the former although the results agree within those errors. It was found, moreover, that some colour combinations of components in the $\varrho\varrho$ (Lorentz) inner product contributing to the 2-qf scalar propagator were comparable with the noise level: no masses could be extracted. All 4-qf operators, however, showed good, i.e., roughly constant, asymptotic behaviour. The fact that one cannot say a priori which operators coupling to a particular channel will perform "best" has also been found in e.g. nucleon mass measurements [Bowler et al 1984], where the unanticipated small residues measured for one particular operator denied a reliable mass estimate. Later, we will observe that this also affects mass measurements on the non-exotic 0^{-+} 4-quark meson (in the 4-qf approximation). In any event, the larger errors in the 2-qf results arose specifically from the the greater spread in the mass estimates from the four colour sums over the

m_q	m_{π^2}	m_ρ	$m(0^{++}(\pi))$	$m(0^{++}(\rho))$	$m(1^{+-})$	$m(0^{++}(\pi))$	$m(0^{++}(\rho))$
3·2895	0·986±0·02	1·058 ± 0·019	2·070± 0·026	2·156 ±0·017	2·199 ± 0·016	2·056±0·041	2·167 ± 0·019
3·1746	0·640±0·021	0·874± 0·015	1·663 ± 0·031	1·761 ± 0·018	1·787 ± 0·018	1·665 ± 0·067	1·827 ± 0·052
3·0769	0·384± 0·020	0·721 ± 0·013	1·274 ± 0·019	1·369 ± 0·011	1·527 ± 0·028	1·291 ± 0·051	1·392 ± 0·042
m_c 2·944 ± 0·010	0·000± 0·039	0·510± $^{0·022}_{0·058}$	0·786 ± $^{0·048}_{0·103}$	0·889 ± $^{0·029}_{0·109}$	1·088 ± $^{0·056}_{0·100}$	0·821 ± $^{0·070}_{0·161}$	0·939 ± $^{0·070}_{0·130}$

Table 4.1 Mass estimates for all the quoted operators at the various values of m_q. The first set of 4-quark operators are those for 4 quark flavours, the second are for two quark flavours.

statistically significant range of time steps.

From now on, all results quoted will specifically ignore contributions from quark annihilation graphs which would lift the mass degeneracy in the 4-quark sector.

In interpreting the data in the 0^{++} channel, two possibilities arise. Firstly, one might discover a 4-quark bound state, below the mass of two pions. Secondly, the data might demonstrate a two pion cut in the spectrum of that operator. If it were assumed that two non-interacting pions would appear, then a fit of the data to the 2 boson propagator

$$\Delta(n_4) = A\,|n_4|^{-3/2} \exp(-m_1(n_4)|n_4|) \qquad (4.16)$$

instead of

$$\Delta(n_4) = B \exp(-m_2(n_4)|n_4|) \qquad (4.17)$$

would be appropriate [Goodyear 1984]. In figure 6, we illustrate the extent to which the "modified" propagator form (4.16) would shift the mass estimates for the scalars. That is, the logarithms of (4.16) and (4.17) are plotted, versus time slice, for a mass $m_1(n_4)=m_2(n_4)=2m\pi$. The actual 0^{++} log propagator data clearly follows (4.17). However, in attempting a free fit to the logarithm of (4.16), it was found that the masses were decreased typically 12%-18% (essentially because of the $t^{-3/2}$ factor) and hence $m(0^{++})/m_\pi < 2.$ with the premise. The implication is, that on the lattice, the pions are interacting and we discuss below other evidence for this. Indeed, since the radii of $Q\bar{Q}$ mesons are likely to be comparable with their separation on this size of lattice, (volume of space-time), one would expect some interaction, i.e., the simple exponential should be used. Finite size effects will be important here of

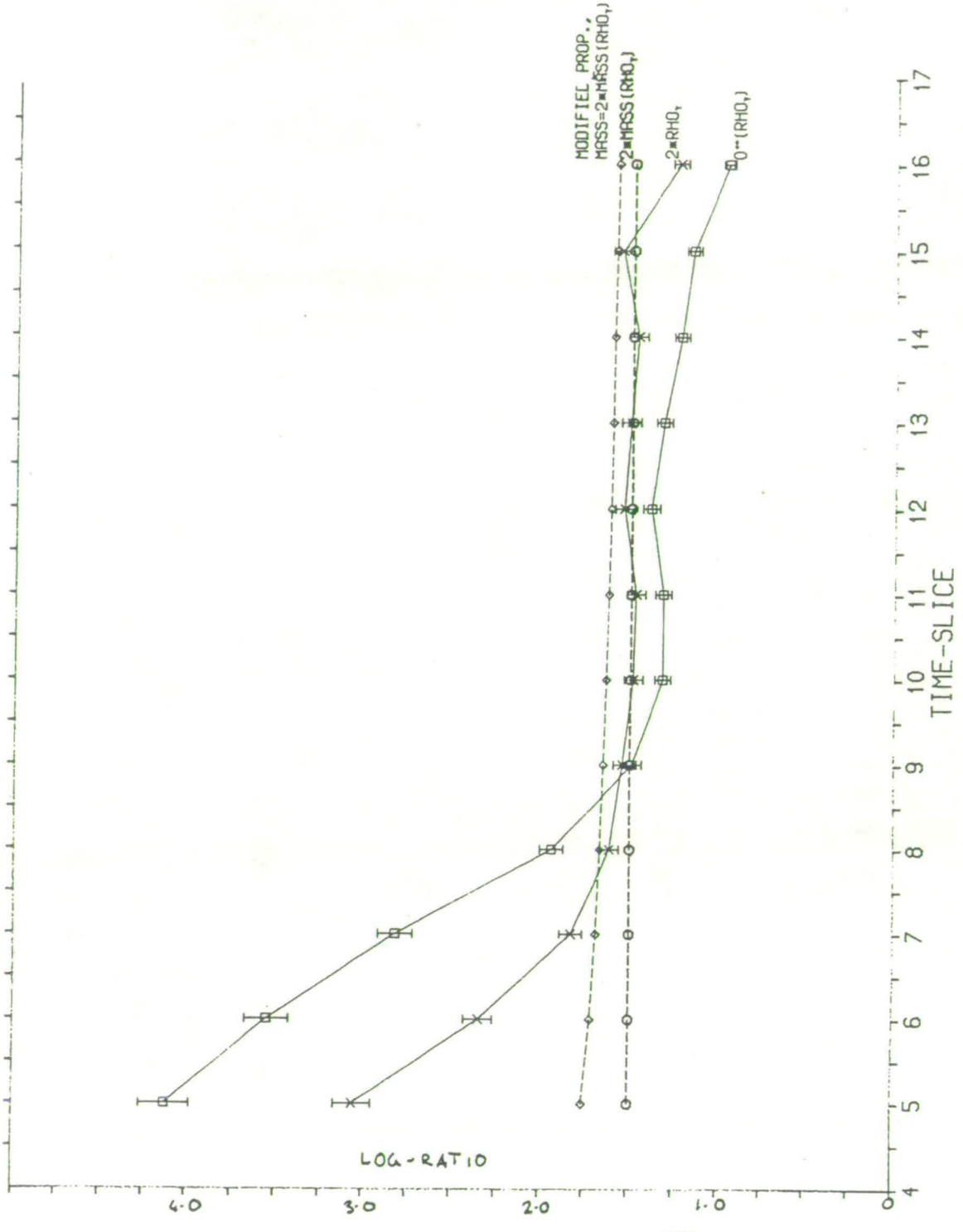

Figure 4.6 The effect of including the $t^{-3/2}$ prefactor on the fitted propagator function. The squares indicate the actual 0^{++} data (with ϱ_y "basis" operators). The crosses are the scaled data for the ϱ $q\bar{q}$ meson (to yield $2m_\varrho$ for comparison). The hexagons then show the extracted mass from the "cross" data and the diamonds show the "mass-shift" that results from plotting eqn (4.16) instead of (4.17) using $2m_\varrho$. $m_q = 3.0709$

course, but the evidence is for a bound state at threshold. One can estimate the value of n_4 where (4.16) and (4.17) will agree within the typical quoted error, ε, i.e., $m_1(n_4)=m_2(n_4)+\varepsilon$. We find that, at the very least, an order of magnitude greater value of n_4 is required.

The relative smallness of the volume of space-time investigated on the lattice thus allows us to probe effectively the internal structure of these 4-quark states. The "crossover" from bound state to 2π cut, as observed by Fucito et al, does not occur. On larger lattices giving an equality between mass estimates from the two different propagators, one could not tell a "resonance" state from the 2-boson cut. For example, in the 0^{++} channel, the two pions would presumably separate to the distances indicated (i.e., minimising the effective mass, see below) and perhaps all interaction or structure would be lost. The lattice size (i.e., infra-red cut-off) thus works in our favour and, as we shall see later, helps to establish resonances in most of the cases (as opposed to two particle "systems"). However, we should bear in mind that this is an artifact of the lattice itself.

More evidence suggesting the interpretation of the 0^{++} as a two pion system is given in figure 7. The crucial observation here is that while the vanishing of m_π^2 as $m_q > m_c$ is found, the ratio of $0^{++}/\pi$ masses is roughly constant for all m_q regardless of the initial $Q\bar{Q}$ operators used to construct the 0^{++}. This point is to be contrasted strongly with the results of Fucito et al [1983]. Also included in this diagram, for comparison's sake, is the corresponding behaviour of the 1^{+-}, but not that of the 2^{++} state. In the latter case, we were unable to deduce a reliable mass estimate from the erratic time-dependent masses produced. The general tensor (i.e., not the traceless form of (4.1)d) is

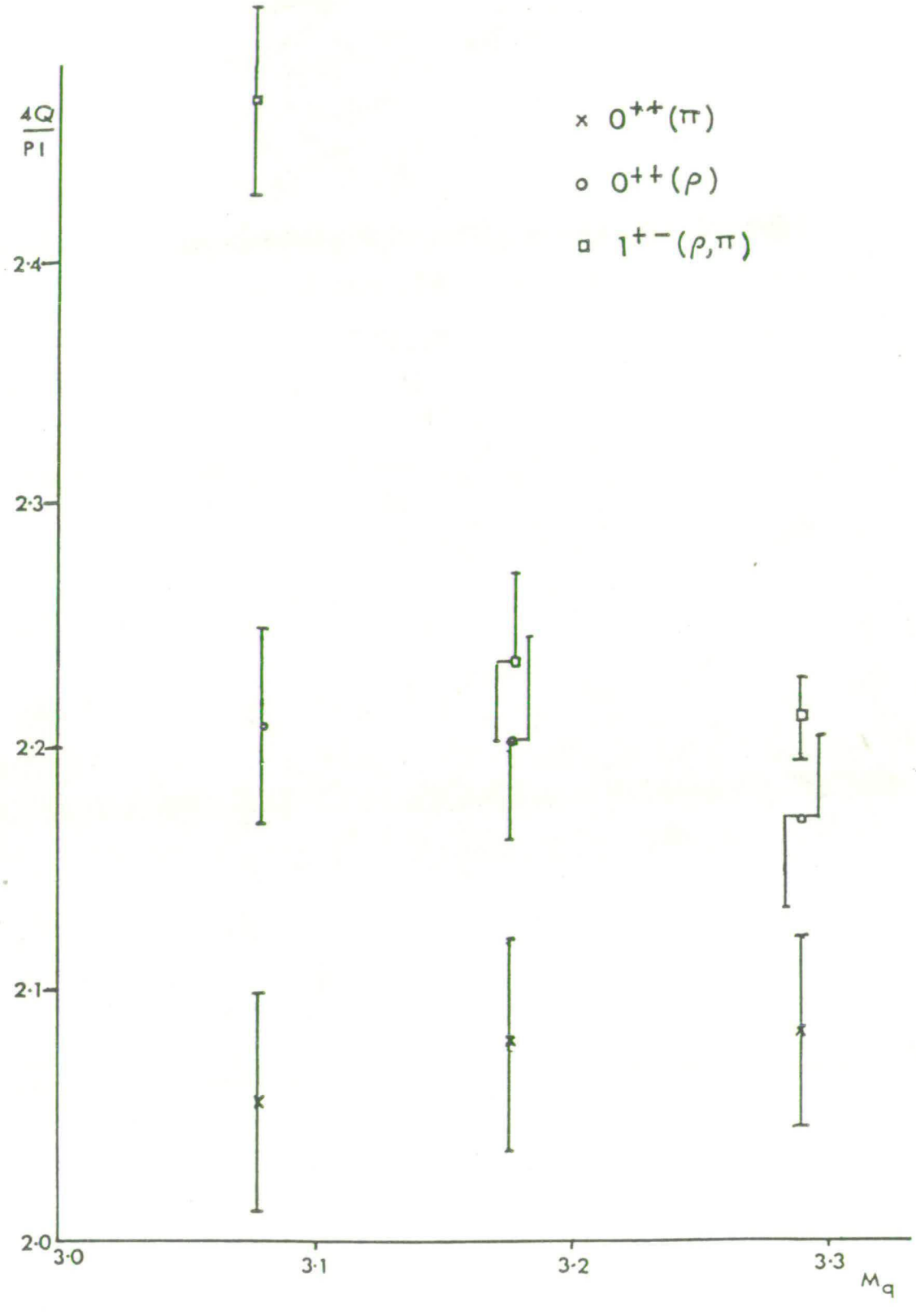

Figure 4.7 Mass ratios of 0^{++} 4-quark operators and the 1^{+-} (as an example of an operator that should not depend on m_π) to the pion mass at all m_q

dominated by the scalar signal; there is no significant spin two component. We are thus unable to say whether a bound state or two pions or two rhos appear in the "asymptotic" region. Bag model calculations [Jaffe 1977a,b] however do not suggest spin 2 $Q^2\bar{Q}^2$ lying much below 2 GeV, whereas most of the "interesting physics" is in spin zero and one mesons around 1-2 GeV. It would be, of course, possible to consider more general operator constructions coupling to $J^P=2^+$.

Fig.8 portrays the $(\text{mass})^2$ of the calculated $0^{++}(\pi\pi)$, $0^{++}(\varrho\varrho)$ and $1^{+-}(\pi\varrho)$ operators, and <u>all</u> but the 1^{+-} (included here again simply to highlight this observation) show a good linear fit. Table 2 correspondingly gives values for the $(\text{mass})^2$ at m_c from a least-squares analysis.

Of the emerging dynamical picture of two pions on the lattice, The major conclusion has to be that even if a $Q^2\bar{Q}^2$ 0^{++} had been successfully constructed (at the space-time origin), 2π appears in the "asymptotic" region, indicating that the 0^{++} simply falls apart. However, when the evaluation of the "effective" mass of the rest-frame propagator is made, we deal in this case with the rest-frame of the <u>system</u>, not that of a single particle (or 4-quark resonance), as in $Q\bar{Q}$ calculations. In other words, one should <u>expect</u> a 3-momentum contribution to the effective mass. Thus we measure for each pion

$$E_\pi(n_4) = m_\pi(n_4)\left[1 + \frac{k_\pi^2(n_4)}{m_\pi^2(n_4)}\right]^{1/2} \qquad (4.18)$$

where $k_\pi(n_4)$ is the pion 3-momentum. Indeed, the $0^{++}/\pi$ mass ratio shows a statistically significant increase over the (particle) rest-frame value of 2. Table 3 details the contribution to the total energy (assumed to be due to a

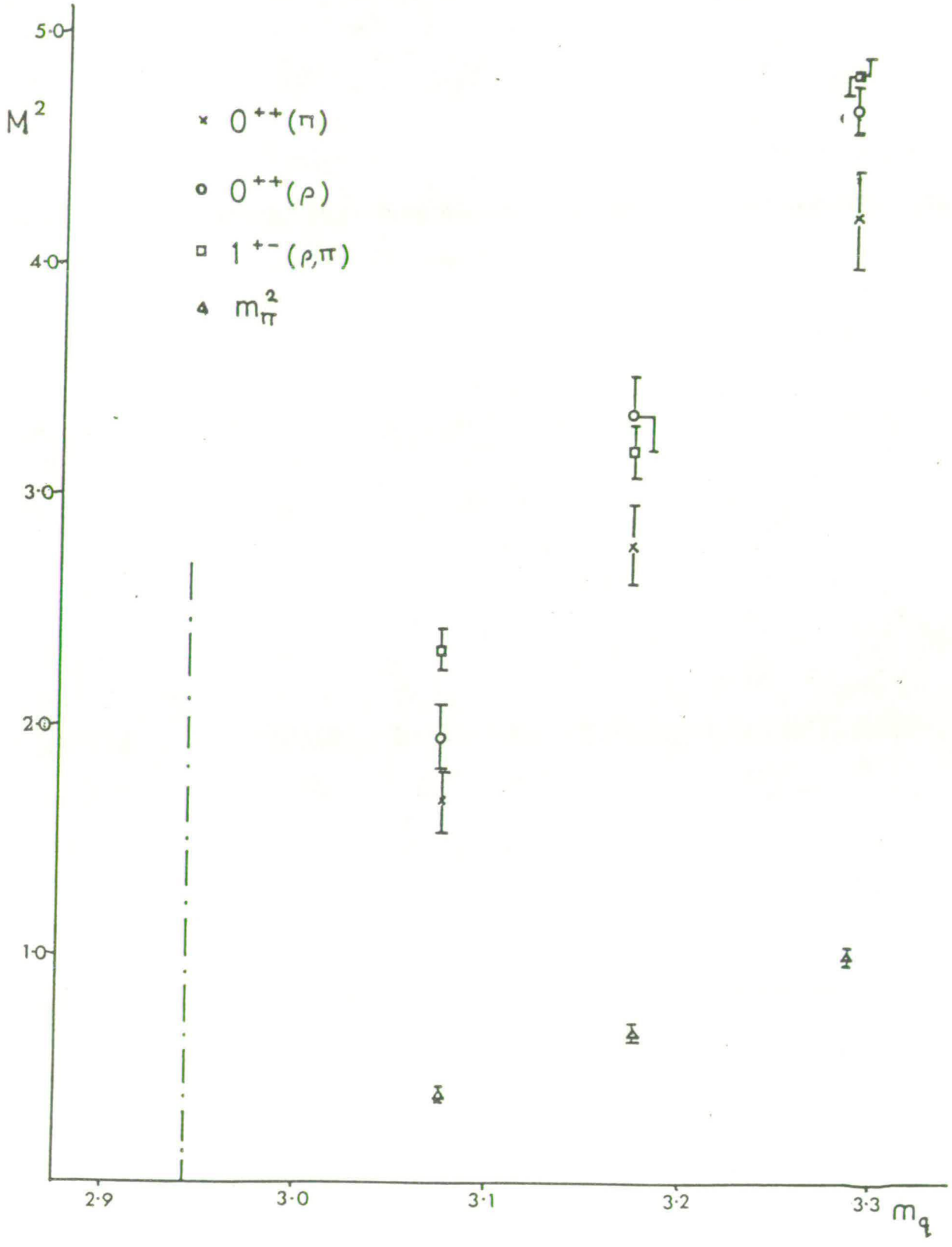

Figure 4.8 Plot of (mass)^2 of the 0^{++} (and the 1^{+-} again) to indicate the "pion-like" behaviour of those scalar states.

operator	$(\text{mass})^2$
$0^{++}(\pi)$	$-0.073\ {}^{+0.155}_{-0.343}$
$0^{++}(\rho)$	$0.121\ {}^{+0.101}_{-0.291}$
$1^{+-}(\rho,\pi)$	$0.653\ {}^{+0.197}_{-0.352}$
ρ	$0.133\ {}^{+0.039}_{-0.102}$

Table 4.2 Values of $(\text{mass})^2$ at the critical quark mass (vanishing m_π) for the relevant scalar operators (estimated by least squares). To illustrate the significance of the error bounds, both 1^{+-} and ρ are also included.

m_q	$0^{++}(\pi)$	$0^{++}(\rho)$	Δk
3.0769	119 ± 42	234 ± 23	115 ± 48
3.1746	239 ± 57	385 ± 36	146 ± 67
3.2895	377 ± 81	541 ± 55	164 ± 98

Table 4.3 Estimation of the effects of non-zero momentum in the effective mass estimates for $0^{++}(\pi\pi)$ and $0^{++}(\rho\rho)$ (by taking half the difference of the 4-quark masses from $2m_\pi$). For comparisons sake, these are translated into MeV at each m_q.

non-zero momentum vector). The lattice itself necessarily provides an infra-red cut-off and the results for each of the $0^{++}(\pi\pi)$ and $0^{++}(\rho\rho)$ operators should be compared with the smallest value of lattice k that is possible. For periodic spatial boundary conditions, the mass centres (assuming that we can adopt this point of view) of the two particles can at most be separated by four lattice spacings (total lattice spatial extent is eight lattice spacings), equivalent to an addition to the effective mass of each pion of approximately 380 MeV (compare again with table 3).

In the C=-1 pseudo-vector channel, extrapolating linearly to the critical quark mass, we find

$$m(1^{+-})/m_\rho = 2{\cdot}13 \pm {}^{0{\cdot}40}_{0{\cdot}28} \qquad (4{\cdot}14)$$

$$m(1^{+-}) = (1640 \pm {}^{310}_{230})\ \text{MeV}$$

This is compatible with the above comments because any possible interpretation of the 1^{+-} as simply $\pi+\rho$ using the respective particle masses plus any 3-momentum contribution does not adequately account for the quoted mass ratios.

Two points are raised by the results of table

(1) In the 0^{++} channel, as m_q decreases, the fraction of the total energy due to the momentum contribution declines; a fact, we believe to be caused by the increased "overlap" of the two pion "bags" as $k \to k_c$, from below. Heuristically, we consider that particle radii, depending on quark propagation, will be roughly proportional to k^l, where k is the hopping parameter and l, some power related to the "average" path-length. That is, smaller k implies a smaller hadron. Unsurprisingly, the best agreement with the

expected result obtains for $0^{++}(\pi\pi)$ at the highest quark mass value (the lowest k, where the pions are, in some sense, more localised). Qualitatively, we understand that attractive magnetic gluon interactions will tend to reduce the interaction energy, the scale of which will depend on the degree of "overlap". Note that in this lattice scheme, in contrast to the conventional MIT bag-model, there will be no rigid constraint that the gluon flux or quark fields vanish at some nominal bag boundary, leading to the possibility of interactions between "leaky" bags.

We stress however, that this result is an artifact of working with an infra-red cut-off; on larger lattices this effect would presumably be absent.

(2) The consistent difference of $k_\pi(t)/m_\pi(t)$ between $0^{++}(\pi\pi)$ and $0^{++}(\varrho\varrho)$ for <u>all</u> m_q is due, we believe, to finite-size effects derived from the two rho operators in the $0^{++}(\varrho\varrho)$ definition. Because of this, there is no real expectation that the value of $k_\pi(t)$ should be of the order of 380 MeV. Note, however, that the reasonably consistent difference in the estimates of the lattice $k_\pi(t)$ between the $0^{++}(\pi\pi)$ and $0^{++}(\varrho\varrho)$ operators is suggestive of finite size effect, which, importantly, act in a direction opposite to the supposed residual gluon interactions.

The addition of some 760MeV (the relative 3-momentum contribution) to the mass of the two pions, means that the next pole in the spectrum of the 0^{++} operator, possibly a 4-quark resonance, must be heavier by at least this amount (n.b., lattice 3-momentum is not a continuous variable). From the expected degeneracy of I=0,..,I=2 4-quark mesons, one should contrast these 0^{++} results with Jaffes's corresponding result [1977a,b] of (1150±50) MeV (the 36-dimensional flavour representation). This is comfortably

greater than the ~760 MeV addition to $2m_\pi$. This value also suggests why the 1^{+-} meson does not fall apart into $\pi+\varrho$ (~900 MeV).

The results of this work indicate no real agreement with that of Fucito et al [1983]. In the 0^{++} 4-quark sector, all masses lie above that of $2m_\pi$. We have shown that the choice of the Γ matrix structure, i.e., the $Q\bar{Q}$ operator basis, is irrelevant in that the extrapolated $(\text{mass})^2$ of the resulting 4-quark operator vanishes as $k \to k_c$, and we would expect that therefore the comparison of $\Gamma_1=\Gamma_2=1$, their ε operator, and the $\pi\pi$ operator would lead to an identical result. Both operators must couple to the lowest pole in the spectrum of the 0^{++} operator, as we have found. Their results may be an effect of the $6^3 \times 10$ lattice they have been using and, we stress that at $\beta=6.0$, one must be wary of the proximity to the deconfinement transition.

There is no reason, of course, to expect accurate estimates of the attractive gluon interaction derived from the data because of the finite size effects: if difficulty is found in putting one meson into the given lattice volume, then problems are virtually guaranteed for two species. Moreover, "mirror reflections" (wrap-around effects due to the periodic boundary conditions) will affect (probably greatly) any attempted estimate of the gluon "potential" in comparison with that in the continuum.

4.4 Masses of other low-spin states

The results of sections 2 and 3 suggest that significant measurements on the 4-quark spectrum are feasible on this

size of lattice, and that we must take the lattice IR cut-off into account when considering any other states. The construction of, and mass calculation from, other $Q^2\bar{Q}^2$ lattice mesons can readily be accomplished using the J^{PC} of more general $Q\bar{Q}$ "basis" operators (quark bilinears) listed in table 4.

Numerical simulations with these were entirely similar to that described in previous sections, involving the same gauge configurations and hopping parameter values.

From all possible combinations of $Q\bar{Q}$ operators in table 4, we selected the following as 4-quark operators (where the $Q\bar{Q}$ basis functions are enclosed in brackets and ? represents the (unobserved quark model exotic) 0^{+-} $Q\bar{Q}$ operator)

$$0^{-+}(\pi\delta)\,;\; 0^{++}(\delta\delta)\,;\; 0^{+-}(\delta ?)\,;\; 0^{--}(\pi ?)\,;\; 1^{++}(A_1,\delta)\,;\; 1^{-+}(A_1,\pi) \qquad (4.20)$$

We comment on a number of points arising from this selection. Firstly, wishing to minimise the number of calculations performed we chose, where possible, only π, δ $Q\bar{Q}$ "basis" operators. One would expect however that all operators with the same quantum numbers should couple to the same state (the lowest mass pole in the spectrum). The particular set of operators chosen represents an attempt to minimise CPU time, and, for example, no attempt was made to investigate the non-exotic 1^{--} 4-quark meson. The second point, which in this case should be emphasised, is that 0^{+-}, 0^{--}, 1^{-+} are all exotic mesons, and so are particularly interesting.

It is, perhaps, noteworthy that in comparison to the sole use of π, ϱ operators, most of these more general

Γ	J	P	C	OP
1	0	+	+	δ
γ_5	0	−	+	π
γ_0	0	+	−	none
γ_i	1	−	−	ρ
$\gamma_5\gamma_0$	0	−	+	π
$\gamma_5\gamma_i$	1	+	+	A
σ_{0i}	1	−	−	ρ
σ_{ij}	1	+	−	B

Table 4.4 The J^{PC} and $q\bar{q}$ meson identification of the 16 $q\bar{q}$ "basis" operators.

propagator signals vanished into noise some 2-3 time steps earlier. The use of the 0^{+-} $Q\bar{Q}$ basis operator may have lead one to anticipate statistical problems in the analysis given that it has no corresponding quark model $Q\bar{Q}$ meson state. However, we obtained results which were statistically as significant as those of any other operator. Even though it was unavoidable in the one case of the 0^{+-} 4-quark meson, its use is doubly significant in that it closes any possible "fall-apart" channel to two $Q\bar{Q}$ mesons involving that 0^{+-} $Q\bar{Q}$ lattice operator.

Let us now review the results obtained in the simulation with firstly the data for the 0^{++} (to complete that discussion), and then the other 4-quark states.

(A) $0^{++}(\delta\delta)$: We emphasised the necessity of exposing the 2π "cut" in any calculation of 0^{++}, arising simply from the lightness of the pion (the approximate Goldstone boson of chiral symmetry breaking). The lowest 0^{++} 4-quark resonance calculated by Jaffe [1977a,b] was some 400 MeV heavier than $m(2\pi)$, though more typical masses (which we must compare with in our approximation) were $\geq$700 MeV higher than $m(2\pi)$. From this simulation, and including a non-zero lattice 3-momentum addition to the "effective mass", we were able to suggest that any resonance in the 0^{++} channel had to be more massive than $\sim(m(2\pi)+ 760)$ MeV (from assuming the dominance of a single exponential in the correlation function at "large" time).

In table 5 we show the results of the mass calculations for both the $0^{++}(\delta\delta)$ and all the other states of (4.20), all m_q. We have not included, for the sake of clarity, corresponding ratios of the $0^{++}(\delta\delta)$to the pion mass (in figure 7) and the 0^{++} $(\text{mass})^2$ extrapolation (in figure 8), but simply present the data in table 5 instead. Typically the

m_q	$m^2(0^{++}(\delta\delta))$	$\frac{m(0^{++}(\delta\delta))}{m(\pi)}$	$m(0^{--})$	$m(0^{-+})$	$m(0^{+-})$	$m(1^{-+})$	$m(1^{++})$
3·2895	$6·833 \pm 0·983$	$2·632 \pm 0·193$	$2·812 \pm 0·210$	$3·154 \pm 0·208$	$3·592 \pm 0·290$	$3·064 \pm 0·119$	$2·951 \pm 0·133$
3·1746	$4·145 \pm 0·509$	$2·545 \pm 0·162$	$2·341 \pm 0·153$	$2·722 \pm 0·203$	$3·588 \pm 0·279$	$2·644 \pm 0·098$	$2·261 \pm 0·090$
3·0769	$2·736 \pm 0·414$	$2·670 \pm 0·213$	$2·003 \pm 0·129$	no fit	$3·468 \pm 0·218$	$1·856 \pm 0·083$	$1·870 \pm 0·068$
m_c 2·944 $\pm$ 0·014	$-0·042 \pm {0·272 \atop 0·748}$	-	$1·484 \pm {0·053 \atop 0·427}$	$1·855 \pm {0·053 \atop 1·131}$	$3·415 \pm {0·008 \atop 0·583}$	$1·109 \pm {0·071 \atop 0·222}$	$1·153 \pm {0·071 \atop 0·288}$

Table 4.5 Tabulation of the masses of all operators used in the final section at the three quark mass values along with the least squares fit at m_c. Included are the values of the $(\text{mass})^2$ and ratio to the pion mass of the $0^{++}(\delta\delta)$ operator.

error bounds are some 3/2-2 times greater on each of these individual measurements (e.g., each of the x,y,z components or each of the four possible colour contractions) than the results reported above in section 3. It may be significant that fitting, for example, the $0^{++}(\varrho\varrho)$ over the same range in time that the $0^{++}(\delta\delta)$ is above noise, results in a mass for the former which is approximately 15% larger than the result we quoted earlier. If, and only if, one could ascribe roughly similar finite size effects to the δ as to the ϱ then this might suggest that all the masses we report on in this section are (at most) too high by roughly this amount. This may be useful to bear in mind, but given the magnitude of the errors we quote, it is not too crucial that this effect may possibly be relevant.

We may conclude from table 5 that all the 0^{++} operators considered do indeed expose the same lowest "pole" (i.e., $m^2(0^{++}(\delta\delta)) \rightarrow 0$ as $k \rightarrow k_c$) and hence do not support Fucito et al [1983] in any respect.

(B) **Other exotic and crypto-exotic 4-quark masses**: Some general comments about the relative magnitudes of the propagator signals and derived errors have already been mentioned, but there are two additional points that we feel that it is important to make. It will be remembered that masses for the vector 4-quark meson masses should, in general, be more reliable (due to averaging over the three possible spin states available). This is underscored by the results of figure 9. However, and more importantly, returning to a point in section 4.2, individual colour combinations of components contributing to both scalar and vector mesons may occasionally fail to give any mass estimate from the two-exponential fit. Essentially, one finds that the residues in the leading exponential are

Figure 4.9 Masses of 0^{+-}, 0^{--}, 0^{-+}, 1^{-+}, 1^{++}, 1^{+-} as a function of quark mass. Also illustrated is the value of the critical quark mass to where the linear extrapolation in masses is carried.

orders of magnitude smaller than corresponding "well-behaved" operators. Since, in the 4-quark calculation, there is an average over the four possible colour contractions, usually at least one of the four operators gives a reliable fit. Only in the case of 0^{-+} at the lowest quark mass did all fail to provide a mass estimate. As a comparison, once again, one should contrast figures 4 and 5 with figures 2 and 3 which contain only π, ϱ basis functions. Thus we are unable to ascribe any real significance to the 0^{-+} mass extrapolation to k_c based on only two values of the hopping parameter.

Using once again the physical mass of the ϱ we find for the measured operators, the masses

$$m(0^{+-}) = (4430 \pm {}^{470}_{460})\text{MeV} \; ; \; m(0^{--}) = (1930 \pm {}^{270}_{360})\text{MeV}$$

$$m(1^{-+}) = (1440 \pm {}^{250}_{350})\text{MeV} \; ; \; m(1^{++}) = (1500 \pm {}^{250}_{430})\text{MeV} \qquad (4.21)$$

All are above the two $Q\bar{Q}$ meson (plus 3-momentum addition) thresholds. One may note that the 0^{-+} mass of $(2400 \pm {}^{320}_{1520})$ MeV with its large uncertainty, is, at best, no more than an order of magnitude estimate.

Previously, we had occasion to compare the results in the 0^{++} channel with the I=0,...,2 (degenerate) multiplet of Jaffe [1977a]. Here, a similar comparison of the the $J^P=1^+$ multiplet finds (1450±50) MeV, whilst the lattice simulation records $m(1^{+-})=(1640 \pm {}^{320}_{220})$ MeV and $m(1^{++})=(1500 \pm {}^{250}_{430})$ MeV. One notes, incidently, that the lowest masses in the Bag Model [Jaffe 1977a] for vector 4-quark mesons are some 200 MeV below this (the 9-dimensional flavour multiplet).

The appearance of low-mass vector exotic and crypto-exotic states suggests the probability of mixing

with $Q\bar{Q}$ and $Q\bar{Q}G$ (hybrid) mesons. As noted by Barnes, Close and de Viron, [1983], one might have expected the mass of the 1^{-+} hybrid to be substantially lower than that of the corresponding 4-quark exotic. Our calculation does not show this. Either a re-scaling of the MIT bag-model spectrum is required or mixing between the 4-quark and $Q\bar{Q}G$ wave functions is indicated.

The masses of the scalars come out heavy, $\geq$2 GeV. It is unfortunate that the 0^{-+} meson gave such an unreliable mass. Some indication as to whether it lay in the region of the controversial $\iota(1400)$, (probably a radially excited η) may have aided understanding of the features of that state. The 0^{--}, in contrast to the 0^{+-}, is within an energy region where its' experimental discovery might be expected. As a comparison though, we might note that the spectrum of scalar hybrid exotics as derived from e.g., QCD sum rules [Govaerts, de Viron, Gusbin and Weyers 1984, Govaerts, Reinders and Weyers 1985] is over 3 GeV.

The general feature of these calculations appear to be the expectation that non-exotic (e.g., 0^{++}, 1^{++}, ..) 4-quark mesons are not overly massive, as suggested by Jaffe [1977a], whilst the scalar exotics are ($\geq$ 2 GeV), and the vector mesons, in general (i.e., exotic or non-exotic), should be experimentally accessible.

CHAPTER 5

Hybrid Mesons in Lattice QCD

5.1 Introduction

A lattice investigation of hybrid, i.e., $q\bar{q}g$ configurations, must necessarily contend with non-locality in any gluon field operator definition. The fundamental variables in lattice gauge theory are the gauge link fields. In chapter 2, we demonstrated that, in the continuum limit of the lattice field theory (in the notation of that chapter), one recovered from the logarithm of the plaquette operator, the field strength tensor i.e.,

$$U_{\square} = e^{ia^2 F_{\mu\nu}^{a}(n)\tau^{a}}\left(1 + \mathcal{O}(a^3)\right) \qquad (5.1)$$

where

$$U(n,\mu) = e^{\frac{ia}{2} A_{\mu}^{a}(n)\tau^{a}}\left(1 + \mathcal{O}(a^3)\right) \qquad (5.2)$$

The physical gluon fields, i.e., the transverse magnetic or electric (TM or TE) modes are elements of this $F_{\mu\nu}$, in a similar manner to the definition of physical photons in the Electromagnetic field strength. Thus we define

$$\begin{aligned} &(TE) \qquad E_i^{a} = F_{oi}^{a} \\ &(TM) \qquad B_i^{a} = \tfrac{1}{2}\epsilon_{ijk} F_{jk}^{a} \end{aligned} \qquad (5.3)$$

The lack of locality represented by (5.1) presents us with a number of problems. Firstly, of central importance to the lattice formulation of gauge theories, we must impose strict gauge transformation properties on any candidate gluon field at any arbitrary lattice site n. Secondly, the lattice $F_{\mu\nu}(n)$ must be uniquely associated with that site n, where the colour contraction with the

$q\bar{q}$ colour octet operator is to be performed. However, we recall that each link variable is associated with two lattice sites, and each plaquette with four. So, from the definition (5.1), we choose a combination of plaquette variables that enforce the above requirements. We consider the following path-ordered operator, traceless in colour and spin [Mandula, Zweig and Govaerts 1983]

$$F_{\mu\nu}(n) = \frac{1}{8ia^2} \sum_{\text{plaquettes } \square} \left(U_\square - U_\square^\dagger \right)_{\text{traceless}} \qquad (5.4)$$

see figure 1. One can readily check that, as $a \to 0$, in a similar manner to that undertaken in chapter 2, (5.4) reduces to the continuum field strength.

For any non-local lattice operator, one should investigate the extent to which the lattice field carries over a unique J^{PC} from the continuum.That this is relevant follows from considering the decomposition of O(4) irreducible representations under the restriction to finite subgroups. In general, any irreducible representation of O(4) will decompose into several irreducible representations of the hypercubic lattice group (i.e., the symmetry group of the 4-dimensional cubic crystal lattice). In turn, these will decompose, again generally non-uniquely, into (3-dimensional) cubic lattice representations [Baake, Gemundes and Oedingen 1982, 1983; Birman and Chen 1971; Verstegen 1984]. In determining which lattice operators contribute to which J^P (continuum) states, one will then inevitably encounter mixing between, say, exotic and non-exotic quantum numbers. There is enough remaining symmetry in the hypercubic group, however, to be able to explicitly identify those lattice operators whose additional spin contributions are much higher (and presumably then also more massive). With these operators, one might hope that lattice Monte-Carlo studies would find them well

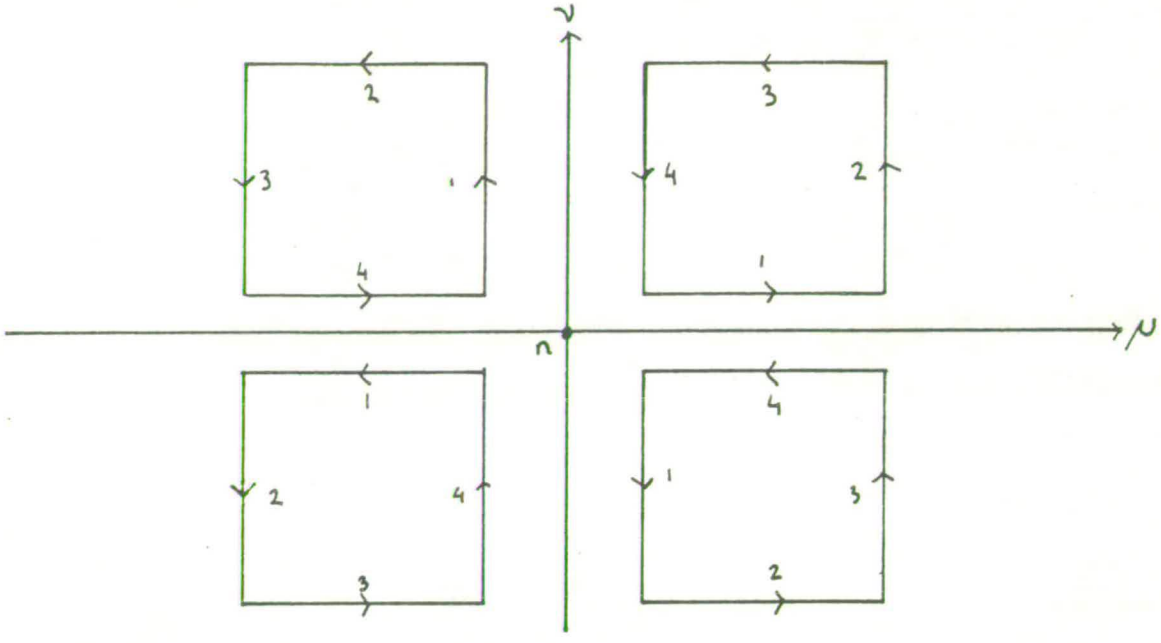

Figure 5.1 The definition of the lattice gluon field, i.e., eqn (5.4).

$$F_{\mu\nu}(n)=(1/8ia^2)[\Sigma_{\square}U_1U_2U_3U_4 - \text{h.c.}]_{\text{traceless}}$$

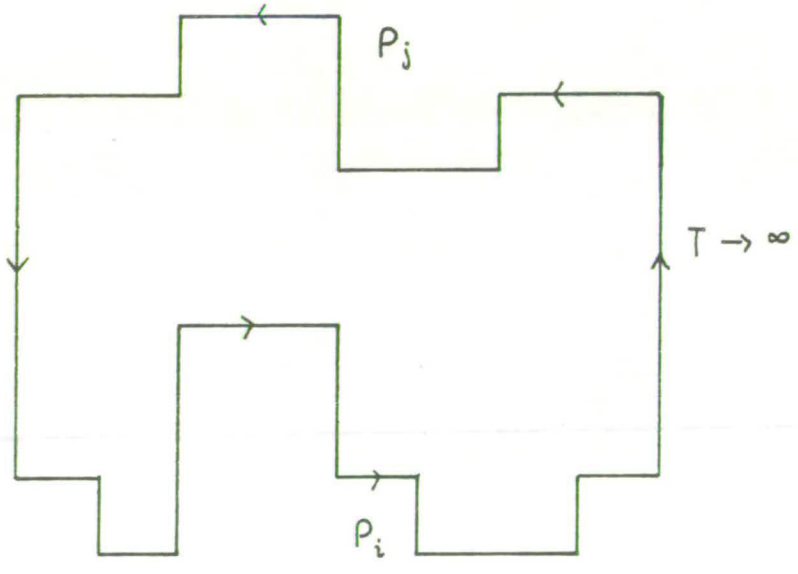

Figure 5.2 The heavy $q\bar{q}$ potential with J^{PC} classified under the lattice rotation/reflection group is extracted from the eigenvalues of this operator, traced in colour space. All "excursions" from the straight string are in space-like directions.

exposed. One can also anticipate that by employing different irreducible lattice fields which contribute to the same J^{PC}, the extent to which they overlap will measure the degree to which the lattice is close to the continuum.

Thus, having defined our lattice gluon field, we now wish to explore the symmetries of the hypercubic lattice, We will then be able to define covariant lattice hybrid fields and measure their correlation functions. A discussion on the lattice symmetry will moreover provide us with a natural introduction to, and a better understanding of, the calculation of Griffiths, Michael and Rakow [1983]; Campbell, Griffiths, Michael and Rakow [1984] on the hybrid spectrum (for heavy quarks) which utilises various closed gauge link paths. This study and its particular problems, will be valuable as a comparison with the difficulties that are encountered in our later approach.

5.2 The Hypercubic Lattice Group

The symmetry group of the 4-dimensional hypercubic lattice is generated by $\pi/2$ rotations in each of the six lattice planes [Mandula et al 1983; Verstegen 1984]. There are 192 elements, grouped into 13 conjugacy classes. Thus there are 13 irreducible representations. In order to demonstrate clearly the spin content of each of these irreducible representations, we will use the isomorphism

$$O(4) \cong (SU(2) \otimes SU(2))/Z_2 \qquad (5.5)$$

Thus a rotation of $\pi/2$ in the 1-2 plane is such that [Mandula et al 1983; Verstegen 1984]

$$R_{12}\left(\tfrac{\pi}{2}\right) = R_3\left(\tfrac{\pi}{2}\right) \otimes R_3\left(\tfrac{\pi}{2}\right) \qquad (5.6)$$

Any rotations that involve the 4-direction, by contrast, affect the $SU(2)xSU(2)/Z_2$ decomposition oppositely [Verstegen 1984]. Thus

$$R_{34}\left(\tfrac{\pi}{2}\right) = R_3\left(\tfrac{\pi}{2}\right) \otimes R_3\left(-\tfrac{\pi}{2}\right) \qquad (5.7)$$

These results follow most staightforwardly from the SU(2)xSU(2) algebra of N_i, $N_i^\dagger$, where $N_i = J_i + K_i$, $N_i^\dagger = J_i - K_i$ and $J_i = 1/2\varepsilon_{ijk}R_{jk}$, $K_i = R_{0i}$. For completeness, note that [Verstegen 1984]

$$R_j(2\pi) \neq I$$
$$R_{ij}(2\pi) = I = R_i(2\pi) \otimes R_j(2\pi) \qquad (5.8)$$

An alternative description of rotations in each of the lattice planes is in terms of a combination of permutation and reflection operations. A moments thought reveals that, for example, $R_{12}(\pi/2)$ has the same effect as a reflection, $P_{2'}$ along the 2-axis followed by swapping axes 1 and 2, i.e., [Mandula et al 1983]

$$R_{12}\left(\tfrac{\pi}{2}\right) = (12)P_2 \qquad (5.9)$$

We can use the permutation group S_4 to provide a labelling of some of the representations of the hypercubic group. There are 5 such representations and we describe them by their Young Tableaux as

(5.10)

with dimensions 1,1,2,3,3, respectively. Importantly, there are 4 irreducible representations of O(4) which, under the restriction to the discrete subgroup, are also irreducible representations of the 4-dimensional lattice. Three of these are (1,0), (0,1), (1/2,1/2) (dimensions 3,3,4), in the SU(2)xSU(2) notation. From these we can construct three

more irreducible representations

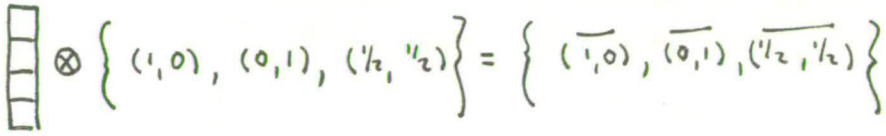

$$\otimes \left\{ (1,0),\ (0,1),\ (\tfrac{1}{2},\tfrac{1}{2}) \right\} = \left\{ \overline{(1,0)},\ \overline{(0,1)},\ \overline{(\tfrac{1}{2},\tfrac{1}{2})} \right\} \qquad (5.11)$$

The remaining representations are $\underset{\sim}{6}$ and $\underset{\sim}{8}$ dimensional [Mandula et al 1983; Verstegen 1984] of which the $\underset{\sim}{8}$ is the remaining irreducible representation of O(4). One may deduce the character table for the hypercubic group from the characters of S_4, SU(2) and also using the orthogonality relations

$$a_r = \frac{1}{N} \sum_{\substack{\text{classes} \\ C}} n_c \, \chi(C) \chi^r(C) \qquad (5.12)$$

for the number of times a character appears in the r-th representation, and where N= the number of elements of the hypercubic group, n_c= the number of elements in the class C, X(C)=character of the class C. Also

$$\chi^{(j_1,j_2)} = \chi^{(j_1,0)} \chi^{(0,j_2)} \qquad (5.13)$$

may be useful, for spins j_1, j_2.

In order to extract fields with a prescribed J^P, it is further necessary to consider the decomposition of these representations under the cubic subgroup of the hypercubic group (which is a subgroup of O(3)). This group has 24 elements in 5 conjugacy classes. Again, one can label some of these irreducible representations by means of S_3 which contains

(5.14)

with dimension 1,1,2 respectively. There is an additional representation (dim 3) called $\underset{\sim}{1}'$ and the final representation is obtained from $\underset{\sim}{1}$ by means of

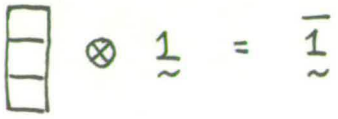

(5.15)

and is called $\bar{1}$ [Mandula et al 1983; Johnson 1982].

In tables 1 and 2, we list the decomposition of the irreducible representations of the hypercubic group under the restriction to the cubic subgroup and also the O(3) spins which contribute to each conjugacy class [Mandula et al 1983; Johnson 1982; Verstegen 1984]. Finally, there is a traditional labelling of these cubic group representations by means of the Octohedral symmetry group irreducible representations as

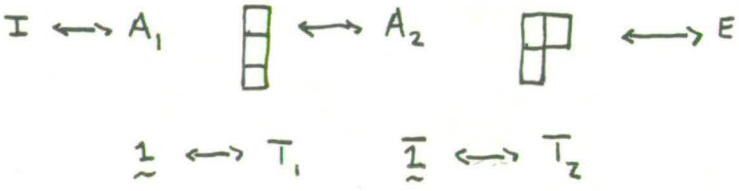

(5.16)

If we think in terms of lattice "string" variables, we may note the following. The notation of (5.16) is such that A,E,T correspond to spin 0,1,2 about the lattice axis and that the subscript 1(2) denotes the symmetry (anti-symmetry) under the interchange of the ends of the "string" by a rotation of π about a lattice axis. In each of these cases, one can also provide a further label g(u) depending on the symmetry (anti-symmetry) under the interchange of ends under inversion in the midpoint [Griffiths et al 1983]. It can be shown that 1(2) is related to the operation of charge conjugation and g(u) to the combined operation of CP on the lattice "string" [Griffiths et al 1983].

Conjugacy Classes of the Hypercubic Lattice Rotation Group			
			Typical Element
Class	Order	Number of Elts.	$SU(2) \otimes SU(2) / Z_2$ Notation*
I	1	1	$I \otimes I$
II	2	6	$R_3(\pi) \otimes R_3(\pi)$
III	2	1	$R_3(2\pi) \otimes I$
IV	4	12	$R_3(-\frac{\pi}{2}) \otimes R_3(-\frac{\pi}{2})$
V	2	24	$R_1(\pi)R_3(-\frac{\pi}{2}) \otimes R_1(\pi)R_3(-\frac{\pi}{2})$
VI	4	12	$R_3(\frac{\pi}{2}) \otimes R_3(\frac{-3\pi}{2})$
VII	3	32	$R_3(\frac{\pi}{2})R_1(\frac{\pi}{2}) \otimes R_3(\frac{\pi}{2})R_1(\frac{\pi}{2})$
VIII	6	32	$R_3(\frac{\pi}{2})R_1(-\frac{\pi}{2}) \otimes R_3(\frac{-3\pi}{2})R_1(-\frac{\pi}{2})$
IX	8	24	$R_2(-\frac{\pi}{2}) \otimes R_3(-\pi)R_2(\frac{\pi}{2})$
X	8	24	$R_3(\pi)R_2(\frac{\pi}{2}) \otimes R_2(-\frac{\pi}{2})$
XI	2	12	$R_1(\pi) \otimes R_2(\pi)$
XII	4	6	$R_3(-\pi) \otimes I$
XIII	4	6	$I \otimes R_3(-\pi)$

*Elements of $SU(2) \otimes SU(2)$ of the form $R_i(2\pi) \otimes R_j(2\pi)$ (any i,j) are equivalent to the identity in O(4).

Table 5.1 Symmetry properties of the hypercubic lattice group. Mandula et al [1983]

Spin Content of Hypercubic Group Representations		
Hypercubic Group Representation	Cubic Group Content	Contributant Spin Representations
I	I	0,4,6,...
		3,6,...
		2,4,5,6,...
	I ⊕ 	0,2,4,5,6,...
	 ⊕ 	2,3,4,5,6,...
(1,0)	1	1,3,4,5,6,...
(0,1)	1	1,3,4,5,6,...
$\overline{(1,0)}$	$\bar{1}$	2,3,4,5,6,...
$\overline{(0,1)}$	$\bar{1}$	2,3,4,5,6,...
$(\frac{1}{2},\frac{1}{2})$	I ⊕ 1	0,1,3,4,5,6,...
$\overline{(\frac{1}{2},\frac{1}{2})}$	 ⊕ $\bar{1}$	2,3,4,5,6,...
6	I ⊕ $\bar{1}$	1,2,3,4,5,6,...
8	 ⊕ 1 ⊕ 1	1,2,3,4,5,6,...

Table 5.2 O(3) spins contributing under the restriction to the cubic subgroup. See Mandula et al [1983]

5.3 Lattice Studies of Hybrid Mesons: The Heavy $Q\bar{Q}$ Potential

Griffiths et al [1983] and Campbell et al [1984] generalise the method of extracting the heavy quark potential from the expectation value of the Wilson loop operator, $\langle \Pi U_{\mu}(n) \rangle$. In the above notation, this would correspond to the straight string (in the spacelike direction) with symmetry A_{1g} (see also Stack [1983]), the "ground state". Qualitatively, one envisages fluctuations in this gluonic string and selects from all possible excursions fron the straight string (of a given length R), those that belong to given irreducible representations of the cubic group (given J^{PC}). So, see figure 2, one traces in group space (SU(3)), the paths P_i at time zero (only spatially directed links) with paths P_j at time T [Griffiths et al 1983; Campbell et al 1984]. These correlation functions $C_{ij}(R,T)$ will correspond to some eigenvalues, λ_a, of the appropriate transfer matrix [Kogut 1983], and one deduces, in the manner of chapter 2, the gluonic potential, for the symmetry α, from

$$\lambda_{\alpha} = e^{-V_{\alpha}(R,T)} \qquad (5.17)$$

From one's intuitive expectation of the statistics of a computer simulation in LGT, only those paths which deviate least from the A_{1g} path are likely to be significant. In fact Griffiths et al [1983] do claim this and find it necessary to perform a matrix variational evaluation of the eigenvalues of the $C_{ij}(R,T)$. The data of Stack [1983] for the heavy quark potential is well reproduced but unfortunately that of the "excited" string states is strongly affected by the statistical fluctuations. Before displaying this, let us note a few of the important lattice parameters. In the SU(3) calculation (for SU(2) see Griffiths et al [1983]), an 8^4

lattice is adopted for $\beta<5.8$ and a 12^4 lattice for $\beta= 5.8$ and 6.0. It is not clear how many configurations were employed in this analysis, a fact that, if glueball simulations are a guide, is of considerable importance. In any event, paths up to 3 spatial lattice links were considered and the resulting energy eigenvalue estimated from that combination of gluonic strings which attenuates least up to 3 temporal spacings. Of importance here is their investigation of the expectation values at several values of β. One then necessarily has to rescale (i.e., normalise) in some manner the resulting data, this being achieved by use of the scaling form (chapter 2), which should be applicable over some range in β, but almost cetainly not valid for $\beta<6.0$ [Barbour et al 1985].

As such, we feel that it is more instructive to place the emphasis less on the numerical values obtained (although these are only fairly rough estimates anyway), and more on the specific features and the general characteristics of their calculation.

The lowest excited energy eigenvalue obtained in the analysis of Griffiths et al corresponded to the E_u symmetry representation (an admixture of exotic and non-exotic quantum numbers). For heavy quarks, the Born-Oppenheimer approximation should be relevant and so the Schrodinger equation is solved in this potential field. The validity of this approach depends on the relative insignificance of the rotational and vibrational modes of the quarks in the potential as compared to the gluonic contribution [Griffiths et al 1983]. Figure 3, from figure 2 of Campbell et al [1984], displays the extent of the evidence they quote for

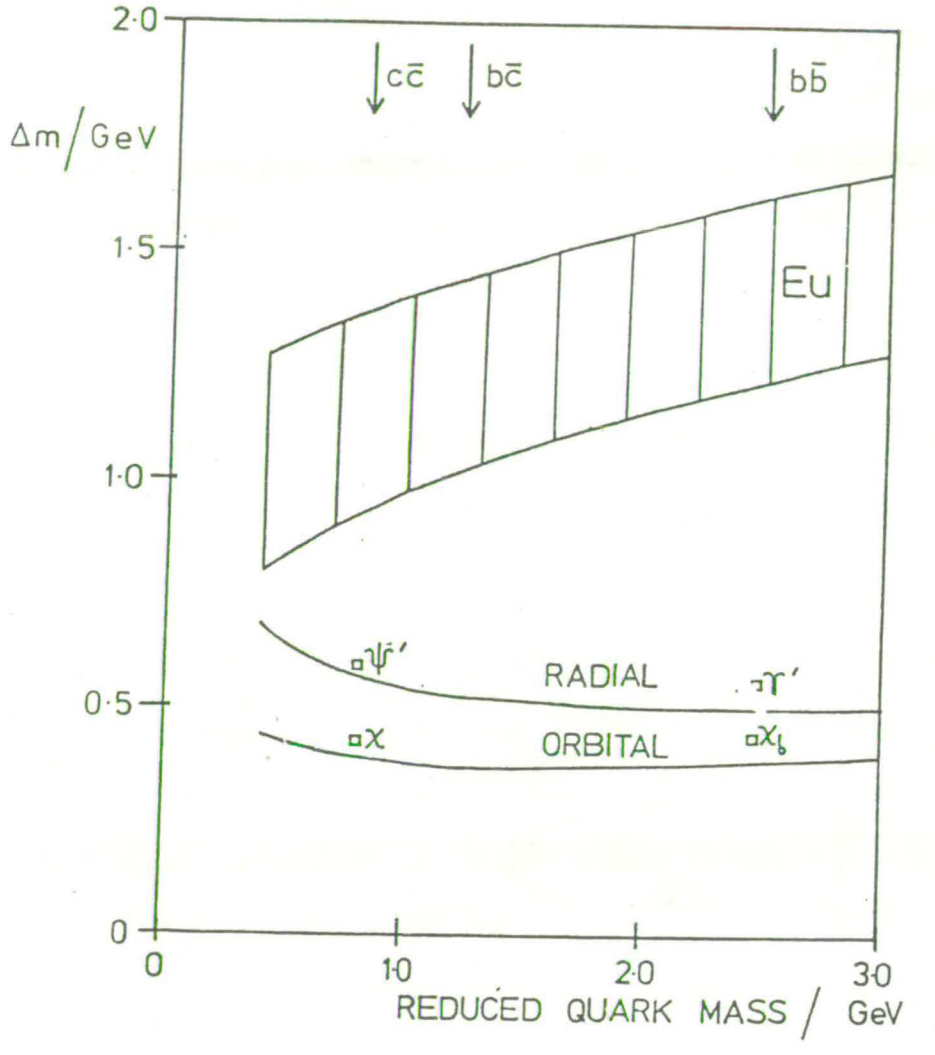

Figure 5.3 The spectrum of mesonic excitations for a given quark mass. The radial and orbital excitations refer to the A_{1g} potential (i.e., 2S and 1P states, relative to the 1S). E_u is the lowest gluonic excitation and the shaded region is the inference drawn by Campbell et al [1984] from their own data. See Campbell et al [1984] for this.

the E_u potential. the source of the linearly-rising part of the potential at larger quark mass derives from an earlier graph (figure 1 of Campbell et al [1984]) which is very flat at all hadronic lengths. However, one might expect the excited potential to always be bounded from below by the A_{1g} (ground) state.

The limitations of their approach, however, are well exposed in this diagram. Evidently, one is unable to extend these results very far to the physically more interesting light-quark regime (see chapter 3). For completeness however, we note that the E_u potential is some 1 GeV above the ground state. In the more extensive study of the potential in the SU(2) gauge theory, Griffiths et al [1983] quote $E_u \sim$ 800 MeV (above A_{1g}), and also $B_{1g} \sim 1$ GeV, $A_{2u} \sim E_g \sim B_{2u} \sim 1.25$ GeV above.

Much of what we learn about the problems of this approach is related to those difficulties of the hybrid calculation we report below, and stem, perhaps unsurprisingly, from the employment of non-local operators on a finite lattice. However, this is an imaginative method which only fails to be significant from being restricted to heavy quarks.

5.4 Hybrid Mesons on the 8^4 DAP lattice

In our approach, we aim to simulate hybrid dynamics with light quarks (i.e., up and down) within the lattice volume. Essentially, we construct a $q\bar{q}$ operator in the adjoint representation of SU(3), entirely in the same way as for the fields of chapter 4. One then takes the trace of this operator with the "cloverleaf" gluon field we defined earlier to obtain the $q\bar{q}g$ colour singlet meson at

the lattice site n. In the continuum, Wilson (four component) fermions transform as $(1/2,0)\oplus(0,1/2)$ (in the SU(2) notation) under O(4). This representation is irreducible under the hypercubic lattice group also (see above). We also know that the (1,0) and (0,1) representations (containing $F_{\mu\nu}(x)$) of O(4) are irreducible with respect to the lattice group. Thus we can write down continuum hybrid fields as in table 3 from which we extract the covariant lattice combinations. Note that the J^{PC} of all the possible fermion bilinears was detailed in chapter 4, and that, in addition,

$$J^{PC}(E_i) = 1^{--}$$
$$J^{PC}(B_i) = 1^{+-} \qquad (5.18)$$

In table 3, we have also explicitly identified those operators which couple to exotic channels. The lattice covariant fields for the 0^{+-} and the 1^{-+} exotic mesons have been constructed by Mandula [1983]. The results are, in the notation of table 3 for the A_μ, V_μ, $T_{\mu\nu}$ (and where $F_{\mu\nu}$ is the field strength tensor)

$$(\tfrac{1}{2},\tfrac{1}{2})\quad 0^{+-} = C_0 = \vec{A}\cdot\vec{B}\ ;\ C_\mu = \tfrac{1}{2}\varepsilon_{\mu\nu\lambda\sigma}F_{\nu\lambda}A_\sigma \qquad (a)$$

$$\underset{\sim}{8}\quad 1^{-+} = H_{i00} = V_0\vec{E} - \vec{V}\times\vec{B}\ ;\ H_{\mu\nu\lambda} = F_{\mu\nu}V_\lambda - \tfrac{1}{3}g_{\nu\lambda}F_{\mu\sigma}V_\sigma - \tfrac{1}{3}g_{\mu\lambda}F_{\sigma\nu}V_\sigma \qquad (b)$$

$$\underset{\sim}{6}\quad 1^{-+} = J_{i0} = \vec{\sigma}_0\times\vec{B} + \vec{\sigma}_i\times\vec{E}\ ;\ J_{\mu\nu} = F_{\lambda\mu}T_{\lambda\nu} + F_{\lambda\nu}T_{\lambda\mu} \qquad (c)$$

$$(1,0)\oplus(0,1)\quad 1^{-+} = K_{i0} = \vec{\sigma}_0\times\vec{B} - \vec{\sigma}_i\times\vec{E}\ ;\ K_{\mu\nu} = F_{\lambda\mu}T_{\lambda\nu} - F_{\lambda\nu}T_{\lambda\mu} \qquad (d)$$

(5.19)

The next exotic spins contributing to these are J=4, and J=3 for the scalar and vector respectively. One can always, of course, alter the PC identification of these to obtain other, non-exotic, fields by means of the swaps $A_\mu \leftrightarrow V_\mu$, $T_{0i} \leftrightarrow T_{ij}$.

O^{++}	O^{+-} exotic	O^{--} exotic	O^{-+}	Definitions
$\vec{V}\cdot\vec{E}$	$\vec{A}\cdot\vec{B}$	$\vec{A}\cdot\vec{E}$	$\vec{V}\cdot\vec{B}$	$S = \bar{\psi}\psi$
$\vec{\sigma_0}\cdot\vec{E}$			$\vec{\sigma_0}\cdot\vec{B}$	$P = \bar{\psi}\gamma_5\psi$
$\vec{\sigma_1}\cdot\vec{B}$			$\vec{\sigma_1}\cdot\vec{E}$	$\vec{V} = \bar{\psi}\gamma_i\psi$
				$V_0 = \bar{\psi}\gamma_4\psi$
				$\vec{A} = \bar{\psi}\gamma_5\gamma_i\psi$
1^{++}	1^{+-}	1^{--}	1^{-+} exotic	$A_0 = \bar{\psi}\gamma_5\gamma_4\psi$
				$\vec{\sigma_0} = \bar{\psi}\sigma_{0i}\psi$
$V_0\vec{B}$	$S\vec{B}$	$S\vec{E}$	$V_0\vec{E}$	$\vec{\sigma_1} = \bar{\psi}\sigma_{ij}\psi$
$\vec{V}\times\vec{E}$	$P\vec{E}$	$P\vec{B}$	$\vec{V}\times\vec{B}$	$\vec{E} = F_{0i}$
$\vec{\sigma_0}\times\vec{E}$	$A_0\vec{E}$	$A_0\vec{B}$	$\vec{\sigma_0}\times\vec{B}$	$\vec{B} = \frac{1}{2}\epsilon_{ijk}F_{jk}$
$\vec{\sigma_1}\times\vec{B}$	$\vec{A}\times\vec{B}$	$\vec{A}\times\vec{E}$	$\vec{\sigma_1}\times\vec{E}$	

Table 5.3 Identification of lattice hybrid operators in terms of the $(q\bar{q})_{\underset{\sim}{g}}$ and $F_{\mu\nu}$ "subsystems". All entries in the table are implicitly expectation values with respect to the gauge action and the trace over colour and spin is understood.

From table 3, we can, using (5.19), see the mixing of the continuum representations that occurs when covariant lattice operators are defined.

In the spirit of chapter 4, let us note the implied colour and spin matrix ordering required to successfully combine the $q\bar{q}$ and gluon operators. The general form for a $q\bar{q}$ octet field with generic gamma matrix, Γ^A, is

$$M^{ab}(n) = \left(\bar{\psi}^a_\alpha \, \Gamma^A_{\alpha\beta} \, \psi^b_\beta\right)(n) \qquad (5.20)$$

The colour singlet hybrid operator is contained in

$$H(n) = \left(\bar{\psi}_\alpha \, \Gamma^A_{\alpha\beta} \, \psi_\beta\right)(n) \cdot F^A(n) \qquad (5.21)$$

where the dot product is in colour space. Lorentz indices have been suppressed for clarity (with all operators carrying such indices denoted by the superscript "A"). The two point correlation function that follows from this is (figure 4)

$$\begin{aligned} \langle H(n) H^\dagger(0) \rangle &= \left\langle \left\{ \left[\bar{\psi}^{a'}_{\alpha'} \, \Gamma^F_{\alpha'\beta'} \, \psi^{b'}_{\beta'} \, F_F^{a'b'}\right](n) \left[\bar{\psi}^b_\beta \, \Gamma^I_{\beta\alpha} \, \psi^a_\alpha \, (F_I^{ab})^\dagger\right](0) \right\} \right\rangle \\ &= \left\langle \left\{ \tilde{\Gamma}^F_{\alpha'\beta'} \, \tilde{\Gamma}^I_{\beta\alpha} \, G^{b'b}_{\beta'\beta}(n,0) \, G^{a'a\,*}_{\alpha'\alpha}(n,0) \, F^{a'b'}(n) \, F^{ba\,*}(0) \right\} \right\rangle \end{aligned} \qquad (5.22)$$

$$\tilde{\Gamma}_{\alpha\beta} = (\Gamma \gamma_5)_{\alpha\beta}$$

in which the expectation value is with respect to the background gauge field, i.e., the "quenched" approximation.

For a given hybrid, the correct J^{PC} is obtained from the O(4) properties of the Γ^A and the component of $F_{\mu\nu}$, from table 3. One may discern from (5.22), the definition of the $q\bar{q}$ "basis" operator (i.e., of a given J^{PC}) extensively employed in the study of 4-quark mesons. If now we look solely at the colour index structure of the product operator then by rewriting the quark propagators and gluon

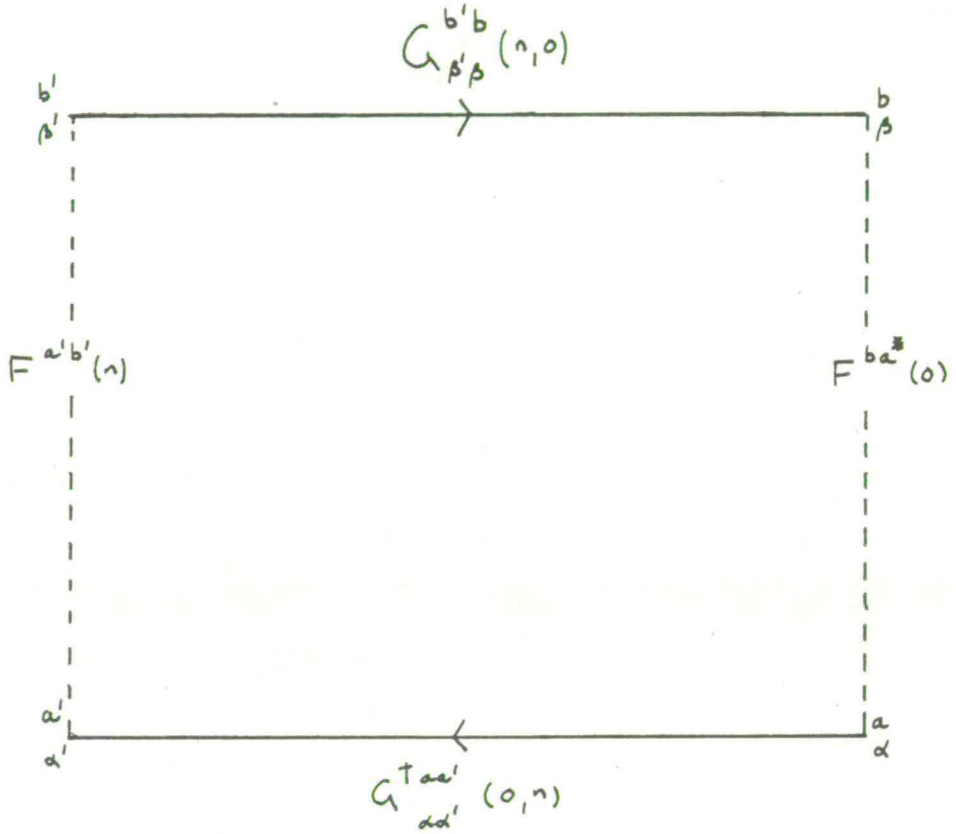

Figure 5.4 A pictorial representation (in the notation) of equation (5.22, representing a generic hybrid propagator.

fields in terms of real and imaginary parts, i.e.,

$$G^{b'b}(n,0) = C^{b'b} + i D^{b'b} \; ; \; G^{a'a*}(n,0) = C^{a'a} - i D^{a'a}$$
$$F^{a'b'}(n) = q_f^{a'b'} + i h_f^{a'b'} \; ; \; F^{ab*}(0) = q_i^{ab} - i h_i^{ab} \qquad (5.23)$$

then the trace reads (in a condensed notation for clarity)

$$\langle H(n) H^\dagger(0) \rangle = \langle M^{b'ba'a} V^{b'ba'a} + N^{b'ba'a} W^{b'ba'a} \rangle \qquad (5.24)$$

In this, there is an implicit sum to project out the zero-momentum state. Here,

$$\begin{aligned} M^{b'ba'a} &= C^{b'b} C^{a'a} + D^{b'b} D^{a'a} \\ N^{b'ba'a} &= D^{b'b} C^{a'a} - C^{b'b} D^{a'a} \\ V^{b'ba'a} &= q_f^{a'b'} q_i^{ab} + h_f^{a'b'} h_i^{ab} \\ W^{b'ba'a} &= q_f^{a'b'} h_i^{ab} - h_f^{a'b'} q_i^{ab} \end{aligned} \qquad (5.25)$$

The advantage of this careful identification is that it allows one to understand the kinds of tests that can be imposed on the calculation. This is most important because, in the light of the results to be presented below, we must be able to correctly interpret the strengths of the method. As some obvious examples, we tried, and found satisfactory (with the unit matrices in colour space)

$$F_{\mu\nu}(n) = F_{\mu\nu}(0) \in \{ \mathbb{1} \, , \, \mathbb{1} + i\mathbb{1} \, , \, i\mathbb{1} \} \qquad (5.26)$$
$$\Rightarrow \langle H(n) H^\dagger(0) \rangle = \{ \langle M(n) M^\dagger(0) \rangle \, , \, 0 \, , \, - \langle M(n) M^\dagger(0) \rangle \}$$

where M(n) is the $q\bar{q}$ colour singlet meson with quantum numbers dictated by Γ^A. By suitably reorganising the storage of the quark green functions and the gluon field components, one can check explicitly that the imaginary parts of the propagators vanish. One also sees that by letting, say, $F_{\mu\nu}(0)=1$ (in colour and spin space), the overlap between hybrid and $q\bar{q}$ meson fields of, for example, the pion, can be estimated (recall chapter 3), from

$$\langle 0^{-+}(q\bar{q}g)(n) \, 0^{-+}(q\bar{q})^\dagger(0) \rangle \qquad (5.27)$$

We shall deal with this below.

The organisation of the calculation was such that the gluon fields were constructed in a separate program from the main hybrid propagator program, through the requirements of memory storage in the DAP (see chapter 6 and the appendix). The six planes of the field strength were computed from the gauge configurations by a well understood series of logical shifts and matrix multiplies which it is unnecessary to detail here. These "cloverleaves" were written to disc store where they were accessed by the main program. The determination of the $q\bar{q}$ "basis" operator was as discussed before (previous chapter) and, with due care exercised on the index sequence, the gluon "propagator" was duly assembled. In order to ameliorate the storage limitations (even in three byte arithmetic), we constructed the program to calculate, at each time step, the product of the $q\bar{q}$ operator with (the maximum possible) four different planes of $F_{\mu\nu}$. Thus we could also compute all the possible "cross-correlations" (as above, but for different J^{PC}) $\langle[q\bar{q}g](n)[q\bar{q}](0)\rangle$ that arise from these. It is inevitable, given that one must set each Γ^A separately in the "host" computer, that any actual data accumulation will be a laborious process unless one restricts the number of operators that are investigated.

An additional check suggested by the necessity of reading large data files to and from DAP store, was the "alignment" of quark green functions and $F_{\mu\nu}(n)$. By this we mean that the original Gauss-Seidel algorithm is reconstructed using the "cloverleaves" and green functions to check the equality of the left- and right-hand sides of

$$2m\, G^{ab}_{\alpha\rho}(n,0) = 2\delta(n)\,\delta^{ab}\delta_{\alpha\rho}$$

$$+\ldots$$

$$\ldots + \sum_{\mu=1}^{4} \Big\{ (\Gamma - \Gamma^A)_{\alpha\lambda}\, U^{ac}(n,\mu)\, G^{cb}_{\lambda\rho}(n,0) + (\Gamma + \Gamma^A)_{\alpha\lambda}\, U^{\dagger ac}(n,-\mu)\, G^{cb}_{\lambda\rho}(n,0) \Big\} \qquad (5.28)$$

to the level of accuracy claimed in Bowler et al [1983, 1984]. This was indeed found.

All of the above detail is necessary to demonstrate that the results we now present are not the result of some programming error. This may have been a significant criticism in the light of those results. However, there is enough information to be extracted from the numerical simulations to suggest that program error is not the problem. We will demonstrate that substantial improvements in statistics are, in fact, the key to a reasonable comparison with the other methods (as outlined in chapter 3).

The simulation was performed entirely analogously to that in chapter 4, so we may summarise, briefly, the values of the various parameters involved. We evaluated the expectation values of 0^{-+}, 0^{+-}, 1^{-+}(dimension=8) and 0^{-+} "cross-correlation" function as detailed above. Three values of the hopping parameter, k, were employed with 16 gauge configurations for each of these (as in chapter 4). The important quantities are those at the critical value of k, k_c, and may be found in equation (4.14).

In figures 5.5, 5.6 and 5.7 we demonstrate the behaviour of the various log-ratios

$$m(n_4) = -\ln \left\{ \frac{\Delta(n_4)}{\Delta(n_4-1)} \right\} \qquad (5.29)$$

$$\Delta(n_4) = \text{particle propagator}$$

as a function of the Euclidean time, n_4, at k=0.1625 (the highest). Immediately we note the scale of the statistical errors. Shown here are the standard errors in the mean over the 16 configurations. Moreover, the fluctuations appear to be such that no "large n_4" limiting value of $m(n_4)$ is approached. The data is barely compatible with a decaying exponential correction (at small n_4) to the mass from a two-exponential fitting function. That is

$$\Delta(n_4) = A e^{-m_1(n_4)|n_4|} + B e^{-m_2(n_4)|n_4|} \qquad (5.30)$$

implies

$$m(n_4) \underset{\substack{n_4 \gtrsim 1 \\ (m_2-m_1)>>0}}{\simeq} m_1(n_4)\left\{1 + \frac{B}{A m_1} e^{-(m_2-m_1)|n_4-1|} + \frac{B}{A m_1} e^{-(m_2-m_1)|n_4|}\right\} + \mathcal{O}\left(\frac{B^2}{A^2 m_1^2} e^{-2(m_2-m_1)}\right) \qquad (5.31)$$

The fluctuations greatly affect the deduced $m(n_4)$, not least in that it requires (experimentally) greater than of the order of eight configurations to trace the hybrid propagator signal out to the furthest time-steps. Thus the method of dividing the 16 configurations into four blocks of four and estimating the statistical error in the average mass from the spread in the masses calculated on each of the blocks separately was not sufficiently reliable. The method we adopted was to similarly calculate masses on two blocks of eight configurations and to corroborate this by a direct comparison with the statistical errors arising from the log-ratio plots themselves (at each k, see, for example figure 5.5 et seq). In a high statistics investigation one would not regard this method of evaluating the errors as particularly satisfactory. However in this analysis we have been keen to establish that the overall method of extracting hybrid masses is valuable and so, for the moment, do not regard this as a critical point. Overall consistency, we feel, is important.

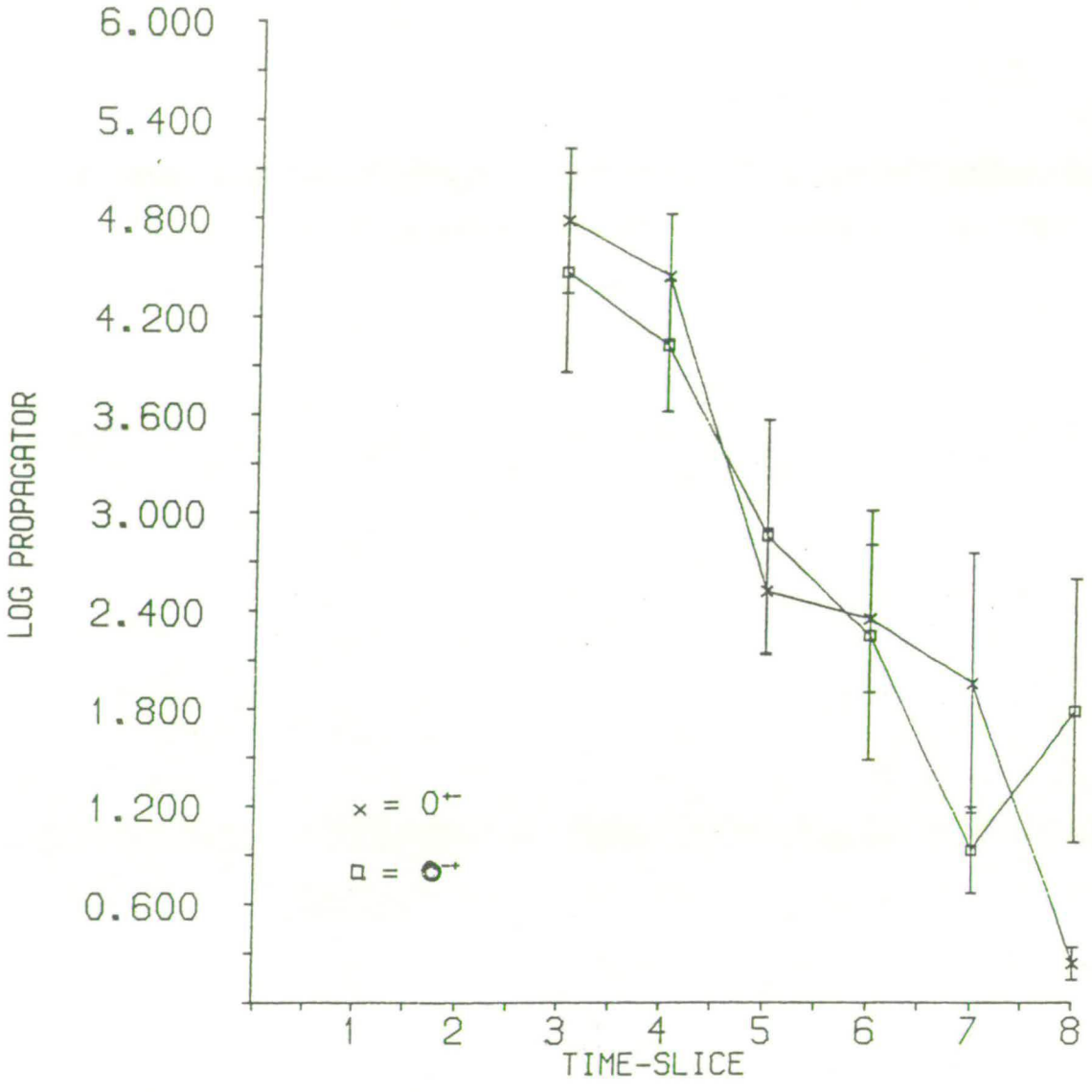

Figure 5.5 Log-ratios, i.e., m(t)= ln(G(t)/G(t-1)) versus time-slice in the (flavour non-singlet) case of the 0^{+-} hybrid exotic and 0^{-+} non-exotic at m_q=3.0769. The errors quoted are the standard errors on the data. The absence of error bars indicates errors off the scale of the diagram, i.e., results commensurate with the noise in the propagator signal.

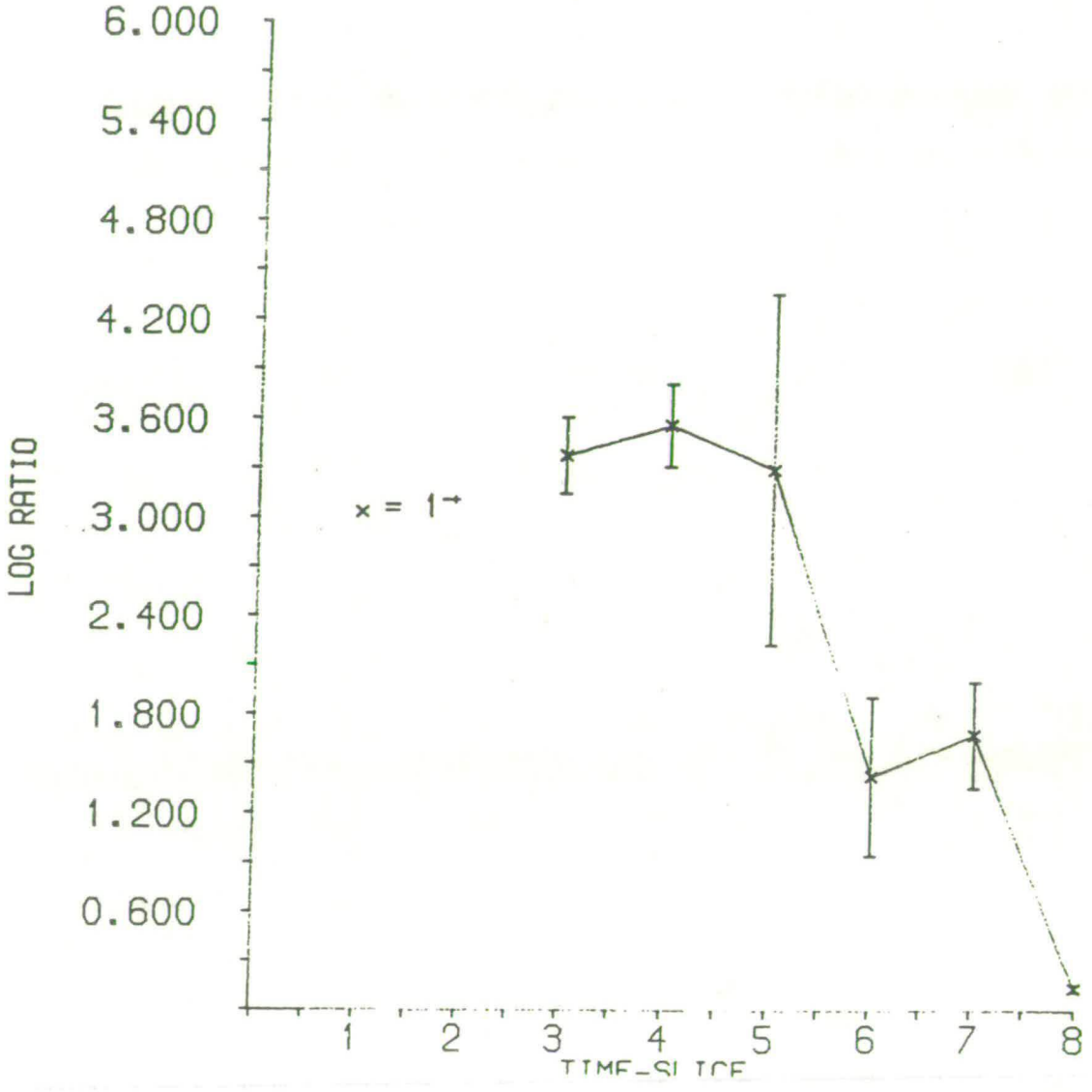

Figure 5.6 Same plot as Fig. 5.5 for the exotic 1^{-+} meson at m_q=3.0769.

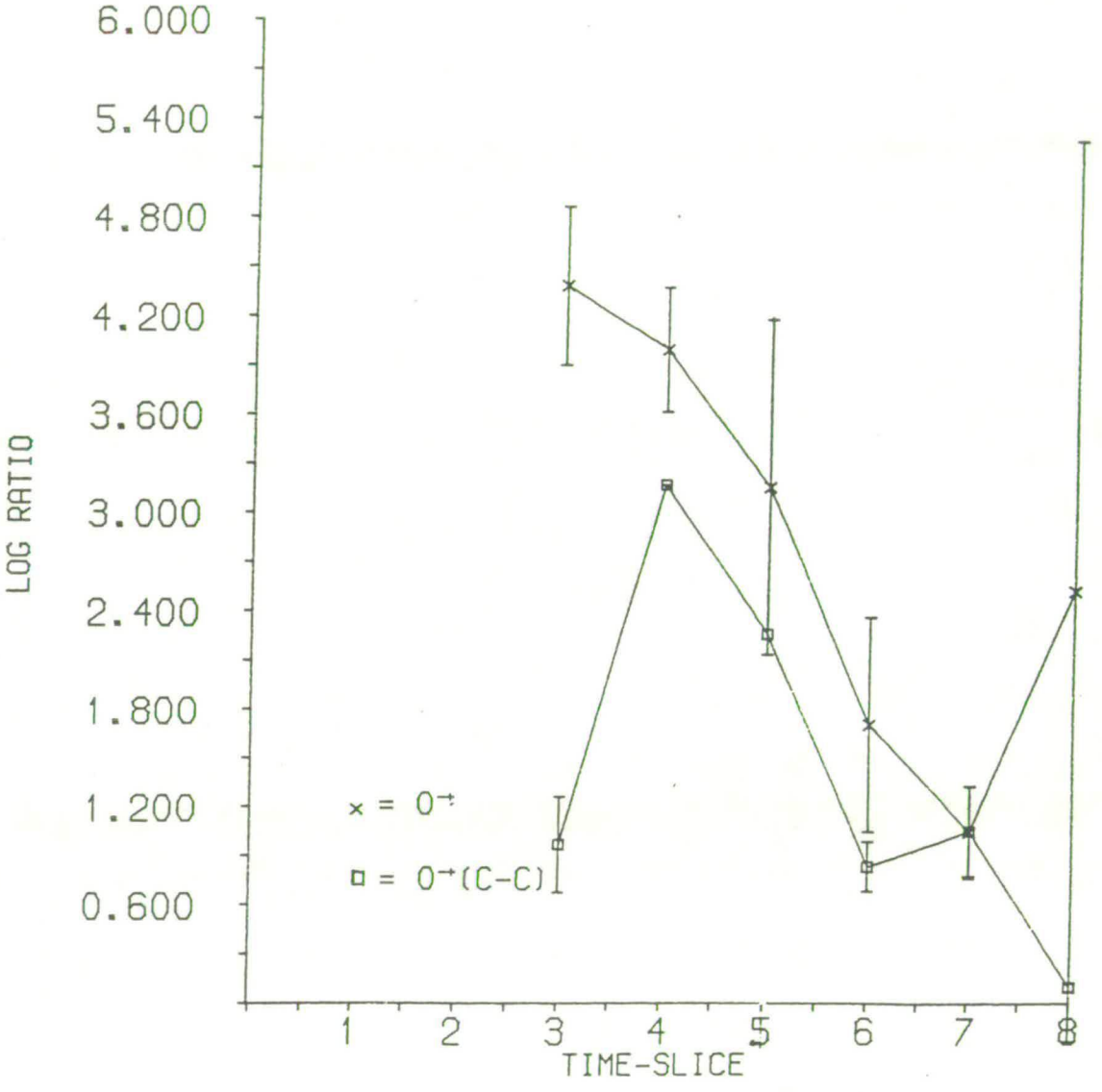

Figure 5.7 Same as Fig. 5.5 in the case of the 0^{-+} and the 0^{-+} "cross-correlation". $m_q = 3.0769$

Moreover, given that the errors on individual data points range from 20%-50%, any resulting mass-estimates will be, in any event, very rough, order of magnitude claims.

Figures 5.8 and 5.9 demonstrate the extent to which varying both the operator definitions and the sample of configurations affects (greatly) the resulting masses and propagators. The first of these is a comparison with the 8 dimensional 1^{-+} field. Here we plot the log-ratios for only the space-like components of (5.19b) (but which itself is covariant in the continuum). The errors are significantly larger. One may also think of this as merely failing to diagonalise the corresponding matrix of propagators which would here include the other, time-like, components. It serves to show the worth of considering as many operators as possible that couple to a given channel. That this should be useful also follows from considering the improvement in the mass of the $q\bar{q}$ ϱ-meson when averaged over the three vector components instead of just ϱ_x or ϱ_y or ϱ_z, say. Figure 5.9 clearly shows the deterioration in the (log-ratio) signal that results from restricting the number of configurations; here only four configurations are used.

We can summarise our interpretation of the error bounds by pointing out the necessity for high statistics in the form of much more extensive sets of gauge configurations and we may also add the probable worth of including more data points (i.e., k-values).

In table 5.4 we have compiled the estimates for the various particle masses along with the extrapolated results (by least squares) to m_c=2.944±0.014 (see chapter 4).

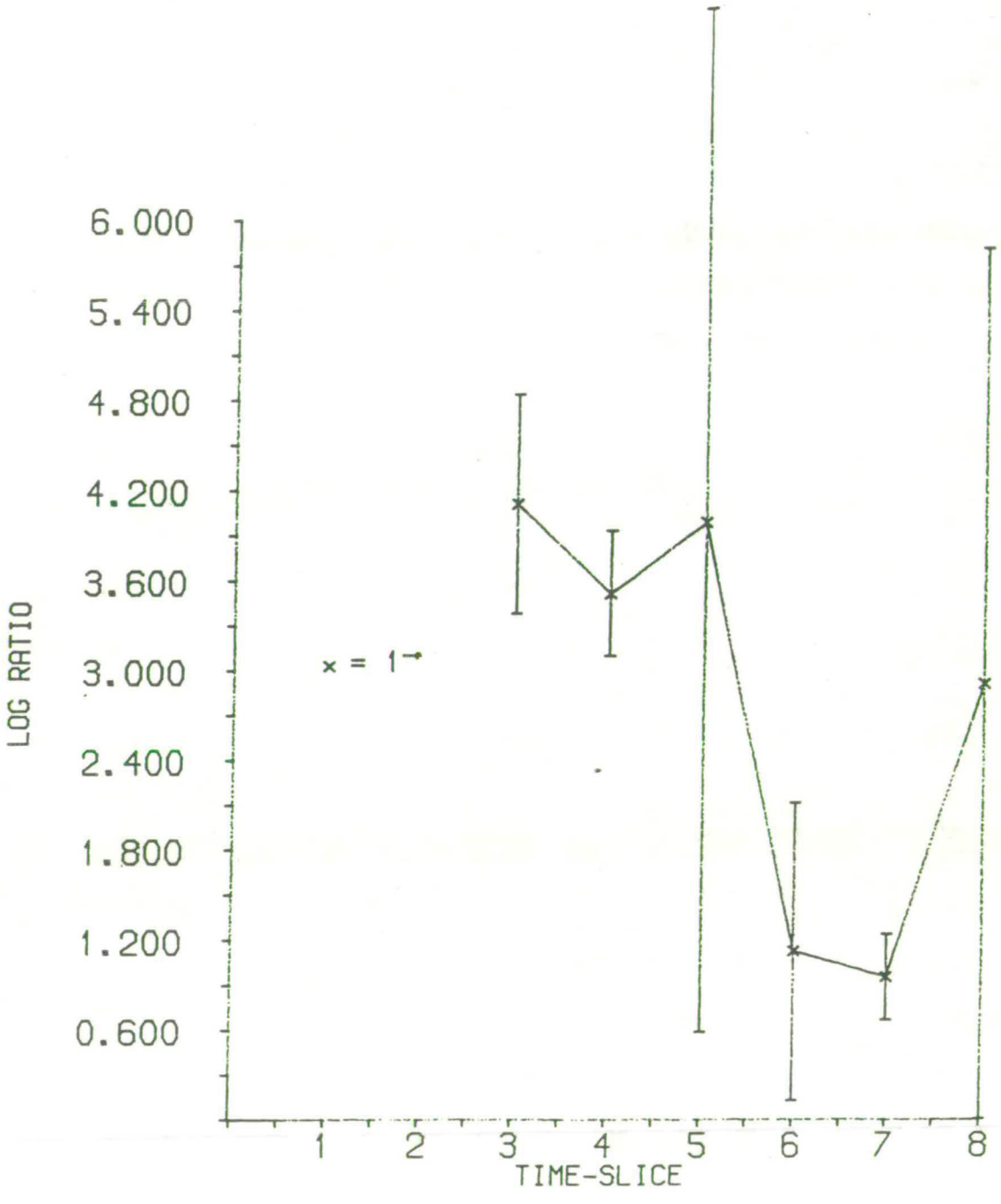

Figure 5.8 Same as Fig. 5.5 for the 1^{-+} at m_q=3.0769 over 16 configurations, but in contrast to Fig. 5.6, here we depict the result for a non-covariant field (the space-like components, see text) under the lattice group. Notably, the errors are much more significant.

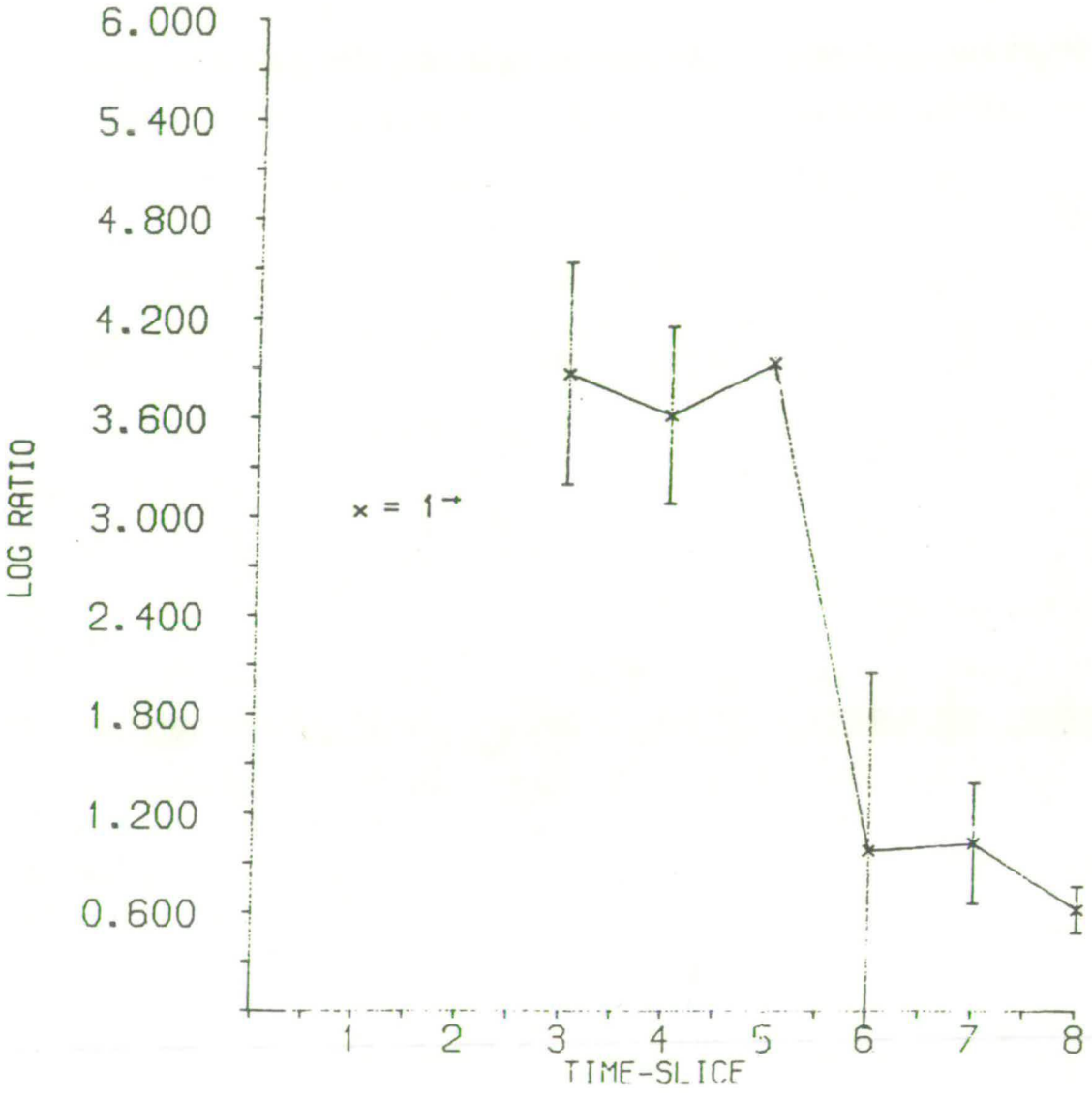

Figure 5.9 The same plot as Fig. 5.5 for the 1^{-+} but here only over four configurations at m_q=3.0769. The importance of averaging over as many configurations as possible is clear from this data.

Table 5.4 Masses of 0^{+-}, 0^{-+} and 1^{-+} as a function of quark mass m_q.

m_l	0^{+-}	0^{-+}	1^{-+}	
3·2895	3·40 ± 0·78	2·36 ± 1·26	1·91 ± 1·05	
3·1746	2·62 ± 0·54	1·83 ± 0·75	1·89 ± 0·80	
3·0769	1·96 ± 0·66	0·97 ± 0·46	1·68 ± 0·47	
m_c 2·944 ± 0·014	1·06 ± 1·56	0·18 ± 1·66	1·58 ± 1·51	$m_\rho a$ $0.516 \pm \begin{matrix}0.027\\0.058\end{matrix}$
MeV	1600 ± 2400	273 ± 2500	2400 ± 2300	m_ρ = 770 (scale)

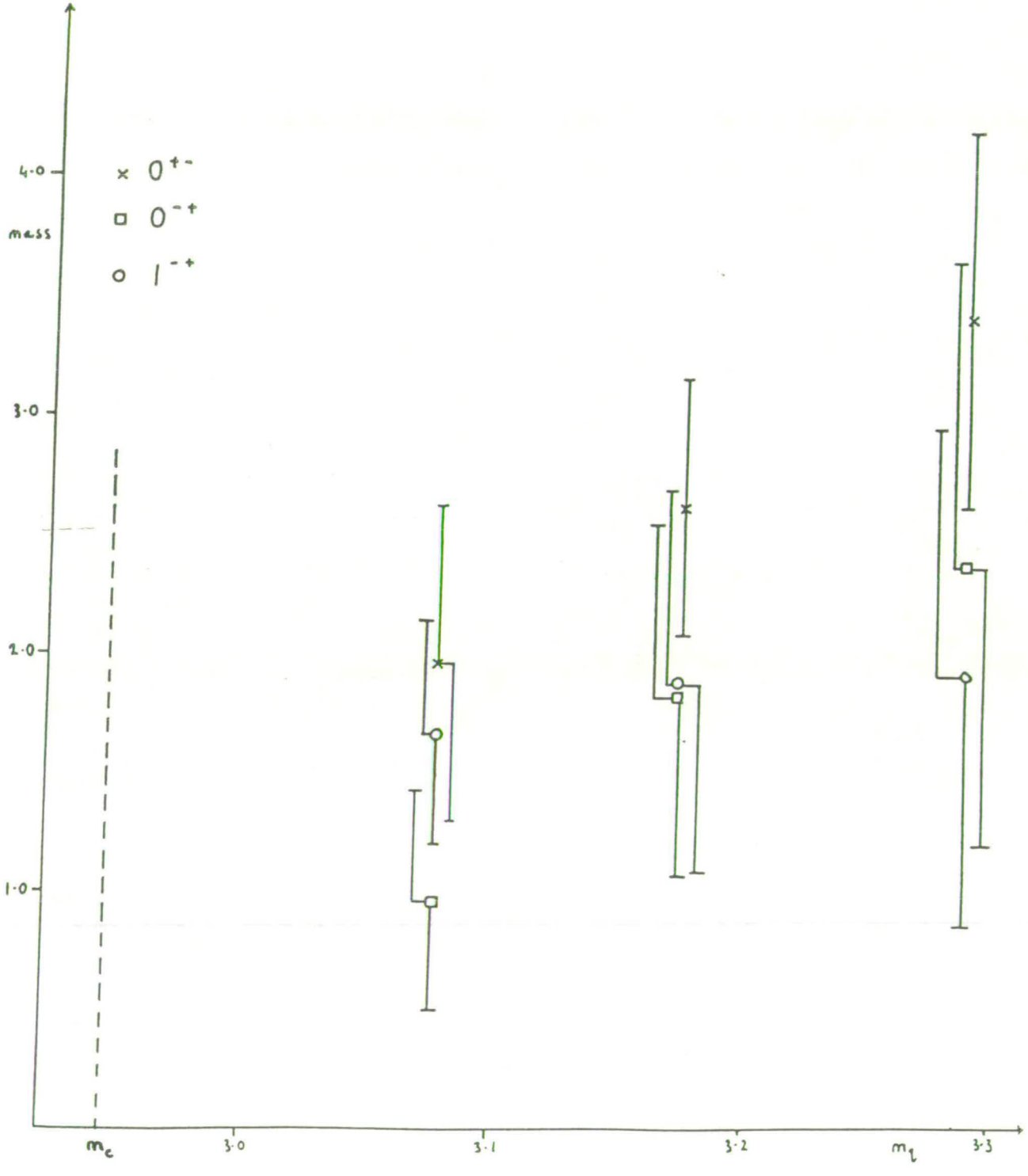

Figure 5.10 Masses of 0^{+-}, 0^{-+} and 1^{-+} as a function of m_q.

Note the absence of any conclusions on the 0^{-+} "cross-correlation" function. By referring to fig. 5.7 it is clear that no significant signal is detectable beyond one time-step from the space-time origin. It would appear probable that only by averaging this "crossed" propagator over all possible starting positions for the quark propagator, i.e., incorporating the fluctuations in the gluon field as defined at each "new" origin, can any improvement be anticipated. To a lesser extent some improvement in hybrid statistics themselves could be forthcoming from this method.

The main conclusions that we may draw from figure 5.10 and table 5.4 are the following. Such are the scales of the errors we report that we may only (just) be able to make a rough assessment of 2 GeV as the characteristic scale of this part of the Hybrid spectrum. In fact, the extrapolated 0^{-+} is far too small (i.e., from the report in chapter 3), whilst the 1^{-+} is more massive than expected and the 0^{+-} perhaps somewhat light. Since the typical error here is itself greater than about 2 GeV, there is obviously little that can be stated uncontroversially. Certainly one expects the fluctuation in the gluon field to be more important than that in the quark propagator, if the studies in glueballs are any guide, but we may also note a slight increase in the statistical errors in the hybrid masses as one moves away from the physical region, i.e., when $k<<k_c$. This could be indicative of the need to remain close to the "physical" quark mass. If we add in the previous observation that no "large-n_4" constancy of log-ratios is found (mass-fits to, say, two-exponential propagators are decidedly more reliable in such a regime, i.e., equation (5.31) where $m_1(n_4)$ is the dominant mass at large n_4), we can see the need to consider bigger lattices

(e.g., 16^4) with gauge configurations closer to the renormalised trajectory, bearing in mind the comment on p59.

It may be encouraging that a scale of 2 GeV is not greatly at variance with other calculations (chapter 3), but we should not over-emphasise this point. It is clear that substantial improvements in the mechanics of the calculation are required and that these should really be based on larger lattices, where, if only to minimise the effect of the inherent non-locality of the gluon operator, we should attempt to improve the agreement of the lattice action as an approximation to the continuum. Then it will be important to include the various improvements suggested above, viz: more configurations; different lattice operators; more values of k; and varying the space-time origin. However, it is vital, in the light of the lack of asymptotic scaling found by Barbour et al [1985], to explore these results as a function of β.

It appears, however, that some positive result can be taken from these calculations. The improvements that we can suggest should not obscure the fact that, from the dynamical point of view, lattice hybrid mesons with a relatively low mass-scale are, even within this study, to be expected. It remains to incorporate some or all of these suggestions to improve on the estimates found within Bag-Model or Sum-Rule calculations.

CHAPTER 6

Summary and Conclusions

QCD has two qualities that are particularly relevant to the work presented in this thesis. Firstly, the non-perturbative features of the theory are, as we discussed in chapters 1 and 2, crucial in providing both "long-range" confinement and dynamical mass generation for hadrons. The physically interesting regime, the confinement scale, denies the value of a perturbation expansion which necessarily cannot include the important (non-perturbative) field fluctuations. However, an effective and computationally efficient method is afforded by the lattice regularisation, a point detailed at length in the second chapter. We saw how lattice QCD possesses a range of pertinent features, from a relatively straightforward strong coupling expansion to an (increasingly) acceptable hadronic spectrum.

The second quality QCD possesses which is relevant here is the additional, colour, degree of freedom. The non-relativistic Quark Model, under the overall constraint that physical states are colour singlets, is readily generalised to include multi-quark and quark-gluon composite hadrons. Importantly though, up to the present time no such hadrons have been experimentally detected. Thus one must attempt to understand the dynamical mechanisms controlling or even inhibiting their production.

In chapter 3 we took up this point and discussed the extent to which it has hitherto been possible to calculate the spectrum of such states. We concentrated on the mesonic sector and detailed three methods; operator inequalities, QCD Sum Rules and the MIT Bag Model. More emphasis was placed on the latter two given that they

were able to yield explicit mass estimates rather than just overall bounds on the spectrum. In both Sum Rule and Bag Model approaches one typically performs an $O(\alpha_s)$ perturbative calculation (at high momentum exchange) but attempts to include the "long-distance" (low momentum) non-perturbative aspects in radically different ways. Whilst the Bag Model imposes overall confinement by a single term, the "bag pressure", Sum Rules (i.e., the operator product expansion) give, in principle, much greater control over the spectrum through including explicitly the fermionic, gluonic and mixed condensates which are non-vanishing in the non-perturbative vacuum. In addition, this method also shares with the lattice transcription the feature of directly relating the hadron spectrum to the fundamental QCD Lagrangian.

In the absence of a definitive $q^2\bar{q}^2$ or $q\bar{q}g$ candidate meson there is no guide to the extent to which the degree of corroboration that is found in the "conventional" spectrum is carried over to these new states. Indeed, the inherent complexity of even $O(\alpha_s)$ calculations has restricted somewhat the range of states whose masses have been calculated. In particular, the 4-quark spectrum has, to our knowledge, only been attempted in the Bag Model. This disappointing lack of certainty in both 4-quark and hybrid sectors is, of itself, suggestive of the value of a lattice simulation. This has been the major investigation of this thesis.

Our calculation proceeded by evaluating the expectation values of appropriate lattice operators, as described in chapters 4 and 5. We comment firstly on the multi-quark simulation. The distinctive non-locality of gluon field (and resulting hybrid) operators will more naturally lead us on to discuss all our results within the context of the

present status of lattice QCD. Three major conclusions are to be drawn from our 4-quark investigations. Firstly we obtained mass estimates for all the scalar and vector exotic and crypto-exotic states with the exception, for reasons of the available computer time, of the 1^{--} non-exotic meson. The results reveal the existence of low-mass (1-2 GeV) vector exotics but scalars more massive than about 2 GeV. Notably, and as we shall discuss immediately below, the bound we find on the mass of any true 4-quark meson in the 0^{++} channel supports the current belief that the S^* and δ are not 4-quark mesons.

A further two conclusions follow from the presence, in the 0^{++} channel, of two pions (shown by the vanishing of the 0^{++} "particle" mass as the quark mass was decreased to the critical value). That the two bosons were not freely propagating on the lattice arose from the inconsistency in the 2-pion "mass" that was obtained from a fit to the (free) two-boson propagator. It was demonstrated that the data was explainable by adding to $2m_\pi$ a 3-momentum contribution, k_π. On an 8^3 lattice with periodic boundary conditions, the lowest possible k_π (i.e., that found in the "large" n_4 region) implied an addition to $2m_\pi$ of some 760 MeV. Thus we deduced that, necessarily, any true 4-quark bound state must be at least of the order of 1040 MeV in mass. This feature of the finite lattice, the existence of an IR cut-off, will determine (depending, of course, on the value of the inverse lattice spacing) whether or not genuine 4-quark mesons are to be found or simply pairs of $q\bar{q}$ mesons. We note, for example, that on this lattice, in the 1^{+-} channel, $m_\pi+m_\varrho$ was not deduced, but rather a state more massive by some 730 MeV, only just within the limits imposed by the implied IR cut-off.

The final point is also a result of the finite lattice size. We noted that, as the quark mass is reduced towards the critical region, the estimate of the 3-momentum contribution was pushed down relative to its expected value (on the basis of the above). This effect, we also noted, was in the opposite direction to the finite size effects deducible from using, e.g., ϱ, δ, rather than π, operators. We thus argued that this decrease was not only an artifact of the finite lattice but could be interpreted as the result of residual attractive gluon interactions (between lattice pions as they more closely approach, from below, their continuum "volumes").

In the Hybrid sector we have presented (at best) order of magnitude mass estimates for 0^{-+}, 0^{+-} and 1^{-+} mesons of around 2 GeV. As with the 4-quark states, this was achieved by using the appropriate lattice operators. The singlemost relevant consideration throughout this particular calculation is the statistical significance that can be attached to the results (in the light of the evident non-locality of the gluon field operator). Indeed, this was necessarily a concern at the outset. On an 8^4 lattice, the gluon operator (whose definition is here fixed by the requirement that it reduces, in the limit, to the continuum field strength) is a sizeable fraction of the lattice volume. With errors up to 50% on individual mass measurements (at each m_q), this has been borne out. At the very least, 8 configurations prove to be necessary to extend the propagator signals out to the furthest time steps, with 16 configurations representing a moderate improvement. Evidently, the mass estimates are rough, but at least result in a mass scale not wholly at odds with that obtained by other methods. However it must be said that at least part of the rationale for attempting this

calculation was to improve on those other approaches. We must therefore concentrate more on those avenues of improvement in which much greater accuracy might be achieved.

Two areas for investigation are suggested. Firstly, there is the rather obvious remark that simulations over greater numbers of configurations (which was not possible during this work) with more values of the quark mass should be a basic requirement of further work. This would be particularly justified at the present time if no quantitative improvement in lattice "technology" were forthcoming. However, and this is the second point, larger lattices themselves, to minimise the non-locality of the gluon field, and gauge configurations which are closer to the renormalised trajectory, are likely to lead to increasing reliability. In common with glueball studies on the lattice, the hybrid calculation is undeniably more sensitive to the fluctuations present in the ensemble of gauge configurations. One should really regard this present calculation as a "first approximation" to the actual mass spectrum but which, encouragingly, demonstrates the value of the method. In addition, recent numerical evidence tends to suggest that the Wilson one-parameter action at $\beta=5.7$ may not be close enough to a renormalised trajectory (see Bowler et al [1985]) to make these investigations final. However, at least the existing software is readily adaptable.

Finally though, the comprehensive study of lattice 4-quark mesons does not, we feel, warrant further calculations in this area until 4-quark states are discovered, which disagree significantly with our estimates. Alternatively, more sophisticated lattice gauge and fermionic actions that reproduce more closely the observed

hadronic spectrum may also suggest a reappraisal. Certainly, much is likely to be forthcoming in the next few years.

The lattice simulations we have presented demonstrate, (we stress) within the overall constraints of the method itself, the belief that QCD does support the existence of multi-quark and hybrid mesons. What is now required is the experimental detection of at least some of these states.

APPENDIX

The numerical simulations involving lattice QCD performed in this thesis were carried out on an ICL Distributed Array Processor (DAP). There are particular characteristics of the DAP architecture that make it well suited to these kinds of Monte Carlo calculations and in this section we would like to discuss some of the ways that one can readily "map" a Lattice Gauge Theory model in a straightforward manner into DAP software. The key feature here is the machines' ability to process in a parallel fashion (i.e., perform simultaneous identical operations on) independant data sets assigned to individual processing elements within the computer memory. The efficacy of the actual structuring of the processing elements should become clearer below when we consider some specific examples taken from both the Metropolis and Gauss-Seidel algorithms for constructing gauge ensembles and quark green functions.

The reader is directed to the review of Bowler [1983 and references therein] and also to the work of Hockney and Jessop [1983] where some consideration of the DAP's performance in comparison with other parallel and "pipelined" (e.g., CRAY-1, CYBER, etc) processors is made.

The DAP is an array of 64x64 processing elements (PE's) each of 4kbits memory capacity with each PE stored on a single chip. The DAP uses only small-scale integration for these elements and this accounts in part for the modest cost of the computer. The total 2Mbytes memory space is also available as store to the ICL 2900 series mainframe system to which it is connected. In one additional respect, the DAP serves as an additional memory module for the "host" computer when not carrying DAP jobs. Access is

gained to the PE's through a Master Control Unit (MCU) which also performs simple (i.e., scalar-type FORTRAN, DO-loop control) operations in parallel-processing mode. In figure 1, we illustrate, in schematic form, the relation of the DAP to the "host" system.

Each PE has, in addition to the input/output multiplexors, three 1-bit registers, an accumulator (Q), a carry store (C) and an "A"-register which allows increased programming control to select individual PE's for operation. This A-register "enables" the processor when the bit stored within it is "TRUE". The 4096 PE's are linked by row and column (figure 2) to their nearest neighbours. The geometry of the resulting assembly is labelled N, E, S, W, (compass points) with a prescription (set by the user) on whether planar or cyclic boundary conditions are enforced. The former defines a zero input at the edge of the array and the latter imposes periodicity in the four directions.

Software features

Communication between DAP and Host is facilitated by shared common blocks with the DAP called as a subroutine in the Host program (i.e., the object file run on the 2900 machine). Once control is transferred to the DAP, processes are executed by means of a modified FORTRAN language, DAPFORTRAN. This implements efficiently the parallel-processing aspects of the system. Word lengths in DAPFORTRAN are 3-8 bytes for REAL-valued variables, 1-8 byte INTEGER variables and LOGICAL variables, as in standard FORTRAN. In addition to FORTRAN scalars, the DAP can process as complete "entities" vector and matrix arrays of 64 and 64x64 entries respectively. Although it is also possible to treat these objects as strings of scalar variables (in the sense of FORTRAN), the power of parallel

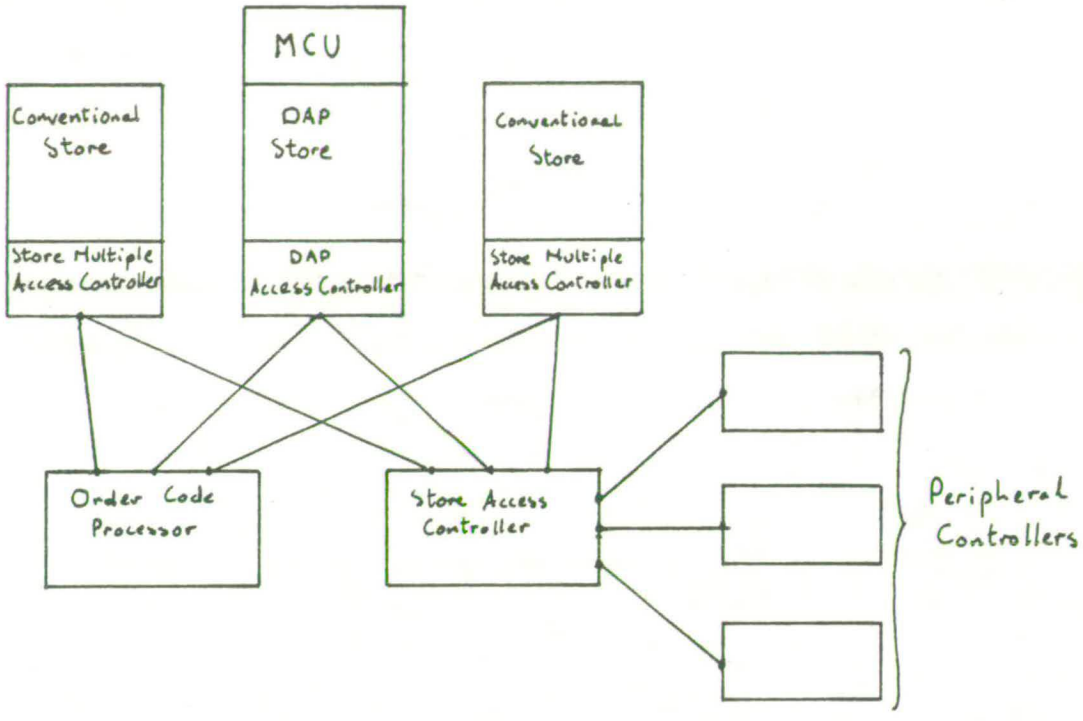

Figure A.1 A schematic illustration of the relation of the DAP to the "host" ICL 2900 machine.

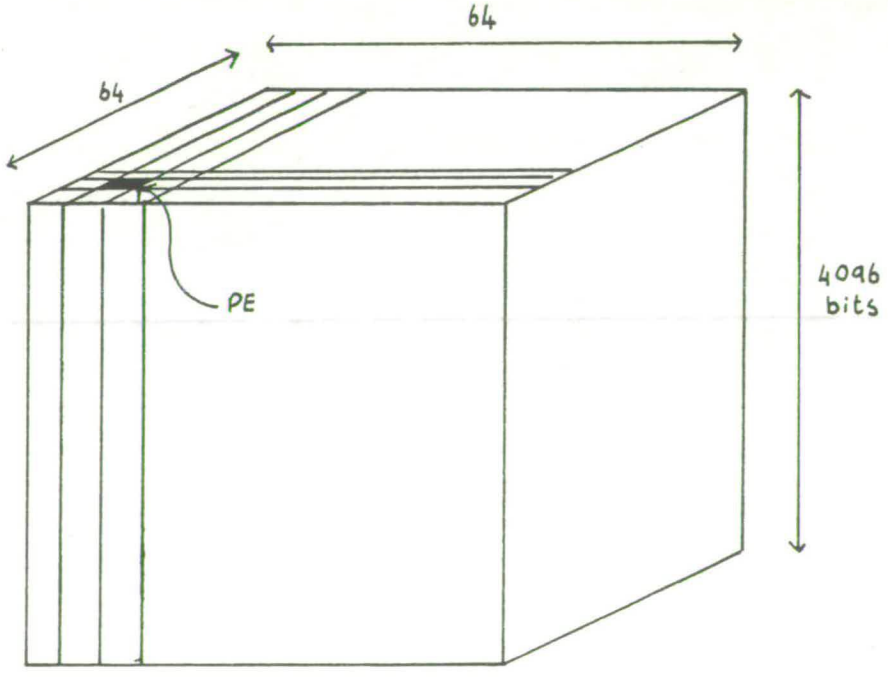

Figure A.2 The organisation of the processing elements (PE's) within the DAP.

processing is demonstrated clearly even by the following simple example, which adds two 64^2 matrices at each PE simultaneously

```
DIMENSION A( , ), B( , ), C( , )          (A-1)
A=B+C
```

The DAP layout introduces two novel features into the associated software. The first is the capability to shift information stored in one (or more) PE to any other PE in the array. Consider the following

```
DIMENSION A( , ), B( , ), C( , )          (A-2)
A=B+SHNC(C,4)
```

which, see figure 3, defines A at each PE to be the sum of B at the same PE and the value of C at the PE four sites away to the "south". In general, one also has SHNC,SHEC,SHWC, for cyclic geometry and SHNP,SHEP,SHSP,SHWP for planar boundary conditions. One can also treat the matrices in "long-vector" mode, i.e., of length 4096 elements, and shift entries left and right a specified number of sites by the commands SHLC,SHLP,SHRC,SHRP.

The second major new feature of DAPFORTRAN is the use of A-register (see earlier) in each of the 4096 PE's to impose logical "masks" on the operation of the assembly of PE's. In particular, the combination of both shift function and built-in logical operations allow the construction of the complicated masks required to mount 4-dimensional lattice QCD in the DAP memory. Thus,

```
LOGICAL LMASK( , )                        (A-3)
LMASK=ALTR(N)
```

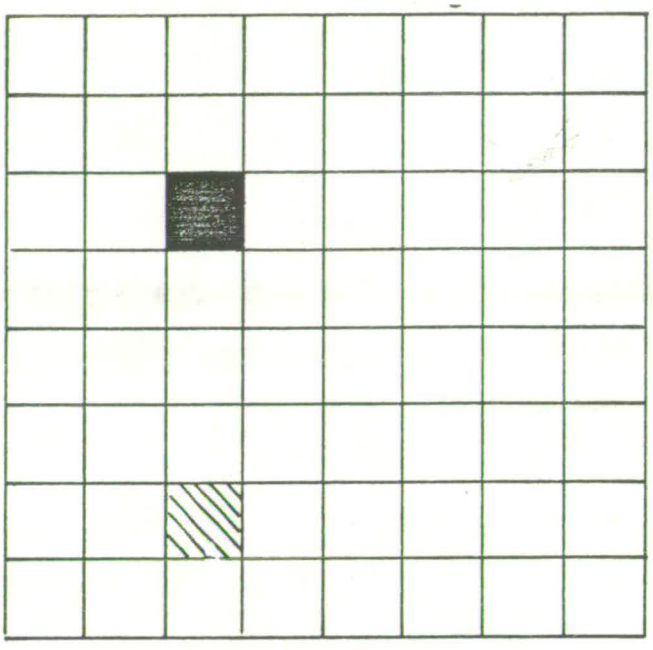

Figure A.3 The effect of A= B+SHNC(C,4). To an arbitrary PE, indicated by the solid square, one adds the contents of B and the contents of C stored 4 PE "away to the south" (cross-hatched).

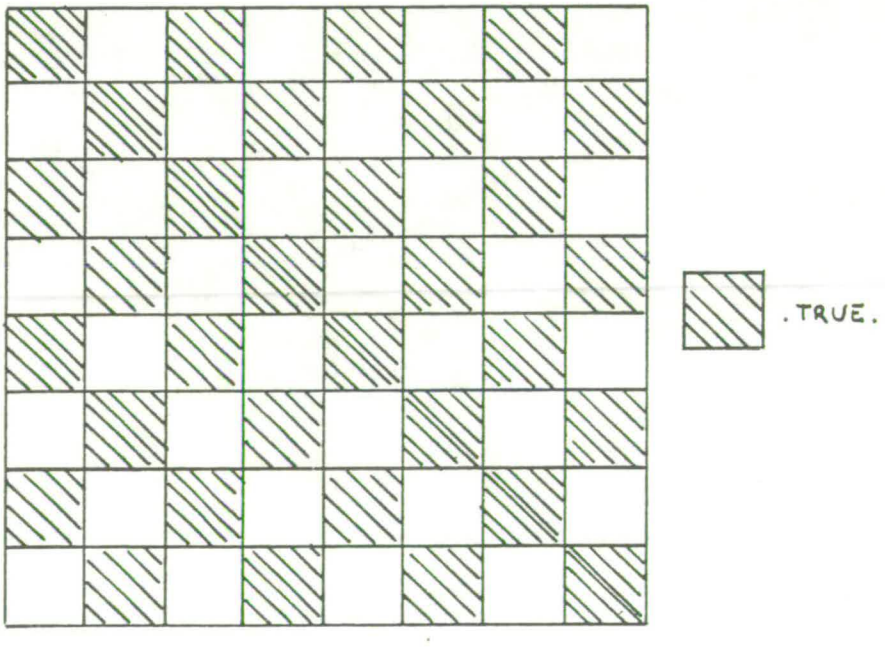

Figure A.4 A DAP logical mask: LMASK= ALTR(1).LEQ.ALTC(1)

is a system function which sets alternate N rows .FALSE. and N rows .TRUE. Using the analogous function for colomns of PE's, we can set up the "checkerboard" mask

```
LMASK=ALTR(1).LEQ.ALTC(1)                    (A-4)
```

which we illustrate in figure 4. Note that the action of this mask is to allow arithmetic functions to be carried out only at those PE's where LMASK=.TRUE.

Finally, the MERGE command makes shift operations conditional upon the truth of some specified mask. So, for instance,

```
Y( , )=MERGE(SHWC(X( , ),1),SHNC(Z( , ),6),LMASK)    (A-5)
```

assigns to Y at each PE <u>either</u> X(,) shifted by one site to the "west" <u>or</u> Z(,) shifted by six sites to the "north" depending on the truth of LMASK at that PE.

DAP Algorithms for Lattice QCD

Earlier in this thesis (chapter 4), we had occasion to discuss specific algorithms for the generation of ensembles of gauge configurations and the quark propagator. We now look at the explicit "mapping" of the 4-dimensional "volume" of space-time that represents the QCD vacuum onto the 2-dimensional DAP array. From the 64x64 assembly of PE's we can identify an 8^4 four dimensional lattice by means of dividing up the 4096 sites into 64 blocks of 8x8 lattice sites. In figure 5 we indicate, for an arbitrary site n, the nearest neighbours that will be involved in calculations involving local field theories. Note that we will typically impose periodic boundary conditions in the 4 co-ordinate directions and so must incorporate the cyclical geometry

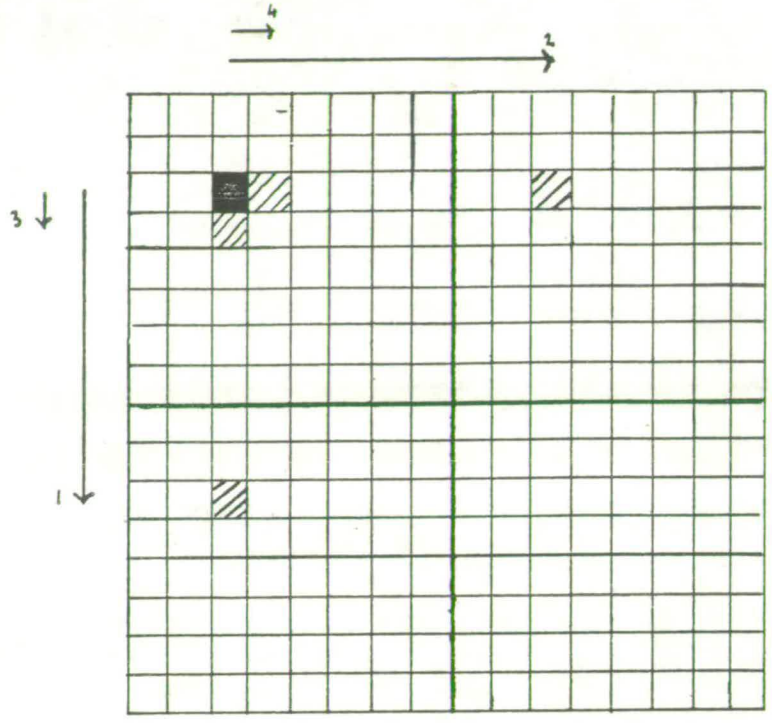

Figure A.5 For an arbitrary site (solid shading) the nearest neighbour PE in the four co-ordinate directions are as indicated (hatched shading).

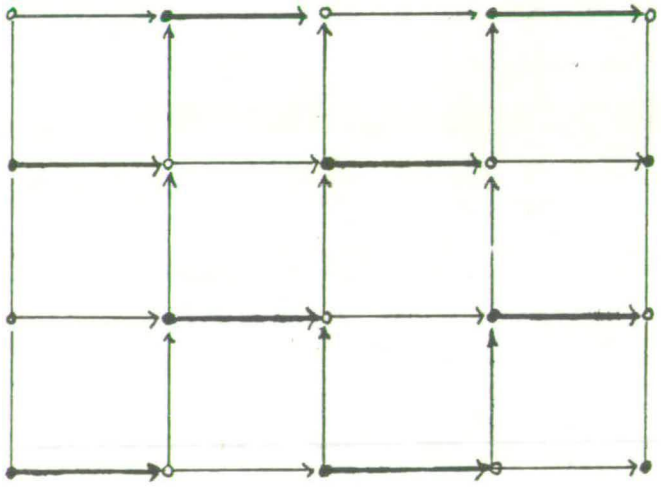

Figure A.6 A two dimensional subspace of the four dimensional lattice space-time. The bold-face arrows indicate those link variables that may be updated simultaneously whilst maintaining detailed balance.

for the two directions that repeat within the 64^2 plane by means of appropriate logical masks.

A subtlety that arises in generating the gauge configurations by means of some (e.g. Metropolis) algorithm is the necessity of maintaining detailed balance throughout. This reduces to some extent the efficiency of any parallel up-dating scheme in computing the change in the gauge action that arises from the selection of a "new" link variable. Recall that the gauge action depends on the elementary squares of the lattice and that the gauge fields are stored at the site from which they emanate in the four co-ordinate directions. It is only possible to test one link at a time whilst executing the algorithm if detailed balance is to be satisfied at all times. To maximise the efficiency of the program then, we label the sites of the lattice even and odd, e.g., $U(n,\mu)$ and $U(n\pm\mu,\mu)$ repectively. One updates the even sub-lattice and <u>then</u> the odd sub-lattice. By referring to figure 6, we can see (for a two-dimensional slice of the 4-d space-time) that indeed only one link per plaquette is updated at any one time. For two sub-lattices, each with four link variables, we achieve a one in eight update efficiency. The mask that facilitates this process is given by

```
LMASK=(ALTR(1).LEQ.ALTC(1)).LEQ.(ALTR(8).LEQ.ALTC(8))   (A-6)
```

This actually provides us with the means to extend the lattice from 8^4 to 8^3x16, twice the length in the time direction. We noted in chapter 4 that the relaxation routine for the quark propagator connects even and odd sites of the lattice. One determines the "improved" approximation to $G(n,\mu)$ on the even sub-lattice and then on the odd sub-lattice. Thus only half the PE's are needed at any stage of the iteration. The redundant PE's, whether

even or odd, are used to extend the lattice by copying the existing 8^4 configuration to those unused sites and update G_{odd} or G_{even} respectively <u>as if</u> the lattice were larger by that extent (because there are no dynamical fermion loops involved this does not feed back to the gauge configurations themselves).

The simulations on the 4-quark and hybrid mesons used much of the software features that have been outlined above. In particular, the construction of the non-local gluon field operator utilised a complicated series of shift operations to "bring" the required link variable to the site where $F_{\mu\nu}(n)$ was to be defined (recall that the SU(3) interactions were localised there) and perform the matrix multiplies. However, there is no great gain to be made in understanding from discussing this in any further detail. For completeness though, we may note that the time-slice quark green functions $G^{ab}_{\alpha\beta}(n,0)$ were stored in DAP memory over 48 3-byte planes. Each plane contained the green function information at the 8^3 lattice sites for all values of the colour label "a", by real and imaginary parts. 48 planes were therefore necessary to store the 3 components of "b" and the 4x4 components of α and β. The use of shift and merge operations, in tandem with various logical masks, proved invaluable in performing the colour and spin summations (as detailed elsewhere).

REFERENCES

Adler S.L., 1969, Phys. Rep. 177, 2476

Aitchison I.J.R., 1983, An Informal Introduction to Gauge Field Theories (Cambridge Univerity Press)

Aitchison I.J.R. and Hey A.J.G., 1982, Gauge Theories and Particle Physics (Adam Hilger, Bristol)

Amit D.J., 1984, Field Theory, The Renormalisation Group, and Critical Phenomena (World Scientific, Singapore)

Anderson P.W., 1958, Phys. Rep. 112, 1900

1963, Phys. Rep. 130, 439

Andrei N. and Gross D.J., 1978, Phys. Rev. D18, 468

Applequist T. and Georgi H., 1973, Phys. Rev. D8, 4000

Baake M., Gemundes B. and Oedingen R.,

1982, J, Math. Phys.23, 944

1983, Ibid 211, 1021

Balitsky I.I., Dyakanov D. and Yung A.,

1982a, Phys. Lett. 12B, 71

1982b, Sov. J. Nucl. Phys. 35, 761

Banks T., Kogut J. and Susskind L., 1976, Phys. Rev. D13, 1043

Barbour I.M., Bowler K.C., Gibbs P. and Roweth D.,

1985 Edinburgh preprint 85/346

Barnes T., 1984, in School of Physics of Exotic Atoms, Erice

Barnes T. and Close F.E., 1982, Phys. Lett. 116B, 365

Barnes T., Close F.E. and Monaghan S.,

1981, Phys. Lett. 110B, 159

1982, Nucl. Phys. B198, 380

Barnes T., Close F.E. and de Viron F.,

1983, Nucl. Phys. B224, 241

Barkai D., Moriarty K.J.M., and Rebbi C.,

1984, Phys. Rev. D30, 1293

Baulieu L., Ellis J., Gaillard M.K. and Zakrzewski W.J,

1978, Phys. Lett. 77B, 290

Bechi C. and Morpurgo G., 1965a, Phys. Lett., 17, 352

1965b, Phys. Rep. 140B, 689

Belavin A.A., Polyakov A.M., Schwartz A.S. and Tyupkin Yu S.,
1975, Phys. Lett. 59B, 85

Bell J.S. and Jackiw R., 1969, Nuovo Cimento 51, 47

Berg B. and Billoire A., 1982a, Phys. Lett. 114B, 324
1982b, Ibid 113B, 65
1983, Nucl. Phys. B221, 109

Berg B. and Luscher M., 1981, Nucl. Phys. B190 [FS3], 412

Bernard C., 1982, Phys. Lett. 108B, 431

Bhanot G., 1982, Phys. Lett. 108B, 337

Bhanot G. and Creutz M., 1981, Phys. Rev. D24, 3212

Bhanot G., Lang C.B. and Rebbi C.,
1982, Computer Physics Comm. 25, 275

Bhanot G. and Rebbi C., 1981a, Nucl. Phys. B180 [FS2], 469
1981b, Phys. Rev. D24, 3319

Binder K., 1979, (ed) Monte Carlo Methods in Statistical
Physics (Springer, New York)

Birman J.C. and Chen L.C., 1971, J. Math. Phys. 121, 2454

Bjorken J.D., 1967, in Proceedings of 3rd International
Symposium on Electron and Photon Interactions
(Stanford, CA)
1969, Phys. Rep. 179, 1547

Bjorken J.D. and Drell S., 1964, Relativistic Quantum
Mechanics (McGraw-Hill, NY)
1965, Relativistic Quantum Fields (McGraw-Hill, NY)

Blanckenbeckler R., Hirsch J. Scalapino D. and Sugar R.,
1982, Phys. Rev. Lett. 47, 1628

Bogoliubov N.N. and Shirkov D.V., Introduction to the Theory
of Quantised Fields, 3rd ed., 147 (John Wiley and Son)

Bowler K.C., 1983, in Proc. of the Three day In-Depth Review
on the impact of Specialised Processors in
Elementary Particle Physics, Univ. of Padova, Italy

Bowler K.C., Pawley G.S., Wallace D.J., Marinari E.
and Rapuano F., 1983, Nucl. Phys. B220 [FS8], 137

Bowler K.C., Chalmers D.L., Kenway A., Kenway R.D.,
Pawley G.S. and Wallace D.J.,

1984, Nucl. Phys. B240 [FS12], 213

Brandelik R. et al, 1977, Phys. Lett. 70B, 387

Bronowski J., 1973, The Ascent of Man (BBC publications)

Cabibbo N. and Parisi G., 1975, Phys. Lett. 59B, 67

Cabibbo N. and Marinari N., 1982, Phys. Lett. 119B, 387

Callen C.G., Dashen R. and Gross D.J.,

1978, Phys. Rev. D17, 2717

1979, Ibid D19, 1826

Campbell N.A., Griffiths L.A., Michael C. and Rakow P.E.L.,

1984, Univ. of Liverpool preprint LTH113

Celik T., Engels J. and Satz H., 1983, Phys. Lett. 125B, 411

Chalmers D.L., 1985, Phys. Lett. B151, 151

Chanowitz M. and Sharpe S., 1983a, Nucl. Phys. B222, 211

1983b, Phys. Lett. 132B, 413

Cheng T.P. and Li L.F., 1984, Gauge Theory of Elementary Particle Physics (Clarendon Press, Oxford)

Chodos A., Jaffe R.L., Johnson K., Thorn B. and Weisskopf V.,

1974, Phys. Rev. D9, 3471

Christ N.H., Friedberg R. and Lee T.D.,

1982a, Nucl. Phys. B216 [FS6], 310

1982b, Ibid B216 [FS6], 337

Close F.E., 1980, Introduction to Quarks and Partons (Academic Press, Lon)

Proc. of Kopai Summer School, ed. J. Ellis

Coleman S., 1977, in The Whys of Subnuclear Physics, Proc. of Int. Sch. in Subnucl. Phys., "Ettore Majorana", ed. A. Zichichi (Plenum, NY)

Coleman S. and Gross D.J., 1973, Phys. Rev. Lett. 31, 851

Copley L.A., Karl G. and Obryk E., 1969a, Phys. Lett. 29B, 117

1969b, Nucl. Phys. B13, 303

Cornwall J.M. and Soni A., 1982, UCLA 82/TEP3

Creutz M., 1980a, Phys. Rev. D21, 2308

1980b, Phys. Rev. Lett. 45, 313

Creutz M., Jacobs L. and Rebbi C.,

1979a, Phys. Rev. Lett. 42

1979b, Phys. Rev. D20, 1915

1983, BNL preprint 3243B NSF-ITP-83-07

Creutz M. and Moriarty K.J.M., 1982, Phys. Rev. D26, 2126

Dashen R., 1969, Phys. Rep. 183, 291

Dashen R. and Gross D.J., 1981, Phys. Rev. D23, 2340

De Forcand P., Schierholz G., Schneider M. and Teper M.,
1985, Phys. Lett. 152B, 107

De Grand T.A. and De Tar C.E.,
1983, Univ. of Colorado preprint COLO HEP66

De Grand T., Jaffe R.L., Johnson K. and Kiskis J.,
1975, Phys. Rev. D12, 2060

De Grand T.A., and Toussaint D., 1980, Phys. Rev. D12, 2478

1981, Ibid D24, 466

De Viron F. and Weyers J., 1981, Nucl. Phys. B185, 391

Dirac P.A.M., 1933, Physikalische Zeitschrift
der Sowietunion 3, 64

Donaghue J., Johnson K. and Li B., 1981, Phys. Lett. 99B, 416

Drell S.D., Levy D.J. and Yan T.M., 1970, Phys. Rev. D1, 1035

Drell S.D. and Yan T.M., 1971, Ann. Phys. (New York) 66, 595

Drell S.D., Weinstein M. and Yankielowicz S.,
1976a, Phys. Rev. D14, 487

1976b, Ibid D14, 1627

Drouffe J.M., 1978, Phys. Rev. D8, 1174

Dubikov M.S. and Smilga A.V., 1981, Nucl. Phys. B185, 109

Dyson F.J., 1951a, Phys. Rep. 82, 420

1951b, ibid, 82, 608

Englert F. and Brout R., 1964, Phys. Rev. Lett. 13, 321

Espriu D., Gross M. and Wheater J.,
1984, Univ. of Oxford preprint

Faddeev L.D. and Popov V.N., 1967, Phys. Lett. 25B, 29

Faddeev L.D. and Slavnov A.A., 1980,
Gauge Fields, Introduction to Quantum Theory
(Benjamin Cummings, Reading MA)

Farhi E. and Susskind L., 1981, Phys. Rep. 74C, 277

Feynman R.P., 1948, Rev. Mod. Phys. 20, 267

Fischler W., 1977, Nucl. Phys. B129, 439

Fuçito F., Marinari E., Parisi G. and Rebbi C., 1981, Nucl. Phys. B180 [FS2], 369

Fucito F., Martinelli G., Omero C., Parisi G., Petronzio R. and Rapuano F., 1982, Nucl. Phys. B210 [FS6] 409

Fucito F., Patel A. and Gupta R., 1983, Phys. Lett. 131B, 169

Gell-Mann M., 1964, Phys. Lett. 8, 214

Gell-Mann M. and Levy M., 1960, Nuovo Cimento 16, 705

Gell-Mann M. and Ne´eman Y., 1964, The Eightfold Way (Benjamin NY)

Glashow S.L., 1961, Nucl. Phys. 22, 579

1967, in Hadrons and their Interactions, Proc. of Int. Sch. of Phys., "Ettore Majorana", ed. A. Zichichi (Academic Press, NY)

Goldstone J., 1961, Nuovo Cimento 19, 154

Goldstone J., Salam A. and Weinberg S., 1962, Phys. Rep. 122, 965

Goodyear S.G., 1984, Univ. of Edinburgh preprint 84-318

Govaerts J., de Viron F., Gusbin D. and Weyers J., 1983a, CERN preprint TH.3823

1983b, Phys. Lett. 128B, 262

Govaerts J., Reinders L.J. and Weyers J., 1985, Univ. of Texas preprint UTTG-06-85

Griffiths L.A., Michael C. and Rakow P.E.L., 1983, Phys. Lett. 129B, 351

Gross D.J., 1975, in Methods in Field Theory, Les Houches (North-Holland)

Gross D.J. and Wilcek F., 1973a, Phys. Rev. Lett. 30, 1343

1973b, Phys. Rev. D8, 3633

Gross M., 1984, in Phase Transitions in the Early Universe, Bielefeld

Guth A.H., 1980, Phys. Rev. D21, 2291

Halliday I.G. and Schwimmer A., 1981, Phys. Lett. 102B, 327

Hamber H. and Parisi G., 1981, Phys. Rev. Lett. 47, 1792

Hammermesh M., 1963, Group Theory

(Addison-Wesley, Reading MA)
Hasenfratz A. and Hasenfratz P., 1980, Phys. Lett. 93B, 165
Hasenfratz P., 1983, Lattice QCD, CERN preprint TH3737-CERN
Hasenfratz P., Horgan P.R., Kuti J. and Richard J.M.,
1980, Phys. Lett. 95B, 299
Hasenfratz P., Karsch F. and Stametescu I.O.,
1983, CERN TH.3636
Higgs P.W., 1964a, Phys. Rev. Lett. 12, 132
1964b, Ibid 13, 509
1966, Phys. Rep. 145, 1156
Hockney R.W. and Jesshope C.R., 1981, Parallel Computers,
(Adam Hilger, Bristol)
Horn D. and Mandula J., 1978, Phys. Rev. D17, 898
Ioffe B.L., 1981, Nucl. Phys. B188, 317
Ishikawa K., Sato A., Schierholz G. and Teper M.,
1983, DESY-83-061
Ishikawa K., Schierholz G. and Teper M.,
1982, Phys. Lett. 110B, 399
Ishikawa K., Teper M. and Schierholz G.,
1982, Phys. Lett. 116B, 424
Itzykson C. and Zuber J.B.,
1980, Quantum Field Theory (McGraw-Hill)
Jackiw R. and Rebbi C., 1976a, Phys. Rev. Lett. 36, 1119
1976b, Ibid 37, 172
Jaffe R.L., 1977a, Phys. Rev. D15, 267
1977b, Ibid D15, 281
Jaffe R.L. and Johnson K., 1976, Phys. Lett. 60B, 201
Johnson R.C., 1982, Phys. Lett. 114B, 149
Kajantie K., Montoner C. and Pietarinen E.,
1981, Zeit. Phys. C9, 233
Karsten L.H. and Smit J., 1978, Nucl. Phys. B144, 536
1979, Phys. Lett. 85B, 100
1981, Nucl. Phys. B185, 20
Kawamoto N. and Smit J., 1981, Nucl. Phys. B192, 100
Kluberg-Stern H., Morel A., Napoly O. and Peterson B.,

1982, Saclay preprint DPh.G.SPT/83/29

Kokkedee J.J.J., 1969, The Quark Model (Benjamin, NY)

Kogut J.B., 1979, Rev. Mod. Phys. 49, 267

1983, Ibid 55, 775

Kogut J. and Susskind L., 1975a, Phys. Rev. D111, 395

1975b, Ibid D111, 1477

Kogut J., Stone M., Wyld H.W., Shigemetsu J., Shenker S.H. and Sinclair D.K., 1982, Phys. Rev. Lett. 48, 1140

Lang C.B. and Rebbi C., 1982, Phys. Lett. 115B, 137

Lattore J.I., Narrison S., Pascuard P. and Tarrach R., 1984, CERN preprint TH.3949

Lautrup B. and Nauenberg M., 1980, Phys. Lett. 95B, 63

Lee B.W., 1975, in Methods in Field Theory, Les Houches, eds. R. Bailin, J. Zinn-Justin (North-Holland, Amsterdam)

Lee B.W. and Zinn-Justin J., 1972a, Phys. Rev. D5, 3121

1972b, Ibid, D5, 3137

1973, Ibid D7, 1049

Levin E.M. and Frankfurt L.L., 1965, ZhETF Pisma 2, 106

Lipkin H.J. and Leck F.S., 1965, Phys. Rev. Lett. 16, 71

Lipps H., Martinelli G., Petronzio R. and Rapuano F., 1983, Phys. Lett. 126B, 250

Lisboa P. and Michael C., 1982, Phys. Lett. 113B, 303

Luscher M., 1982, Nucl. Phys. B200 [FS4], 61

Mach G. and Petkova V.B., 1980, Ann. Phys. (NY) 125, 117

Maciel A.K.A. and Paton J.E., 1982, Nucl. Phys. B197, 201

Mandelstam S., 1976, C23, 245

Mandula J.E., 1983, private commumication

Mandula J.E., Zweig G. and Govaerts J.,

1983, Nucl. Phys. B228, 91

1982, Los Alamos Preprint LA-UR-82-3585

Manton N.S., 1980, Phys. Lett. 96B, 328

Marinari E., Parisi G. and Rebbi C.,

1981a, Phys, Rev, Lett. 47,1795

1981b, Nucl. Phys. B190, 266

Menotti P. and Onofri E., 1981, Nucl. Phys. B190, 288

Metropolis N., Rosenbluth A.W., Teller A.H. and Teller E.,
1953, J. Chem. Phys. 21, 1087
Michael C. and Teasdale I., 1983, Nucl. Phys. B215, 109
Morpurgo G., 1965, Physics 2, 95
Munster G., 1981, Nucl. Phys. B128 [FS2], 23
1981, Ibid B190 [FS3], 439
Neilsen H.B. and Ninomiya M., 1981, Nucl. Phys. B185, 20
Nikolaev N.N., 1981, Usp. Fiz. Nauk. 134, 370
Nussinov S., 1984, Phys. Lett. 136B, 93
Okubo S., 1962, Prog. Theo. Phys. 27, 949
1963, Phys. Lett. 5, 163
Otto S.W. and Stack J.D., 1984, Phys. Rev. Lett., 52, 2328
1984, Ibid 53, 1028E
Parisi G. and Petronzio R., 1980, Phys. Lett. 94B, 429
Particle Data Group, 1982, Phys. Lett. 111B
Pietarinen E., 1981, Nucl. Phys. B190, 349
Politzer H.D., 1973, Phys. Rev. Lett. 30, 1346
Polyakov A.M., 1978, Phys. Lett. 72B, 477
1979, Nucl. Phys. B120, 429
Ramond P., 1981, Field Theory: A Modern Primer
(Benjamin Cummings, Reading MA)
Rebbi C., 1980, Phys. Rev. D21, 3350
Reinders L.J., Yazaki S. and Rubenstein H.R.,
1982, Nucl. Phys. B196, 125
1983a, Phys. Lett. 120B, 200
1983b, CERN TH.3737
Salam A., 1968, in Elementary Particle Physics
(Nobel Symposium No.8) ed. N. Svartholm
(Almqvist and Wilsell, Stockholm)
Scalapino D. and Sugar R., 1981, Phys. Rev. Lett. 46, 519
Schierholz G., 1984, in Fundamental Forces,
Scottish Universities Summer School in Physics,
eds. R. Turnbull, C. Froggat
Schwinger J., 1951, Phys. Rep. 82, 914
1979, Particles, Sources and Fields,

(Addison Wesley, Reading MA)
Shifman M.A., 1980, Nucl. Phys. B173, 13
1982, Soviet J. Nuc. Phys. 26, 749
Shifman M.A., Vainshtein A.I. and Zakharov V.I.,
1979a, Nucl. Phys. B147, 385
1979b, Ibid B147, 447
Shuryak E.V., 1980, Phys, Rep. 61C, 71
1982a, Nucl. Phys. B203, 93
1982b, Ibid B203, 116
1983, Ibid B214, 237
Shuryak E.V. and Vainshtein A.I., 1982, Nucl. Phys. B201, 141
Stack J.D., 1983, Phys. Rev. D27, 412
Susskind L., 1979, Phys. Rev. D20, 2610
1976, in Weak and Electromagnetic Interactions
at High Energies, Les Houches,
eds. R. Bailin, C. Lewellyn-Smith (North-Holland)
Sutherland D.G., 1966, Phys. Lett. B23, 384
Swendsen R.H., 1979, Phys. Rev. Lett. 42, 859
1984, in Statistical Problems and Particle Physics:
Common problems and Techniques,
eds. K.C. Bowler, A.J. McKane, SUSSP,
Univ. of Edinburgh
Symanzik K., 1979, Comm. Math. Phys. 23, 49
1982, in Mathematical Problems in Theoretical Physics,
ed. R. Schroder, Lecture Notes in Physics 153
(Springer, Berlin)
Tarimoto M., 1982, Phys. Lett. 116B, 198
t'Hooft G., 1971a, Nucl. Phys. B33, 173
1971b, Ibid B35, 167
1976, Phys. Rev. Lett. 37, 8
1976b, in High Energy Physics, ed. A. Zichichi, Palermo
(Editrice Compositori, Balogna)
t'Hooft G. and Veltman M., 1972, Nucl. Phys. B44, 159
Tomboulis E., 1981, Phys. Rev. D23, 2371
1982, Ibid D25, 606

Verstegen D., 1984, Univ. of Edinburgh preprint 84-309

Weinberg S., 1967, Phys. Rev. Lett. 19, 1264

1976, Phys. Rev. D13, 974

Weingarten D., 1982, Phys. Lett. 109B, 57

1983a, Phys. Rev. Lett. 51, 1830

1983b, Nucl. Phys. B215 [FS7], 1

Wilson K.G., 1969, Phys. Rev. 179, 1499

1974, Phys. Rev. D10, 2445

1977, in New Phenomena in Subnuclear Physics,
Erice 1975, ed. A. Zichichi (Plenum NY)

1979, in Recent Developments in Gauge Theories,
ed. G. t'Hooft Cargese (Plenum NY)

Yang C.P., in Proc. of Symposium in App. Math. Vol XV, p351

Yang C.N. and Mills R., 1954, Phys. Rev. 96, 191

Zee A., 1973a, Phys. Rev. D7, 3630

1973b, Ibid D8, 4038